INFLUENCE OF LININGS ON STRESS AND DEFORMATION IN ROCK AROUND ELLIPTICAL TUNNELS

A THESIS SUBMITTED IN PARTIAL FULFILMENT OF THE DEGREE OF MASTER OF ENGINEERING

IMIYA RALALAGE PRIYANTHA GUNATILAKA

DEPARTMENT OF CIVIL ENGINEERING
UNIVERSITY OF MORATUWA
SRI LANKA

October 2001

DECLARATION

The work included in the thesis in part or whole, has not been submitted for any other academic qualification at any institution.

....

Signature of the Candidate

Certified

UOM Verified Signature

....

Dr. U.G.A.Puswewala
Supervisor

ABSTRACT

Stress and deformation behavior in rock surrounding elliptical tunnels with concrete liners is investigated by finite element analysis. The loading condition is limited to hydrostatic pressure applied inside the tunnel and it is assumed that the constitutive behaviors of both rock and concrete are according to isotropic linear elasticity. Plain strain conditions are assumed to prevail for the tunnels, which is the case when tunnels with straight axis in uniform rock media are considered.

Three elliptical tunnel geometries with major to minor axis ratios of 1.156, 1.358 and 1.500 are considered for the study. Each problem geometry was analysed for liner thickness varying from 0.0 m (unlined case) to 1.0 m in steps of 0.2 m, assuming that the Young's Modulus for rock is $1/10^{th}$ of that of concrete. The result for stress and deformation are presented for the rock domain, both in tabular and graphical forms. These numerical results illustrate the effect of concrete liner thickness and tunnel geometry on stress and deformation in rock.

A limited parametric study is conducted by varying the Young's Modulus of rock for a selected tunnel geometry with a concrete liner thickness of 0.2 m.

The present research makes a significant contribution to tunnel engineers, providing numerical tools to arrive at an optimum tunnel geometry and liner thickness, by striking a balance between cost and efficiency.

ACKNOWLEDGEMENT

This report is the final outcome of the great encouragement, idea and opportunity given by the Geotechnical Engineering Division of the Department of Civil Engineering, University of Moratuwa.

I would like to give my greatest thanks to the project supervisor Dr. U.G.A. Puswewala, for his valuable advice, guidance, criticism and suggestions to make this project a success in every possible way.

I must also be thankful to Dr. S.A.S.Kulathilaka, the course coordinator for the Master of Engineering in Geotechnical Engineering Course(1997/1998) for arranging for us a research program as part of a successful academic course.

I am deeply indebted to the former Head of Department of Civil Engineering, Associate Professor S.S.L.Hettiarachchi and other academic staff members who have made contributions to the course in every possible way to make it a success.

A special word of thanks goes to Miss. Pradeepa Peires and the staff at the Geotechnical laboratories of the department, for their kind coorperation. Also I must thanks to Eng. K.A.D Weerathunge, Eng. B. Senaratne and Eng. U.S.Karunarathne for their kind encouragement to do this course.

Imiya Ralalage Priyantha Gunatilaka

October 2001

CONTENTS

ABBREVIATIONS

eg - exempli gratia (example)

etc - et ceteri or cetera (and the others)

hr - hour

i.e. - id est (that is)

kN - kilo Newton

m - metre

m^2 - square metre

mm - millimetre

N - Newton

N/m^2 - Newton per square metre

N/mm^2 - Newton per square millimetre

No - Number

Pa - Pascal

% - Percentage

$<$ - Less than

$>$ - Greater than

^{0} - Degree

ν - Poisson's ratio

ρ - Density of soil

τ - Stress in tangential direction

σ_H - Stress in horizontal direction

σ_v - Stress in vertical direction

CHAPTER 01

INTRODUCTION

Tunnel construction was first introduced for mining operations in late 16^{th} and early 17^{th} centuries in Europe and United States of America. These tunnels were mainly used to reach mineral deposits and coal deposits. Most of these tunnels consisted of a vertical part and a horizontal part or an angle part depending on the ground condition. In the early designs in tunneling operations, people had to face problems of roof collapse on the working areas. This was overcome by making the tunnel roof as an arch which is a structural form that can take high compressive load. The exception was coal mines; roof of the coal mine was flat. In some cases temporary roof support was achieved by using steel or timber structures. But with the advancement of science and technology, people started to construct underground road systems (highways and railways) to minimize the traffic congestion. These tunnels had to be protected from collapses of roof. For this purpose, tunnel linings were introduced as a protective measure for highway tunnels. Tunnels have many more uses other than highways and railways, as discussed in chapter2. Tunnels may be constructed through rock or soils.

Tunnels in rock constitute an important area in civil and mining engineering. Tunnels can be classified according to many aspects, e.g. based on the shape, utility, location, media, etc. A comprehensive documentation on tunnels and tunnelling has been compiled by Szechy (1973).

Stress and deformation fields in rock surrounding tunnel excavations are of considerable importance in tunnel engineering. The stress fields set up due to different load systems that are imposed on the tunnel walls can be used to identify potential failure regions in the surrounding rock. Many instances arise where stresses transmitted to the surrounding rock need to be reduced by some appropriate means. An example for this is the tensile normal tangential stress set up in rock surrounding a circular or elliptical tunnel conveying water under pressure, which causes hydraulic fracturing of the rock at high magnitudes. A concrete lining is often introduced to tunnels to prevent generation of high stresses in the surrounding rock mass, in addition to other potential purposes such as protecting the exposed rock surface from weathering/erosion, controlling seepage of water, and preventing rock falls.

The calculation of the stress distribution around a circular hole in an infinite plate was first solved with the aid of mathematical theory of linear elasticity by Kirsch in 1898 (Herget, 1988). Herget (1988) gives a summary of the typical stress distribution patterns around a circular opening. According to the Kirsch equations, Jaeger (1979) gives the analytical solutions for unlined and lined circular openings in rock. More complex shapes of underground openings have also been considered in the literature, which are useful in mining and civil engineering (e.g. Obert et al. 1960). Finite element analysis has been proposed/used by many authors (e.g. Goodman 1976). The boundary integral equation method has been used to calculate stresses by superimposing two stress systems, which are the original stress state, and the stresses induced by superimposing negative surface stresses which result from the removal of material which originally existed in the excavation (Hocking 1976). Boundary element method has been used to analyse tabular ore bodies, under the concept of displacement discontinuity models (Crouch and Starfield, 1983).

This work illustrates the effect of tunnel lining on the stress distribution and deformation behaviour in the surrounding rock mass for elliptical tunnels (Szechy 1973), through the use of finite element analysis. Three elliptical tunnels with different ratios of major radius/minor radius are considered. Concrete linings of different thickness are introduced to investigate the stress and deformation behaviour in the rock mass numerically. It is assumed that material behaviour for both the rock-mass and concrete is isotopic linear elastic, and that conditions of plane strain prevail in all cases considered.

Stress and deformation behaviour in rock surrounding lined elliptical tunnels subjected to hydrostatic pressure is investigated here. The influence of different elliptical shapes of the tunnel, thickness of the concrete liner, and the variation of rock stiffness, on the stress and deformation behaviour of the rock surrounding the tunnel is derived through a parametric finite element study. Elliptical tunnels having three different ratios of major to minor radii (ratios of 1.156,1.358, and 1.500) are considered. The different tunnel geometries are analysed assuming plane strain conditions, for different concrete liner thicknesses (thickness changing from 0.0m to 1.0 m, in steps of 0.2m). A limited parametric study is conducted by varying the Young's modulus of the rock while keeping the other variables constant. The results show the effect of tunnel shape, liner thickness and rock stiffness on the stress and deformation distribution in rock surrounding elliptical tunnels

This analysis is useful in identifying the effect of liner thickness on critically stressed areas, the optimum liner thickness for a tunnel in a particular rock type, and a convenient geometrical shape as far as stress and deformation in rock are concerned.

CHAPTER 02

2. TUNNELS IN ROCK AND SOIL

2.1. Tunnel Classifications

2.1.1. Classifications Based on Service

Tunnels can be classified according to their service as follows (Szechy 1973; Jeager 1979).

(a). Highway Tunnels

Highway tunnels accommodate all types of vehicles permitted on public highways, except that their use by bicycles and horse drawn vehicles may be limited or prohibited.

(b). Railroad Tunnels

Railroad tunnels service standard railroad trains and may need special clearances for electrical traction from catenaries.

(c). Rapid Transit Tunnels

These tunnels service urban and metropolitan rapid transit trains, and are designed to meet the requirements of particular systems.

(d). Aqueducts and Sewer Tunnels

Used to convey fresh water or sanitary wastes and storm water, the sizes and construction of these tunnels vary according to local conditions.

(e). Underground Caverns

These are tunnels built to house underground hydroelectric power plants, hardened defense facilities, and special waste storage (e.g. nuclear waste).

(f). Shafts

There are vertical or inclined excavations that serve as access to mines or tunnel construction or for tunnel ventilations. They are built according to the particular requirements.

(g). Special Tunnels

Tunnels are also used to carry water pipes, electrical cables or other utilities specially in urban centers.

2.1.2. Classification Based on Tunnel Locations

Tunnel may be classified according to location as follows

(a). Underwater Tunnels

These are built by various methods under rivers, harbours or other waterways to serve any one of the purpose listed above. These tunnels are used when clearance requirements, land use, and sometimes the environment prevent construction of bridges (e.g. Channel Tunnel, built from London to Paris, underneath the English channel).

(b). Mountain Tunnels

Tunnels through mountains are used to carry transportation facilities or water (e.g. Canyon tunnel in Sri Lanka). These are frequent in some mountainous areas of the world (e.g. Switzerland, Austria, etc).

(c). Tunnels at Shallow Depths and Beneath City Streets

These are primarily used for rapid transit and other transportation in urban areas. Large metropolitan areas in the world are usually serviced by these system (e.g. London, New York, Vancouver, etc.)

(d). Bored vs Cut–and-Cover Tunnels

Bored by whatever means, these tunnels require a minimum overburden depending upon soil conditions. Shallow tunnels are most economical by cut-and-cover construction unless other conditions preclude this method.

2.1.3. Classification Based on Tunnel Media

Geological conditions greatly affect the cost of tunnel construction as indicated below:

(a). Rock Tunnels

Rock tunnels are excavated in a firm, cohesive medium which may vary from relatively soft marl and sandstone to the very hard igneous rocks such as granite. Bedding and fissuring of rock layers and the presence of water are major factors that control construction methods and pose difficulties.

(b). Soft Ground Tunnels

This category indicates all tunnels built in soft, plastic or non-cohesive soils where water may or may not be a problem.

(c). Mixed Phase Tunnels

These tunnels have part of their cross-sections in rock and part in soft ground, with rock interface often weathered. There are frequent construction difficulties.

2.1.4. Some Aspects in Tunnel Construction

The methods for tunnel constructions vary according to geological conditions, hydrological conditions, length of tunnels, size and shape of tunnel section, type of equipment to be used for excavations and its intended purpose. Out of these, sub surface (geological) conditions, and size and shape of tunnel cross-section are the main factors governing the construction process of tunnel.

2.2. Factors Influencing the Tunneling Operation

Owing to the number of factors influencing the design, loading, location and construction of tunnels, various tunneling systems have been developed.

The major influencing factors are as follows:

(1). Geological conditions.
(2). Shape and cross-sectional dimension of the tunnel.
(3). Intended purpose.

The construction of tunnels involves carrying out of the following operations.

(1). Excavations.
(2). Support.
(3). Transportation of excavated materials.
(4). Lining or coating, sealing, draining and ventilation.

The tunneling operations vary according to the conditions discussed earlier. While excavation and the transport of the excavated material is always an indispensable necessity, the type of working conditions and the means of transportation used may differ widely, and the importance and extent of both the support of the excavated cavities and the process mentioned at (4) above can vary likewise, within a wide range. Thus required operations can be carried out by various methods which can be grouped into the following categories.

(1). Full -face tunneling without temporary support .
(2). Full-face tunneling with support .
(3). Combined underground and open surface(cut-and-cover method).
(4). Pre-cast element and caisson sinking method.
(5). Pre-cast element method.
(6). Shield driving method.
(7). New Austrian Tunneling Method (NATM).

The first method can only be applied in solid rocks having RQD(Rock Quality Designation) 90% or more whereas the methods belonging to group (2) which afford supports of variable extent and strength can be applied in other rocks. In loose and weak rocks and in cohesive and granular soil all the other methods except at (1) and (2) can be applied. Methods mentioned at (5) and (6) afford good results in exceptionally soft and loose ground. The NATM is a flexible tunnel construction method which is adoptable in varying ground conditions from hard rock to soil.

2.3. Methods of Tunnel Linning

Most tunnels require temporary support during the boring operation prior to the introduction of permanent support. It is the usual practice to place permanent lining after excavation of the entire tunnel is complete (even in large tunnels).

A shallow masonry construction was used for lining in early highway tunnels. Until recently, railroad tunnels relied on timber supports. Many early sewer tunnels were lined with brick (e.g. sewer tunnel under Darley Road, Colombo). Presently concrete lining, usually cast in place, has largely replaced all other materials in all types of tunnels. Concrete lining is frequently placed without reinforcement, but where bending effects are serious, reinforcement may be required. Low-pressure grout is usually used to fill the voids that would otherwise always occur in the tunnel roofs. If the tunnel design relies on the rock to resist internal pressures of a water conveying tunnel, high-pressure grout is usually used to fill shrinkage cracks between the concrete and rock. Shotcrete, used for temporary support, is receiving more favour as permanent lining where smooth surfaces are not required. Rock bolts are sometimes used for permanent support. In this case, they must be grouted for protection against corrosion and are usually used with wire mesh, covered with a thin layer of shotcrete. Highway tunnels sometimes have a tile lining on the walls, attached to the main concrete lining.

Example:
Canyon Tunnel Details:
Canyon hydro-electricity project consist of a reservoir with concrete gravity dam, conveying tunnel, steel penstock and power house.

The geological condition of this area was fairly good. But in some locations there were weak zones. Hence the geotechnical investigation report emphasised to line the entire tunnel. (The rock encountered mainly consists of Charnokitic rock and Gneisses).

This tunnel was a horseshoe shape tunnel with internal diameter of 3.40 m (see figure 2.1) and the tunnel discharge capacity of 19.8 cumecs (700 cusecs). To prevent erosion of tunnel wall and seepage of water through tunnel wall, the tunnel was lined with a reinforced concrete liner, whose thickness varied from 0.1 m onwards.

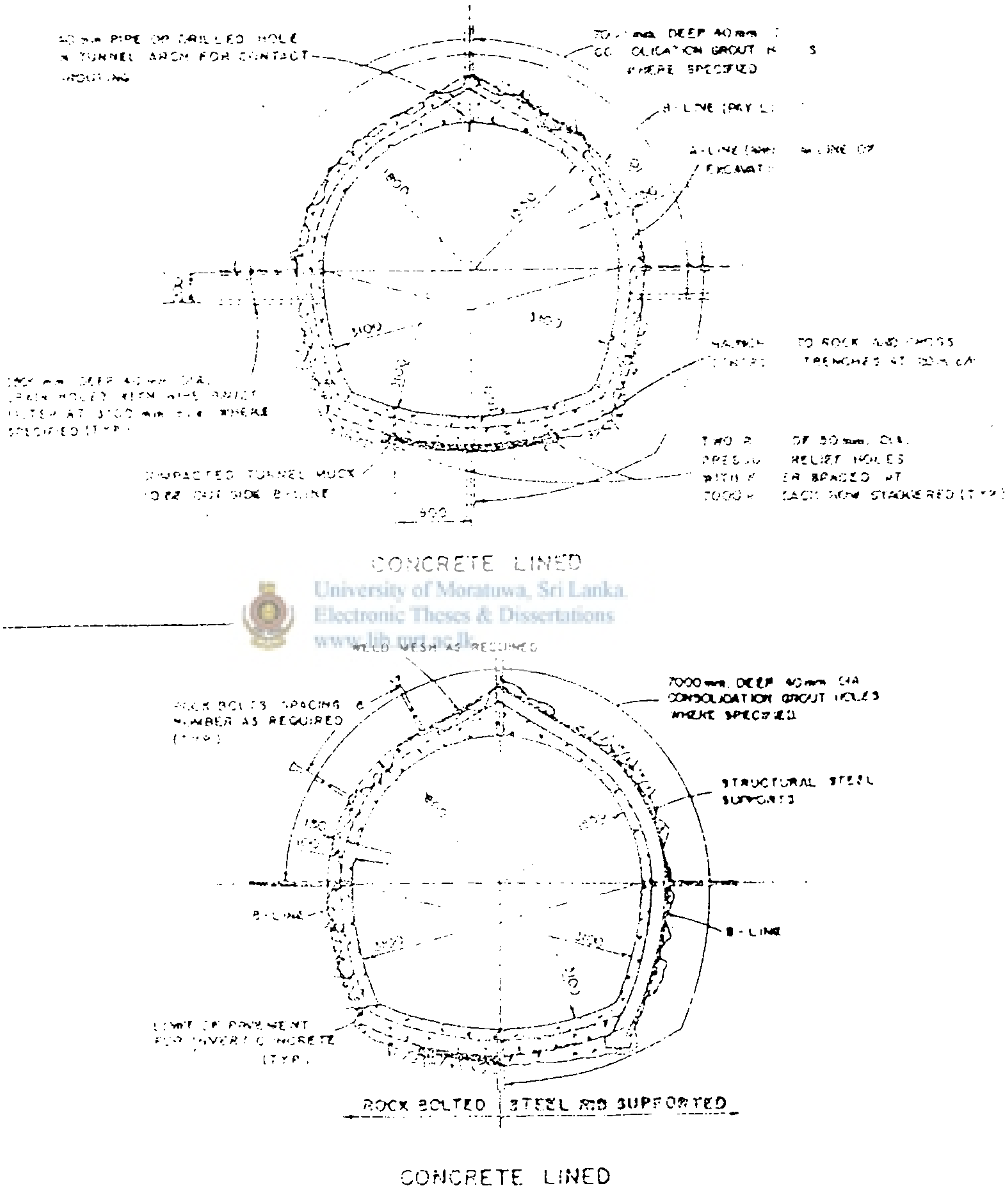

Figure 2.1 Tunnel Section After Introduction of Concrete Liner

2.4. Stress and Strain in Rock

2.4.1. Stresses in Rock

Stresses in rock masses are a fundamental concern in the design of underground excavations in Civil and Mining Engineering projects (Herget 1988; Jaeger 1979). Only an assessment of stresses in rock will allow the application of strength determination and failure theories to a rational design for excavation in rock.

Rock masses in nature are usually under the influence of a stress field. This is known as the natural stress field of the rock, according to its origin. The stress distribution in a rock–mass at a given point of time in his history depends on the history of its constitutive behaviour. Rock–mass may deform according to various constitutive models like elasticity, plasticity, creep, etc, depending on the magnitude and duration of the loading, material properties and boundary conditions. Often, materials display a combination of these various constitutive models. The actual constitutive behaviour of a material is referred to as the rheology of the material.

When man-made excavations or structures are imposed on rock, the naturally occurring stress fields are affected and changed. Such changes are of great concern to rock mechanists. Stress changes induced due to activity of man are known as induced stresses.

2.4.2 Natural Stresses

2.4.2.1. Gravitational Stress

Gravity stresses result from the weight of the column of rock per unit area above in the earth's crust. The vertical component of this stress σ_v can be calculated from.

$$\sigma_v = \int \rho g \, dz \text{ ------------(2.1)}$$

where ρ is the density of rock, g is the acceleration of gravity and z denotes depth.

While the vertical component can be easily defined, the horizontal component is more difficult to define because of the effect of different boundary conditions and rock mass properties. The stress distribution at a point depends on the constitutive behaviour (stress–strain relationship) of the material through its history of existence.

If the rock mass is assumed to be homogeneous, isotropic and elastic with the boundary conditions not allowing horizontal displacement, the horizontal stress σ_H is given by

$$\sigma_H = \nu\sigma_v /(1+ \nu) \text{ -----------(2.2)}$$

where ν is the Poisson's ratio.

If the rock material is not elastic and allowance need to be made for creep because of viscosity, it will not sustain shear stresses in the long term, i.e., the rock will flow. In such cases,

$$\sigma_H = \sigma_v \qquad \text{-----------(2.3)}$$

Thus in general it can be written as;

$$\sigma_H = K\,\sigma_v \qquad \text{-----------(2.4)}$$

where K is a parameter in the range, $0 < K < 1$.

Equation (2.3) describes a hydrostatic stress field, but in relation to rocks, it is preferable to use the term ***'lithostatic'***. In the case of a lithostaic stress field, the weight of the overburden acts in all directions; such situations can be found in areas where sedimentation is ongoing, and the sediments have a high water content. A lithostatic stress field is also expected to exist at great depth in the earth's crust.

In the general case defined by equation (2.4), K can vary from 0, with no lateral support, to K = 1 for a lithostatic stress field.

2.4.2.2. Tectonic Stresses

The earth is not an inert body; movements in the earth's crust occur continuously and seismic events related to these deformations are recorded often. Tectonic plates in the crust move upon the relatively plastic mantle below it due to the driving force provided by the heat differences between the hot core of the earth and the cooler crust.

Teconic stresses are stresses induced in rock crust by the movement of tectonic plates. Some of these stresses may have been locked up in the crust for very long periods of time. Some stresses are subsequently relieved through rock deformation. Regional differences in stress result from the different thicknesses of crustal material which restrict mantle flow in certain regions. Horizontal stresses are generally larger than the vertical stresses. These are difficult to quantity or measure with respect to magnitude and direction, unless there are recent tectonic movements and seismic activity.

One can conceptually distinguish between current or active tectonic stresses and remnant or previous tectonic stress (Herget, 1988). Remnant tectonic stresses are left-over stresses which were not fully relieved by rock deformation. However, due to lack of data, it is difficult to generally distinguish between the current and remnant stress fields. There is some evidence to suggest that current tectonic stresses lead to relatively consistent stress fields over large areas, and seismic events and current deformation suggest a current tectonic stress regime (Herget, 1988).

2.4.2.3. Residual Stresses

Residual stresses are self- equilibrating stresses. These stresses are locked–in by the rock fabric while the outer surface of the rock sample is free of stress.

2.4.2.4. Thermal Stresses

Thermal Stresses are set up due to heating or cooling of rock (Heating may be due to sunlight close to the earth's surface, or by radioactivity or other geological processes deep inside the crust). As an example, a typical liner coefficient of thermal expansion for sandstone would be $10.8x10^{-8}$ per 1^0 C of temperature.

2.4.3. Induced Stresses

Induced stresses are the result of excavation activity and therefore are of great concern in underground excavation design. Stress distribution in the back and wall of an excavation are different from those existing in the unmined rock because material had been removed.

2.5. Stress Distributions in the Earth's Crust

The stress distribution inside the earth's crust has much relevance in the field of Geotechnical and Rock Engineering today. There are many theories developed by researchers during the last two to three decades(Hast 1969, Artyushkove 1971, Herget 1980)

2.5.1. Horizontal Stresses for Canadian Shield

Equations 2.5, 2.6 & 2.7 show horizontal stress components from stress determinations in the Canadian Shield. The relationship of the average horizontal stress component with depth being greater than σ_v is not constant. Three relationships have been identified for $\sigma_H > \sigma_v$ by Herget (1980) and updated in 1988:

1. 0-800 m, σ_H =0.0581 MPa/m, -------- (2.5)
2. 800-2200 m, σ_H = 35.79 MPa + 0.0111 MPa/m, -------- (2.6)
3. Extreme values σ_H = 14.45 MPa + 0.0563 MPa/m.------- (2.7)

Relationship 3 in Figure 2.2(Herget 1988) relates to determinations where the vertical stress components were also found to be high. Although areas with extremely high horizontal stresses appear to be of limited extent, they could produce their own stability problems as the areas are approached underground.

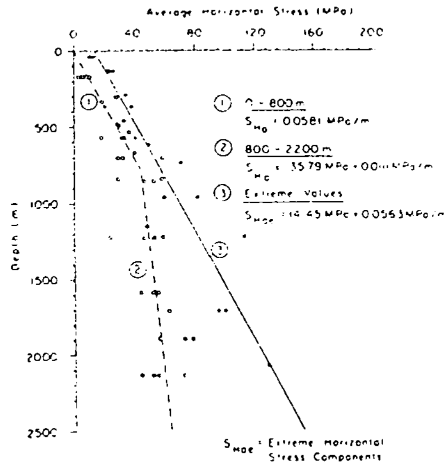

Figure 2.2. Variation of horizontal stress components with depth for Canadian Shield(after Herget, 1988)

2.5.2. Vertical Stress for Canadian Shield

Figure 2.3(after Herget, 1988) shows the vertical stress with the depth for Canadian Shield. However, the simple gravity relationship does not explain all the observations which have been made. A second relationship is shown in figure 2.3 also which gives a gradient of 0.0603 MPa/m. These values may be found in the vicinity of faults or shear zones.

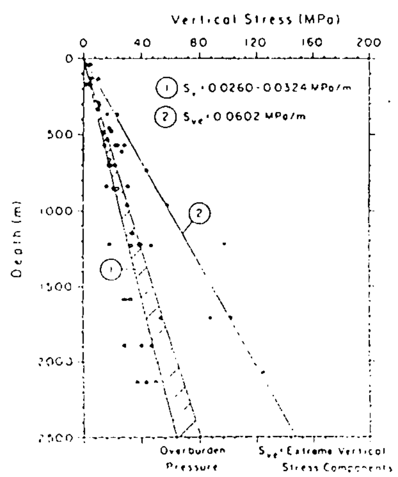

Figure 2.3. Variation of vertical stress components with depth for Canadian Shield(after Herget, 1988)

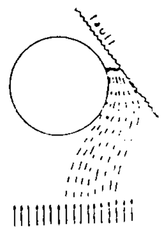

Figure 2.4 The influence of a geological fault on the stress distribution in the vicinity of the underground opening(after Herget, 1988)

Figure 2.4 shows the influence of a geological fault on the stress distribution in the vicinity of the underground opening for the Canadian shield (after Herget, 1988)

A useful way of summarizing the above results is given by plotting the ratio (k) of horizontal to vertical stress components with depths.

Figure 2.5 presents the ratio of maximum σ_H / σ_v to depth for the Canadian Shield of Northern Ontario based on an inverse relationship (Herget 1988).

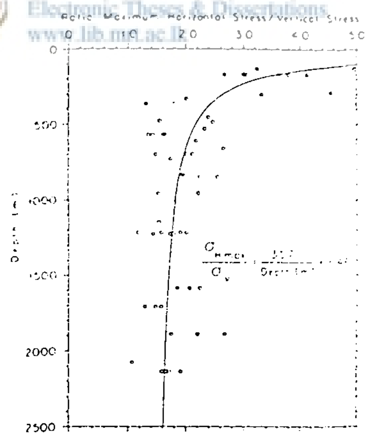

Figure 2.5. Change of maximum horizontal stress to vertical stress ratio with depth(after Herget, 1988)

The separation of the horizontal stress components into maximum, average and minimum values is given in figure 2.6(Herget 1988). These Graphs show the tendency of the ratio of the horizontal to vertical stress components to approach 1 to 1.5 at a depth 3000 metres.

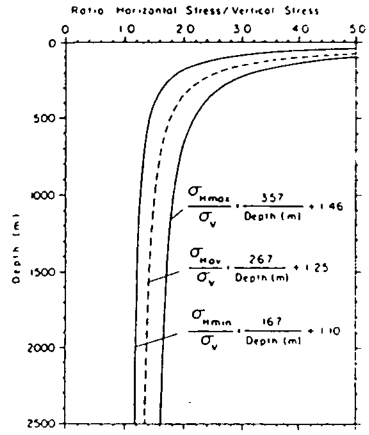

Figure 2.6 Change of maximum and minimum horizontal stress to vertical stress ratio with depth(after Herget, 1988)

2.5.3. Vertical Stress Based on World Data

Figure 2.7(after Herget, 1988) shows a plot of vertical stress components with depth which were determined over a range of depth from surface to a depth of 2400m. Over this depth the magnitude changes between zero to 100MPa.

According to the range of density for the rocks close to the surface of the earth, the gravity stress gradient will vary between 0.025 MPa/m for acidic rock and 0.035MPa/m for basic rock with an average of 0.026 MPa/m(after Hergte, 1988).

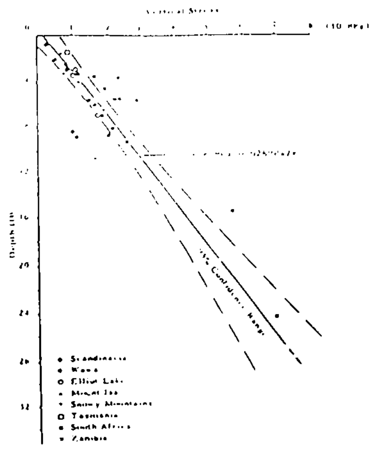

Figure 2.7 Increase of Vertical Stress with depth(after Herget, 1988)

2.5.4. Horizontal Stress

From figure 2.8(after Hergte, 1988) it can be seen that the case where stress in a horizontal direction are lower or equal to vertical stress are rather rare, and that frequently horizontal stresses are higher than vertical stresses. Horizontal stresses close to the surface are rather high at approximately 10Mpa.

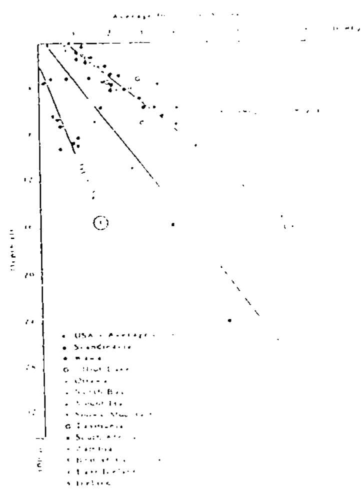

Figure 2.8 Increase of Horizontal Stress with depth(after Herget, 1988)

2.6. Stresses Around Underground Openings

All rock in the ground are subjected to compressive stresses, and if an excavation is made, the rock left standing has to take more load because the original support made by the rock within the excavation has been removed.

The changes in stress around the circular opening in elastic material is shown in the figure 2.9 by the trajectories of the maximum principal compressive stress. Trajectories identify the direction of principal stress by the tangent at each point of the trajectory. The relative magnitude of stresses may be judged by the number of the lines per unit width.

Figure 2.9 shows a crowding of the maximum principal stress trajectories on the side of the opening and a widening at the top and bottom. Crowding indicates an increase in compression and a wider spacing indicates a reduction in stress. It can also be seen that the direction of the maximum principal compressive stress is vertical at the top and bottom but deviates considerably from vertical in the vicinity of the opening.

The closest analogy to this behavior is the stream line analogy for laminar flow. If a round object similar in shape as the cross section of this opening is placed as an obstruction in the flow line, a crowding of stream lines (acceleration of flow) at the sides and a spreading (slowing of flow) in front and behind the obstacle is observed. Calculation of stresses around the opening can be carried out by mathematical theory, numerical modeling, photo elasticity and by using analog models(Herget, 1988).

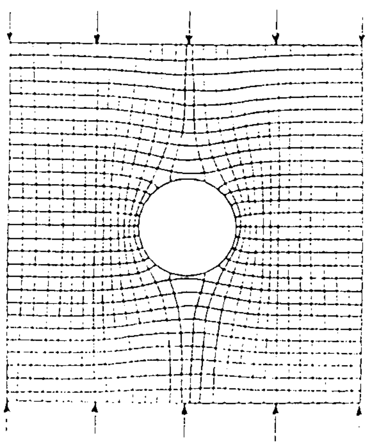

Figure2.9 Principal Stress Trajectories (after Herget, 1988)

2.6.1. Circular and Elliptical Openings in Media

The calculation of the stress distribution around the circular opening in an infinite plate was first solved by with aid of mathematical theory of linear elasticity by Kirsch in 1898 (Herget, 1988). The plate is considered to be under a stress field designated by σ_x and σ_y as shown in the figure 2.10

In general, mathematical difficulties are reduced if the boundary of an opening can be made to coincide with the coordinates that are used for circular opening. The relationships between rectangular coordinates and polar coordinates are:

$$X = r\cos\theta \quad \text{------------(2.8)}$$
$$Y = r\sin\theta \quad \text{-------------(2.9)}$$

The Kirsch equations give the radial stresses, tangential stresses and shear stresses at any point in an infinite plate with polar coordinates with θ defined from the direction of the normal stress component noted first. These are as given below by equations.

$$\sigma_r = 0.5 (\sigma_x + \sigma_y)(1-a^2/r^2) + 0.5 (1+ 3a^4 / r^4 - 4a^2/r^2)\cos 2\theta \quad \text{----------(2.10)}$$

$$\sigma_t = 0.5 (\sigma_x + \sigma_y) (1 + a^2/r^2) - 0.5(\sigma_x + \sigma_y) (1+ 3a^4/r^4) \cos 2\theta \quad \text{----------(2.11)}$$

$$\tau_{rt} = 0.5 (\sigma_x + \sigma_y) (1- 3a^4/r^4 + 2a^2/r^2) \sin 2\theta \quad \text{----------(2.12)}$$

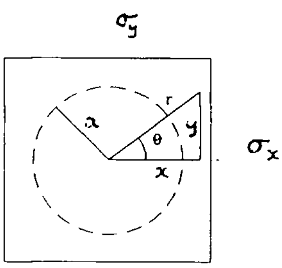

Figure 2.10 Stress field on a plate

In a biaxial stress field, the tangential boundary stresses at the end of the axes of an elliptical opening (with height = H, width = W) are given from elastic theory by the following equations.

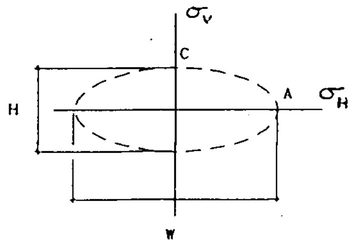

Figure (2.11)Elliptical Excavation in a Plate

$$\sigma_A = \sigma_v + \sigma_v\, 2\ W/\ H - \sigma_H \quad \text{------------- (2.13)}$$
$$\sigma_C = \sigma_H + \sigma_H\, 2\ W/\ H - \sigma_H \quad \text{------------- (2.14)}$$

2.6.2. Solution for Lined Tunnels Under Internal Pressure

Jeager (1979) considered (concrete) lined tunnels, and expressed analytical solution for a uniform pressure loading imposed internally (see figure2.12 for configuration). For concrete lined circular tunnels Jaeger (1979) gives the following solutions

For $c < R < \infty$, the stress σ_r is given by

$$\sigma_r = \frac{m_2 E_2}{m_2 - 1} B_2 - \frac{m_2 E_2}{m_2 + 1} \frac{C_2}{R^2}, \quad \text{-------------- (2.15)}$$

$$\sigma_r = -\sigma_t \qquad B_2 = 0 \qquad m_2 = 1/\ \nu_2$$

For R = c on the rock side;

$$\sigma_r = \frac{m_2 E_2}{m^2 + 1} \frac{C_2}{c^2} = p_c = \lambda p,$$

$$C_2 = -\frac{p_c c^2 (m_2 + 1)}{E_2 m_2}, \text{ with } B_2 = 0$$

The radial displacement u for R = c in the rock is

$$u_{R=C} = B_2 R + \frac{C_2}{R} = \frac{p_c c}{E_2} \frac{m_2 + 1}{m_2},$$

The stresses in the concrete lining are:

For R = b:

$$\sigma_{rb} = p,$$

$$\sigma_{tb} = -\frac{c^2 + b^2 - 2\lambda c^2}{c^2 - b^2} p;$$

For R = c:

$$\sigma_{rc} = \lambda p,$$

$$\sigma_{tc} = -\frac{2b^2 - \lambda(c^2+b^2)}{c^2-b^2}\,p$$

In the concrete

For R = b

$$\sigma_{R=b} = \frac{m_1E_1}{(m_1-1)}B_1 - \frac{m_1E_1}{(m_1+1)}\frac{C_1}{b^2} = p \text{ ---------(2.18)}$$

For R =c

$$\sigma_{R=c} = \frac{m_1E_1}{(m_1-1)}B_1 - \frac{m_1E_1}{(m_1+1)}\frac{C_1}{c^2} = \lambda_p \text{ ----------(2.19)}$$

$$C_1 = -\frac{m_1+1}{m_1E_1}\,\frac{c^2b^2}{(c^2-b^2)}\,(1-\lambda)p$$

$$B_1 = -\frac{m_1-1}{m_1E_1}\,\frac{(b^2-\lambda c^2)}{c^2-b^2}\,p$$

Equating the elastic displacement

For R = c

$$u_{R=c} = B_1c + \frac{C_1}{c} = B_2c + \frac{C_2}{c} \text{ -----------(2.20)}$$

$$\frac{m_1-1}{m_1E_1}\,\frac{(b^2-\lambda c^2)}{c^2-b^2}\,cp + \frac{m_1+1}{m_1E_1}\,\frac{c^2b^2}{(c^2-b^2)}\,(1-\lambda)p = \frac{m_2+1}{m_2}\,\frac{c}{E_2}\,\lambda_p$$

$$\lambda = \frac{p_c}{p} = \frac{\dfrac{2b^2}{E_1(c^2-b^2)}}{\dfrac{m_2+1}{m_2E_2} + \dfrac{(m_1-1)c^2+(m_1+1)b^2}{m_1E_1(c^2-b^2)}} \text{ -----------(2.21)}$$

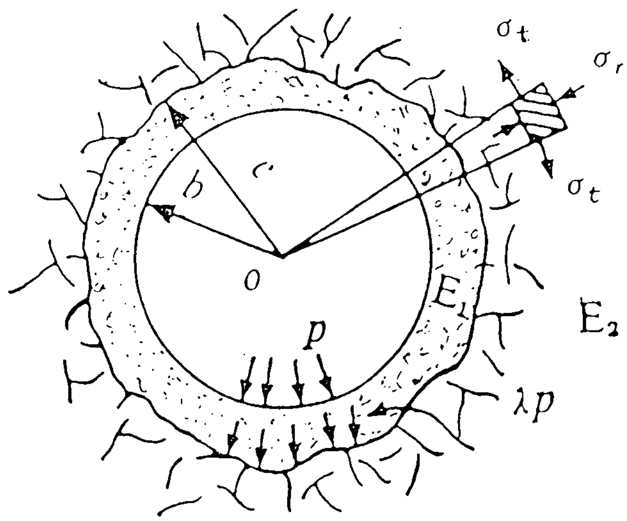

Figure 2.12 Tunnel Section With Concrete Liner

2.6.3. Stress Distribution due to Gravity Around Circular Tunnels

Herget (1988) gives the solution for stress distribution due to gravity around circular tunnels. There are depicted in figure 2.13 and 2.14.

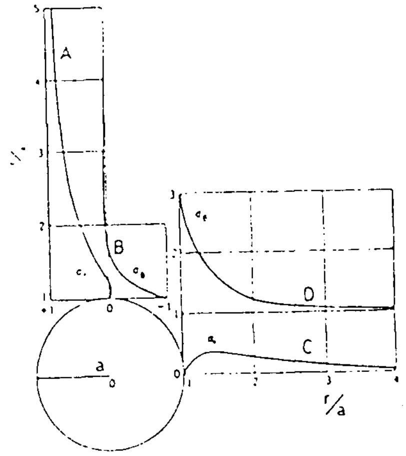

Figure 2.13 Radial and Tangential Stress for a Circular Opening Subjected to Uniaxial stress(after Herget, 1988)

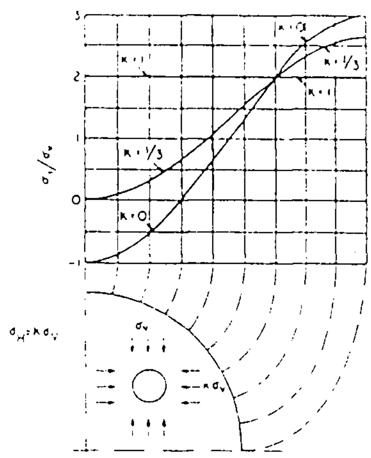

Figure 2.14 Tangential Stress For k=0, 0.33 &1(after Herget, 1988)

CHAPTER 03

PROBLEM GEOMETRY AND FINITE ELEMENT IDEALASATION

3.1 Tunnel Shapes and Geometry

As discussed in chapter two there are various types of tunnel shapes used in the world depending on their practical usage, geotechnical conditions, technology available and the financial resources.

For this research, three elliptical tunnel with different a/b values have been considered, where a= major radius and b= minor radius of the elliptical tunnel opening, as depicted in figure 3.1. These three tunnel geometries are as follows.

1. Elliptical tunnel – a/b = 1.156
2. Elliptical tunnel – a/b = 1.358
3. Elliptical tunnel – a/b = 1.500

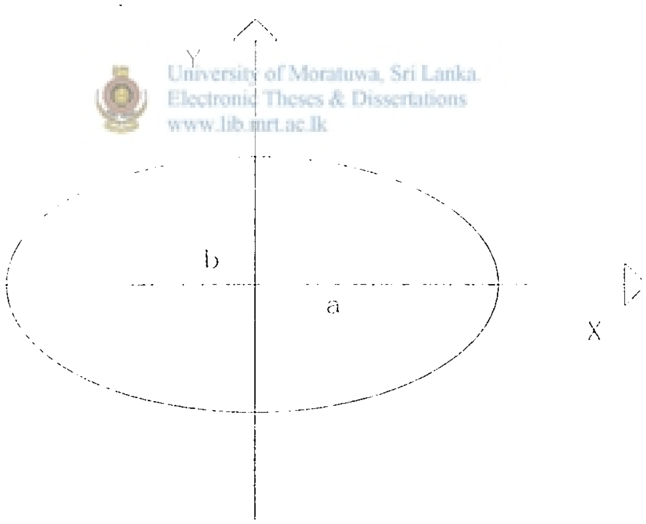

Figure 3.1 Elliptical tunnel geometry

The above values are based on actual tunnel dimensions used in practice in Sri Lanka for hydro-electric power projects. The three different tunnel shapes and the rock domain surrounding them considered for the finite element analysis here are as shown in figures 3.2, 3.3 and 3.4.

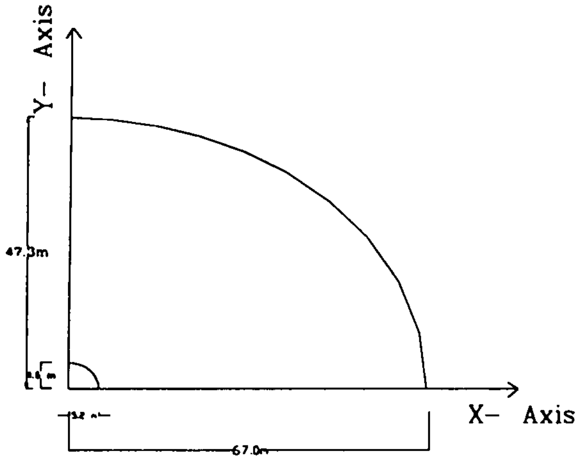

a/b = 1.156

No. of Nodes = 253

No. of Elements = 230

Figure 3.2. Elliptical Tunnel With a/b = 1.156

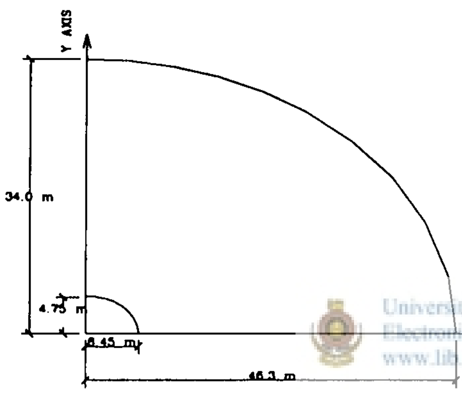

a/b=1.358

No. of Nodes - 200

No. of Elements - 190

Figure 3.3. Elliptical Tunnel With a/b = 1.358

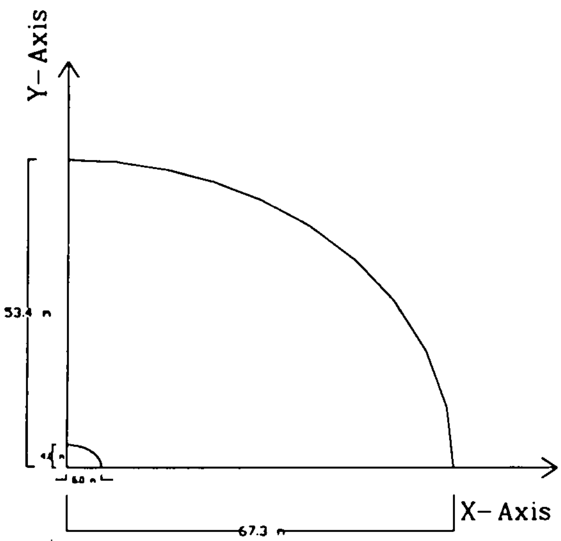

a/b = 1.500

No. of Nodes = 253

No. of Elements = 230

Figure 3.4. Elliptical Tunnel With a/b = 1.500

3.2. Concrete Lining

As discussed in Chapter 2, there are various types of linings used in tunnel construction (locally and in other countries)

In this research only concrete linings are considered. The discretized finite element domain for one of the tunnels, after the introduction of concrete liners, is shown in figure 3.5. The liner thickness is varied from 0.0m(unlined case) to 1.0m, in steps of 0.2m.

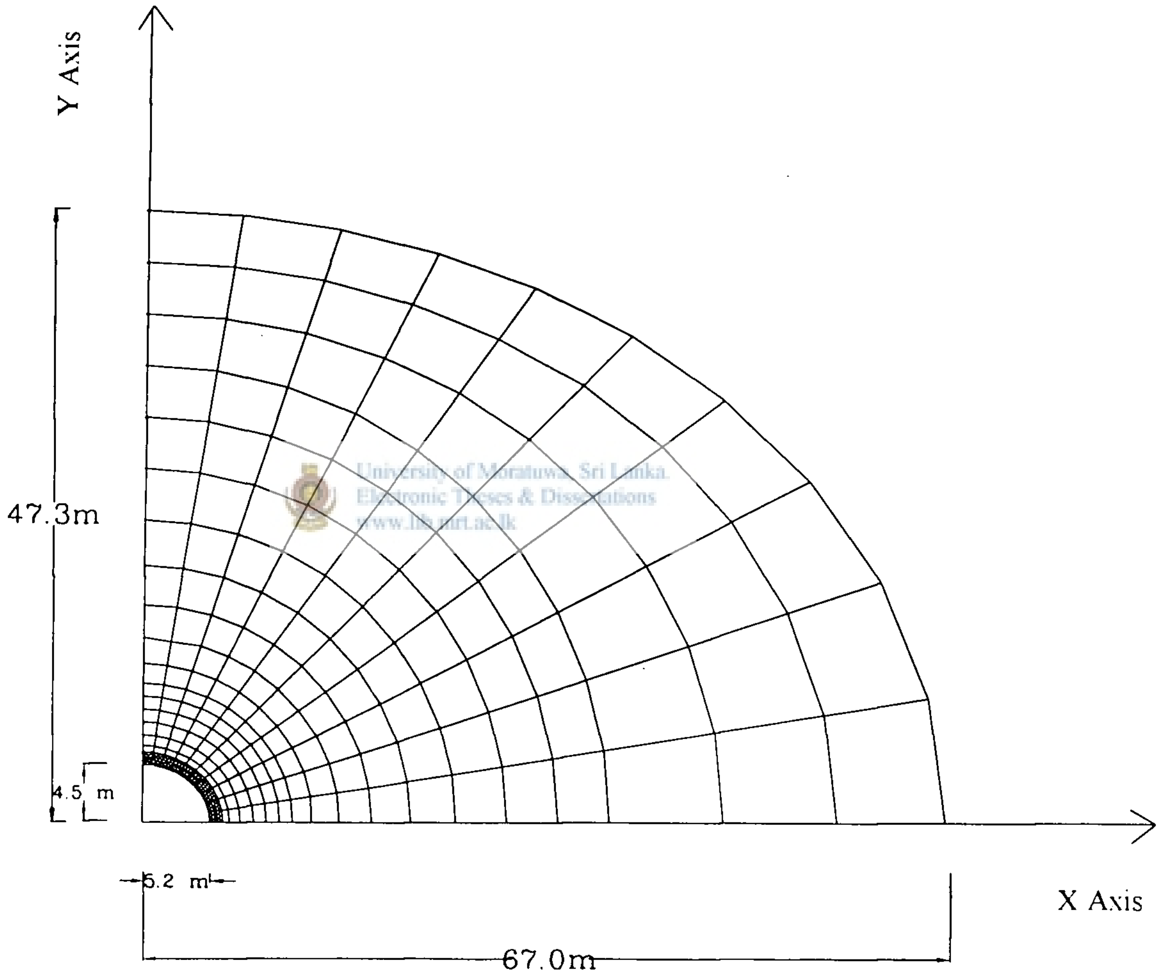

Figure 3.5 Finite element discretisation of the rock domain, after the introduction of the concrete liner.

3.3. Material Properties

In this research, only two types of materials were assumed, these being rock and concrete.

The constitutive behavior of rock domain and concrete in liners are assumed to be according to isotropic linear elasticity. Thus the Young's Modulii of concrete and rock are denoted by E_c and E_r, respectively, and Poisson's ratio of concrete and rock are denoted by ν_c and ν_r, respectively.

The effect of liner thickness on the stress and deformation behavior inside the rock surrounding the three elliptical tunnel geometries was first investigated for a fixed moduli ratio E_c/E_r of 10.0. The material properties selected to represent the assumed behavior of rock and concrete for the above analyses are as given in table 3.1(Rock properties after Selvadurai, 1979):

Table 3.1

Material	Young's Modulus E (kN/m^2)	Poisson's Ratio ν
Rock	0.21×10^7	0.30
Concrete	0.21×10^8	0.20

In order to investigate the effect of varying rock stiffness on the stress and deformation inside rock material, the Young's Modulus of rock material was then varied such that a realistic range of E_c/E_r ratios (varying from 5 to 100) was obtained.

3.4. Finite Element Programme

The analysis for this work is carried out by using the finite element analysis program (FEAP) originally developed by Professor R.L. Traylor, University of Berkely, California (Zienkiewiz,1977). The program was later expanded at the Asian Institute of Technology by Professor Worsak Kanok Nukulchai (1984). This program was modified and installed in a pentium micro-computer with 16 MB of RAM (Random Access Memory) at University of Moratuwa by Dr. U.G.A. Puswewala.

The program FEAP can be utilized to solve one, two and three dimentional finite element analysis problems which may be linear or non-liner. With appropriate modification it can be upgraded to solve transient problems.

The program is written in FORTRAN computer language; it follows a modular concept, by which flexibility to change or modify various modules of the program without affecting the rest of the program is allowed. This enables users to incorporate various additional features in the program in the form of new algorithms or element subroutines. Another feature of the program is the Macro programming language; under this, the various stages of a finite element analysis are performed by specifying a series of Macro commands. Each Macro command instructs the program to access a certain set of subroutines in order to perform a certain task.

The program can be basically divided into three parts as main program, system sub-routines and the element subroutine library. Main program controls the overall memory allocation and the start and end of the analysis. System sub-routine constitute the body of the finite element algorithms, and control the input (data) and the output (results of the program). Element subroutine library contains a number of element subroutines, each subroutine for a specific type of finite element. This arrangement allows the users to write their own element subroutines to solve their specific programs.

3.5. Finite Element Discretisation

The typical finite element meshes are shown in figure 3.6(elliptical tunnel with a/b = 1.156) figure 3.7(a/b=1.358) and figure 3.8(a/b=1.500) respectively. Four noded finite elements were used to discretise the material domains. Memory limitations of the personal computer used to analyse these problems meant that meshes could not be made much finer than shown in figures 3.6, 3.7 or 3.8.

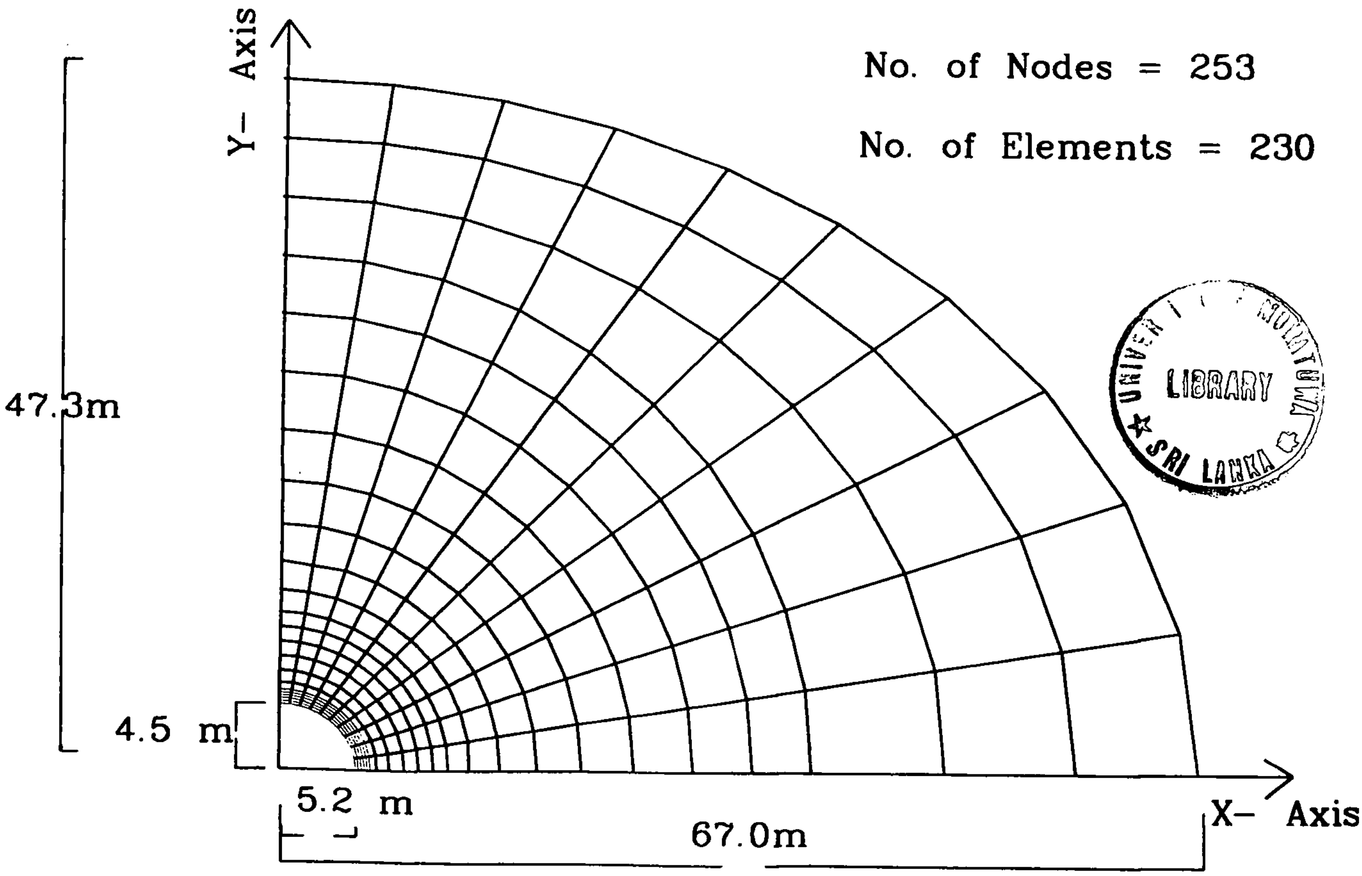

Figure 3.6 Finite element mesh for elliptical tunnel with a/b = 1.156

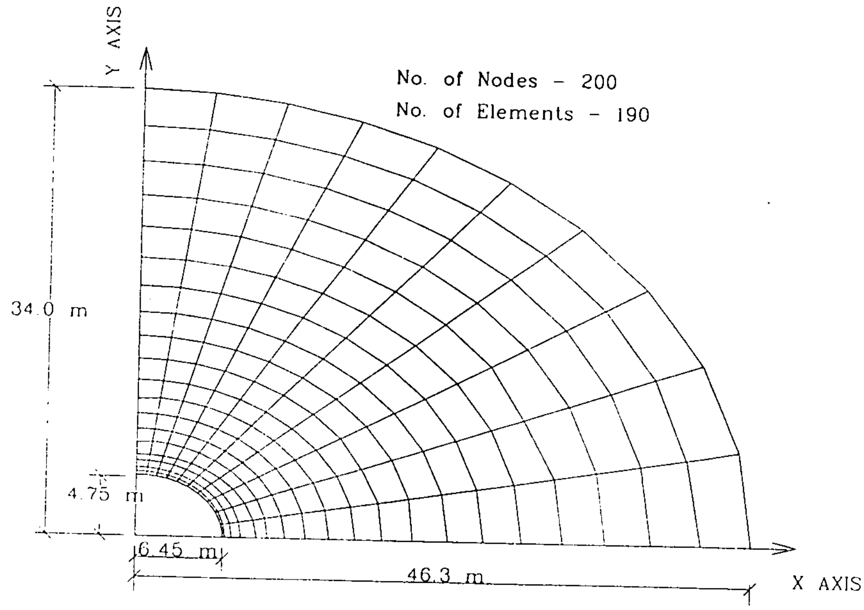

Figure 3.7 Finite element mesh for elliptical tunnel with a/b = 1.358

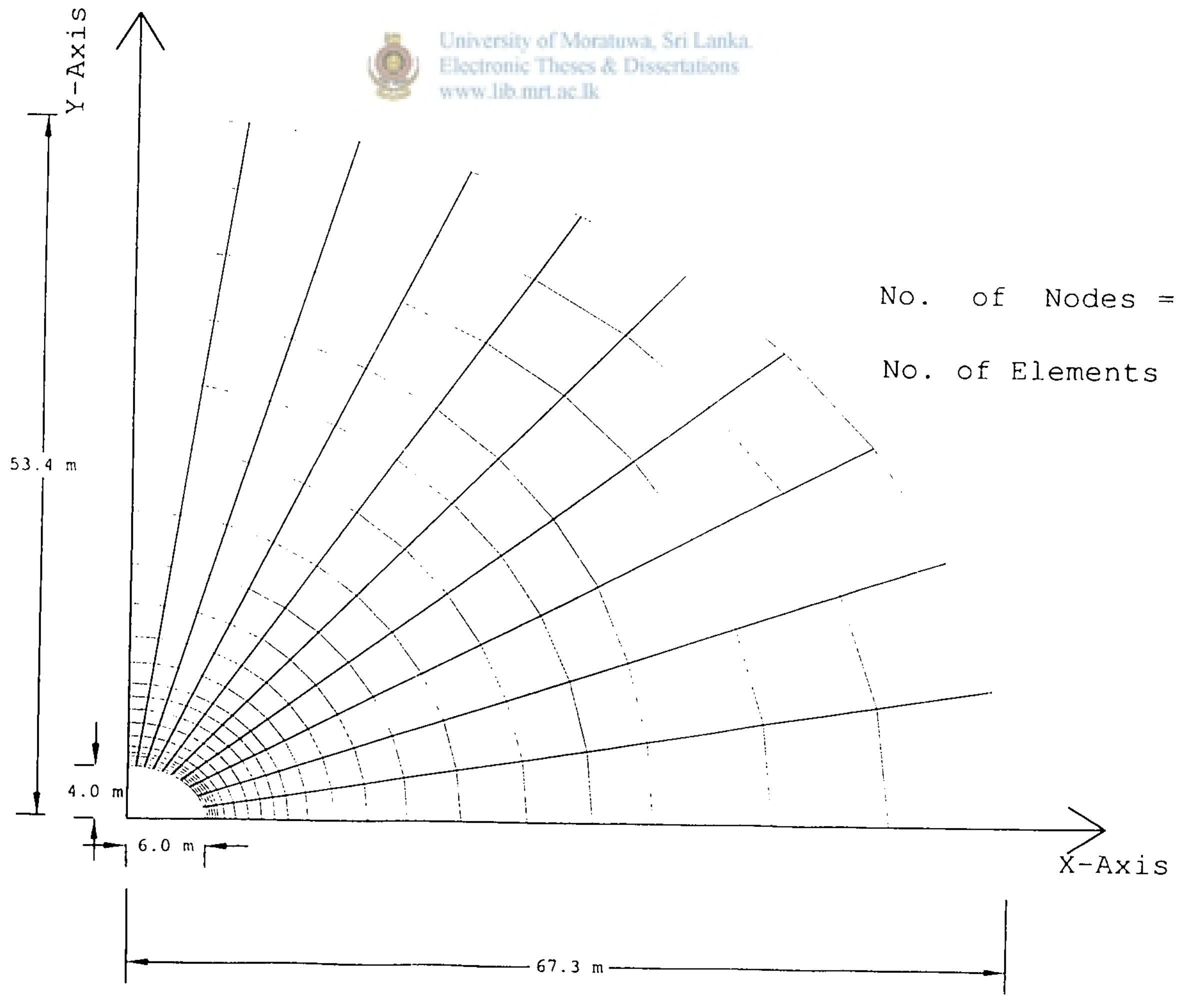

Figure 3.8 Finite element mesh for elliptical tunnel with a/b = 1.500

3.6. Boundary Conditions and Loadings

3.6.1. Loading Conditions

The loads in the domain are

1. Gravity Force
2. Fluid Pressure

Gravity force is not considered here. It is assumed that the rock domain has reached equilibrium under gravity, before the application of the hydraulic loading inside the tunnel.

Fluid pressure acts perpendicular to the surface of the openings. Equivalent nodal forces were computed and input into the computer program. Figure 3.9 shows the application of hydraulic pressure at nodal points

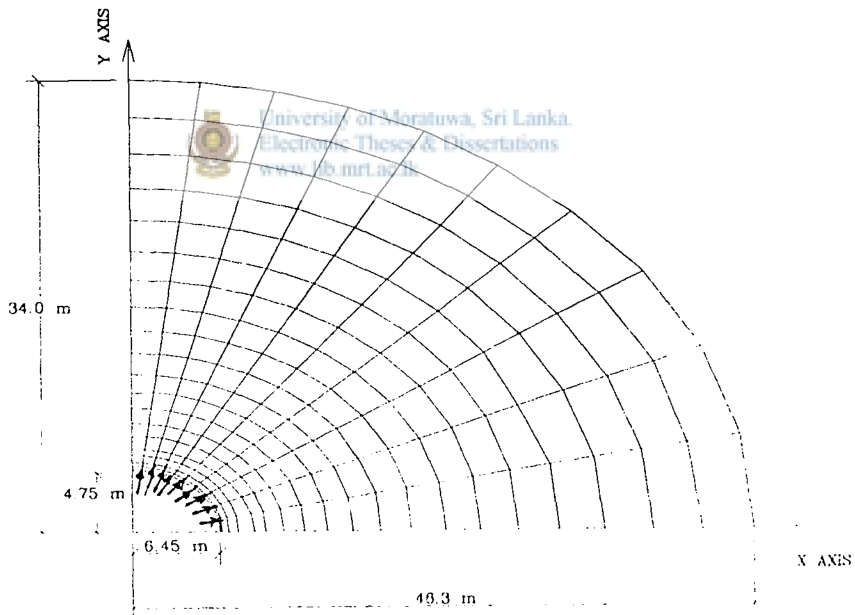

Figure 3.6 Tunnel section after introduction of fluid pressure

3.6.2. Boundary Conditions

Figure 3.10 shows the boundary conditions used for the analysis.

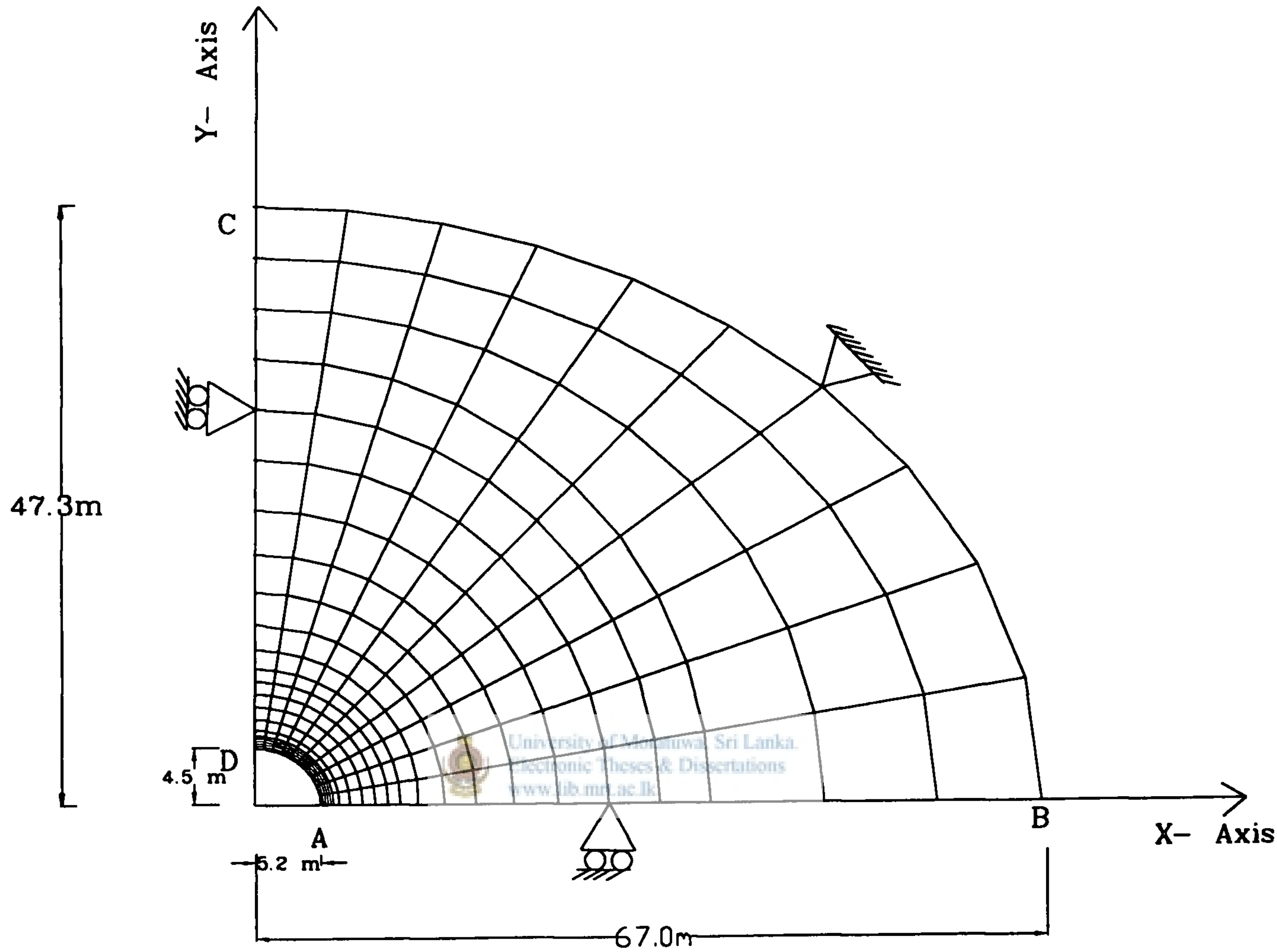

Figure 3.10 Tunnel Section With Boundary Conditions

AB- "y" Displacement is Fixed (line of symmetry)
BC- "x" and "y" Displacements are Fixed (the far boundary)
CD- "x" Displacement is Fixed (line of symmetry)
DA- "x" and "y" Displacements are Free (loading surface)

3.7. Verification of Finite Element Programme Using a Circular Tunnel

Analytical solution for a lined tunnel of a circular cross-section is given by Jaeger(1979). The finite element program FEAP was used to simulate a problem including circular tunnel geometry of selected dimension and parameter, and the comparison of numerical results from FEAP with analytical result of Jaeger(1979) is given in Appendix A.

CHAPTER 4.0

RESULTS FOR ELLIPTICAL TUNNEL a/b = 1.156

4.1. Influence of Liner Thickness on Stress and Deformation in Rock Around Tunnel

Principal stresses were investigated along three radial lines AB, CD and EF, shown in figure 4.1 radiating from the center of the tunnel. For the tunnel with a/b = 1.156, variation of the major principal stress along the radial line AB for different liner thicknesses is shown in figure 4.2, and the variation of the minor principal stress along the same line for different liner thicknesses is shown in figure 4.5. Corresponding results for the same tunnel along line CD are shown in figures 4.3 and 4.6, respectively. Figures 4.4 and 4.7 respectively, show the corresponding results for the same tunnel along line EF.

Figure 4.8 shows the circumferential line considered for analysis. Figure 4.9 shows the variation of major principal stress along an elliptical (circumferential) line of a shape similar to that of the tunnel opening, but at some distance inside the rock mass from the tunnel face, as the liner thickness is varied, for the tunnel with a/b = 1.156. The circumferential line along which the stresses shown in figure 4.9 are evaluated is similar to the line GH shown on figure 4.8.

For the elliptical tunnel with a/b = 1.156, influence of the concrete liner thickness on displacement at points inside the rock mass are illustrated by figures 4.10 and 4.11. figures 4.10 and 4.11 show displacements at points inside the rock mass located along an elliptical (circumferential) line GH, which is shown on the scaled diagram of 4.8.

Figure 4.2,4.3 & 4.4 show the variation of major principal stress along radical line AB,CD &EF respectively.

In the case of line AB (figure 4.2), for the tunnel a/b=1.156 major principal stress at a point inside the rock(element number 51) when there is no lining, which is 420.9kPa decreases by 18.34% when a liner of thickness of 0.2m is introduced. The corresponding reductions are 35.64% for a liner thickness of 0.4m thickness and 58.97% for a liner of 1.0m.

In the case of line CD (figure 4.3), for the tunnel a/b=1.156 major principal stress at a point inside the rock(element 56) reduce by 31.51% when a liner of thickness of 0.2m is introduced as compared to the stresses in the case of unlined tunnel. The corresponding reductions are 45.56% for a liner thickness of 0.4m thickness and 59.43% for a liner of 1.0m.

In the case of line EF (figure 4.4), for the tunnel a/b=1.156 major principal stress at a point inside the rock(element number 60) reduce by 40.10% when a liner of thickness of 0.2m is introduced as compared to the stresses in the case of unlined tunnel. The corresponding reductions are 54.33% for a liner thickness of 0.4m thickness and 73.75% for a liner of 1.0m.

The numerical results and the comparison of figures 4.2, 4.3 & 4.4 show that the line EF is the critical line along which maximum principal tensile stresses occurred.

Figures 4.5, 4.6 and 4.7 show the influence of concrete liner thickness on the compressive principal stress around the tunnel with *a/b* = 1.156. According to figure 4.5, the minor principal stress at a point inside the rock closure to point A reduces by 28.13% when a 0.2 m thick concrete is introduced to the originally unlined tunnel; this reduction is 39.73 for a 0.4 m thick liner and 52.32% for a 1.0 m thick liner. Figure 4.6 shows similar behavior of the minor principal stress along the line CD. Figure 4.7 shows that large percentage stress reductions occur in the case of the minor principal stress along line EF. This stress reduces at a point inside the rock closure to point E by 57.70% when a 0.2 m thick liner is introduced to the unlined tunnel; the corresponding reduction is 79.25% for a 0.4 m thick liner, and 98.46% for a 1.0 m thick liner.

Figures 4.9 & 4.10 shows the variation of major principal stress and minor principal stress along circumferential line GH respectively, which is in rock.

The major principal stress reduction is 18.34% when 0.2m liner is introduced as compared to the stress in the case of unlined tunnel closure to point A(Element number 51). Where as reduction is 35.64% at point closure to E when 0.2m liner is introduced as compared to the stress in the case of an unlined tunnel.

Figure 4.10 shows the minor principal stress variation along line GH. It also shows the same pattern of reduction as in the major principal stress mentioned above.

According to the results in figures 4.11 and 4.12 the percentage reduction of x-displacement and y-displacement over the rock domain varies with the location. Figure 4.11 shows relatively large percentage reductions in the x-displacement at the x-axis as the tunnel liner thickness is increased (this is 40.01% when a 0.2 m thick liner is introduced on the unlined tunnel; and about 83.86% for a 1.0 m thick liner).

Figures 4.13.4.14 & 4.15 are shows the variation of major principal stress with the introduction of concrete liner on three elements close to point A,C & E respectively.

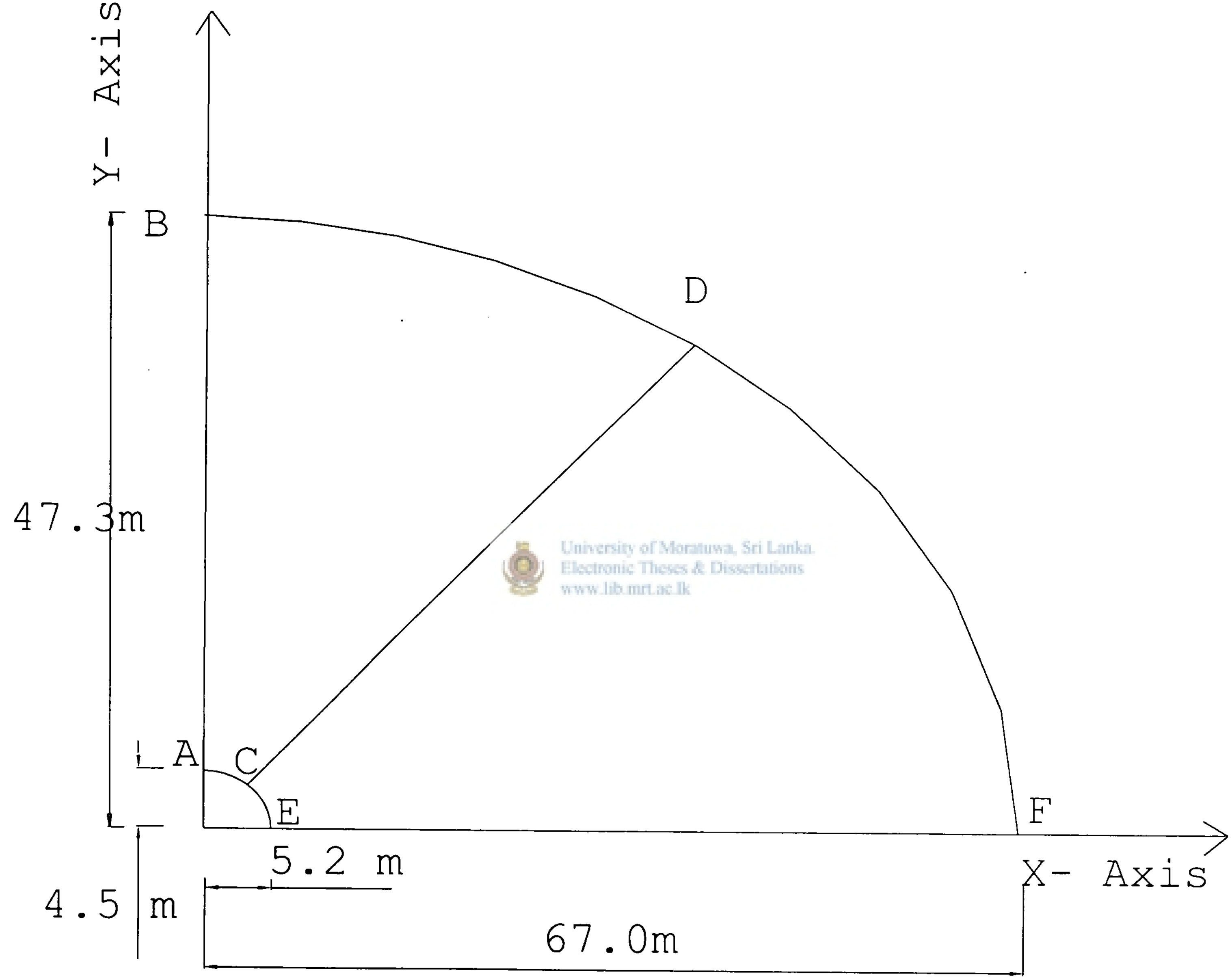

Figure 4.1 Radial lines (For elliptical tunnel-1, a/b = 1.156)

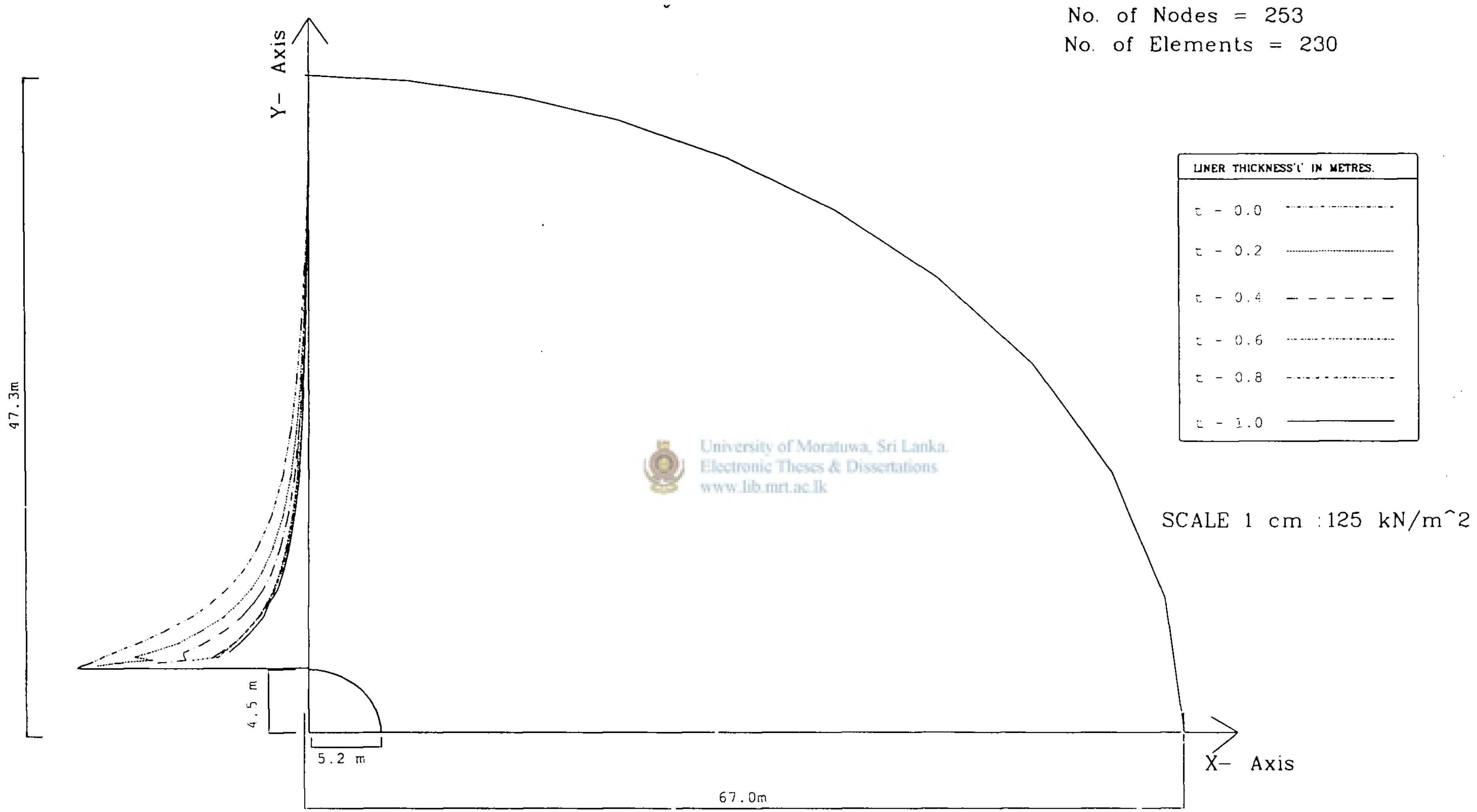

Figure 4.2 Variation of major principal stress along radial line "AB"
(For elliptical tunnel-1, a/b = 1.156)

VARIATION OF MAJOR PRINCIPAL STRESS ALONG RADIAL LINE "AB"
(FOR ELLIPTICAL TUNNEL-2, a/b = 1.156)

ELEMENT NUMBER	MAJOR PRINCIPAL STRESSx10^3 (kN/m^2)						
	LINER THICKNESS (m)						
	t = 0.0	t = 0.2	t = 0.4	t = 0.6	t = 0.8	t =1.0	
1	0.4999	6.4820	4.8740	3.1910	3.1850	2.7730	LINER ELEMENTS
11	0.4914	0.4568	4.8580	3.1370	0.3169	2.7840	
21	0.4712	0.4169	0.3281	3.0140	3.1270	2.7600	
31	0.3836	0.3352	0.2639	0.1520	2.5560	2.1630	
41	0.4457	0.3678	0.2689	0.1946	0.2065	2.6790	
51	0.4209	0.3437	0.2709	0.1840	0.1910	0.1727	
61	0.3690	0.2874	0.2256	0.1603	0.1623	0.1496	
71	0.3099	0.2315	0.1824	0.1335	0.1326	0.1220	
81	0.2526	0.1835	0.1446	0.1083	0.1059	0.0972	
91	0.2115	0.1510	0.1191	0.0907	0.0878	0.0850	
101	0.1770	0.1250	0.0987	0.0761	0.0731	0.0669	
111	0.1140	0.1008	0.0798	0.0621	0.0593	0.0543	
121	0.1107	0.0769	0.0610	0.0480	0.0455	0.0417	
131	0.0804	0.0555	0.0441	0.0351	0.0331	0.0303	
141	0.0565	0.0383	0.0310	0.0249	0.0234	0.0214	
151	0.0387	0.0265	0.0212	0.0712	0.0161	0.0148	
161	0.0253	0.0173	0.0139	0.0114	0.0107	0.0098	
171	0.0159	0.0109	0.0088	0.0073	0.0068	0.0062	
181	0.0092	0.0063	0.0051	0.0043	0.0040	0.0037	
191	0.0039	0.0027	0.0022	0.0018	0.0017	0.0016	
201	0.0010	0.0007	0.0005	0.0003	0.0002	0.0002	
211	0.0020	-0.0139	-0.0011	-0.0008	-0.0007	-0.0007	

Table 4.1

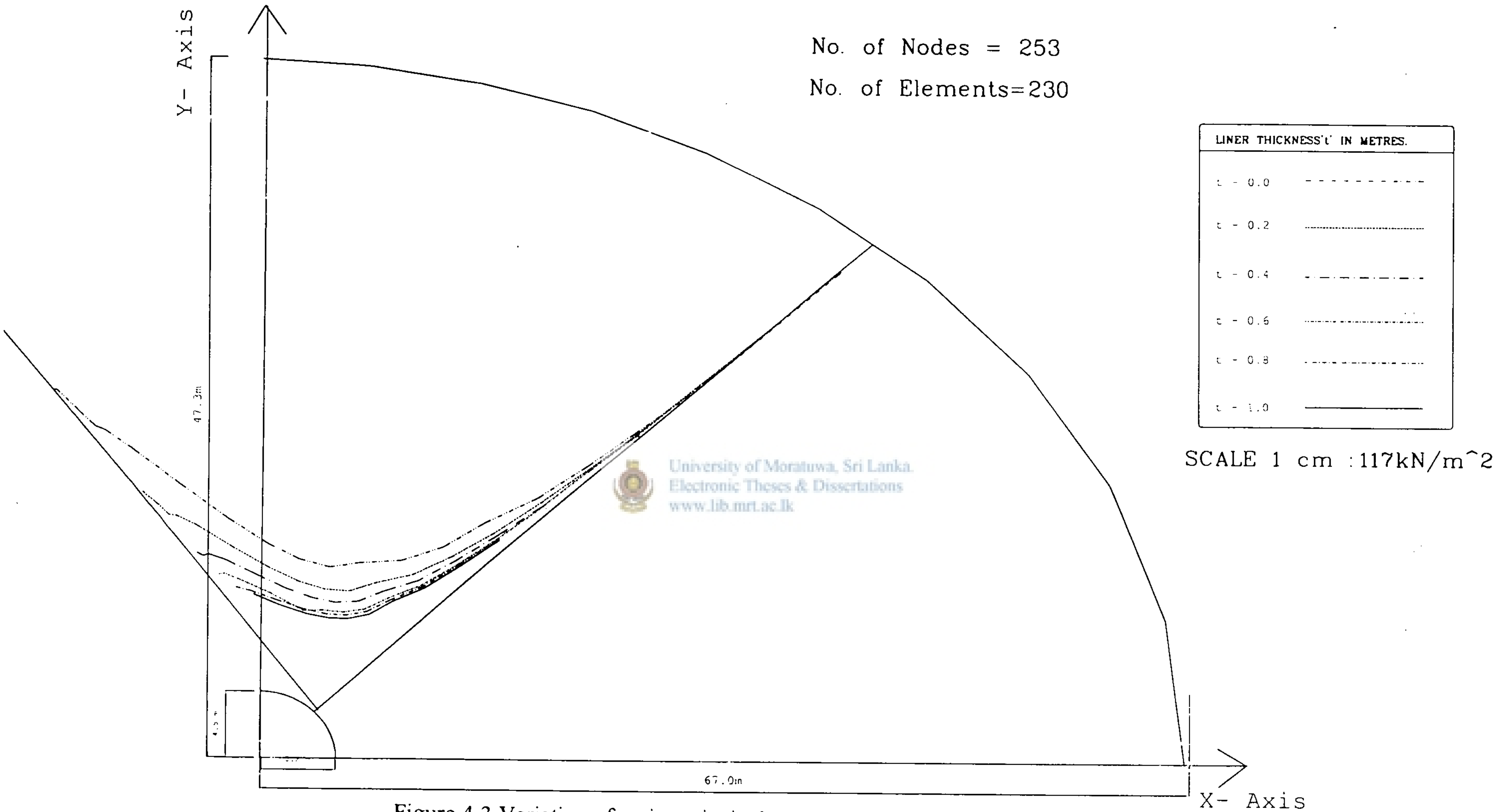

Figure 4.3 Variation of major principal stress along radial line "CD"
(For elliptical tunnel-1, a/b = 1.156)

VARIATION OF MAJOR PRINCIPAL STRESS ALONG RADIAL LINE "CD"
(FOR ELLIPTICAL TUNNEL-2, a/b = 1.156)

ELEMENT NUMBER	MAJOR PRINCIPAL STRESSx10^3 (kN/m^2)						
	LINER THICKNESS (m)						
	t = 0.0	t = 0.2	t = 0.4	t = 0.6	t = 0.8	t =1.0	
6	0.8419	7.8140	5.5030	4.0300	3.6300	3.1300	LINER ELEMENTS
16	0.8378	0.5621	5.0482	4.2230	3.7690	3.2830	
26	0.7772	0.5275	0.3975	4.3780	3.8920	3.4350	
36	0.7279	0.4909	0.3830	0.3350	3.9210	3.5120	
46	0.7105	0.4805	0.3802	0.3296	0.2938	3.7070	
56	0.6402	0.4385	0.3485	0.2936	0.2678	0.2597	
66	0.5236	0.3593	0.2893	0.2390	0.2219	0.2079	
76	0.4089	0.2818	0.2273	0.1687	0.1741	0.1610	
86	0.3174	0.2191	0.1767	0.1447	0.1349	0.1243	
96	0.2519	0.1740	0.1401	0.1146	0.1067	0.0981	
106	0.2004	0.1381	0.1110	0.0906	0.0843	0.0773	
116	0.1677	0.1158	0.0931	0.0760	0.0707	0.0659	
126	0.1169	0.0802	0.0644	0.0527	0.0489	0.0448	
136	0.0830	0.0570	0.0457	0.0372	0.0345	0.0316	
146	0.0055	0.0377	0.0302	0.0245	0.0227	0.0208	
156	0.0359	0.0246	0.0169	0.0159	0.0147	0.0134	
166	0.0218	0.0149	0.0118	0.0095	0.0088	0.0080	
176	0.0128	0.0088	0.0069	0.0055	0.0051	0.0046	
186	0.0070	0.0048	0.0037	0.0029	0.0027	0.0024	
196	0.0021	0.0015	0.0011	0.0008	0.0008	0.0006	
206	-0.0013	-0.0009	-0.0007	-0.0006	0.0005	-0.0005	
216	-0.0033	-0.0022	-0.0017	-0.0132	-0.0120	-0.0011	

Table 4.2

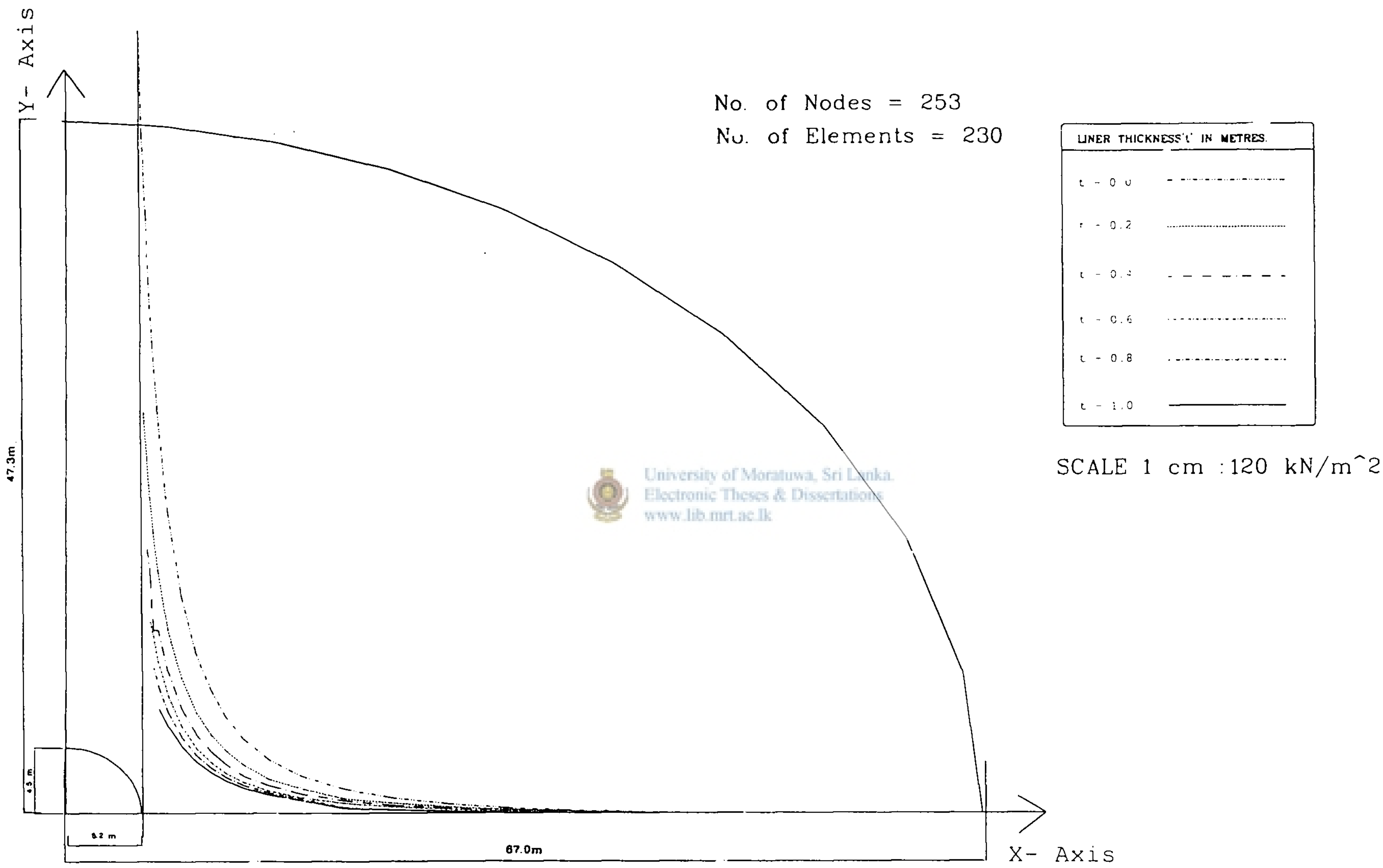

Figure 4.4 Variation of major principal stress along radial line "EF"
(For elliptical tunnel-1, a/b = 1.156)

VARIATION OF MAJOR PRINCIPAL STRESS ALONG RADIAL LINE "EF"
(FOR ELLIPTICAL TUNNEL-2, a/b = 1.156)

ELEMENT NUMBER	MAJOR PRINCIPAL STRESS$\times 10^3$ (kN/m^2)					
	LINER THICKNESS (m)					
	t = 0.0	t = 0.2	t = 0.4	t = 0.6	t = 0.8	t = 1.0
10	1.6050	10.9200	8.7150	7.6750	6.8050	6.2020
20	1.3960	0.8186	6.7370	6.0250	5.4390	5.0240
30	1.2270	0.7210	0.5380	4.5710	4.2910	4.0600
40	1.0890	0.6421	0.4820	0.3916	3.1970	3.1770
50	0.9618	0.5747	0.4374	0.3611	0.2994	2.3540
60	0.8195	0.4909	0.3743	0.3095	0.2584	0.2151
70	0.6184	0.3766	0.2905	0.2416	0.2071	0.1786
80	0.4464	0.2768	0.2151	0.1786	0.1563	0.1378
90	0.3275	0.2067	0.1615	0.1334	0.1184	0.1056
100	0.2530	0.1619	0.1268	0.1043	0.0933	0.0837
110	0.1992	0.1289	0.1011	0.0828	0.0746	0.0671
120	0.1535	0.1002	0.0786	0.0640	0.0579	0.0522
130	0.1104	0.0727	0.0571	0.0462	0.0420	0.0379
140	0.0761	0.0505	0.0396	0.0318	0.0290	0.0262
150	0.0502	0.0335	0.0262	0.0208	0.0191	0.0172
160	0.0319	0.0213	0.0166	0.0131	0.0120	0.0101
170	0.0191	0.0128	0.0099	0.0077	0.0070	0.0063
180	0.0108	0.0073	0.0055	0.0042	0.0038	0.0034
190	0.0056	0.0038	0.0028	0.0021	0.0019	0.0016
200	0.0011	0.0077	0.0005	0.0003	0.0002	0.0002
210	-0.0020	-0.0014	-0.0012	-0.0008	-0.0008	-0.0007
220	-0.0027	-0.0013	-0.0013	-0.0010	-0.0009	-0.0008

LINER ELEMENTS

Table 4.3

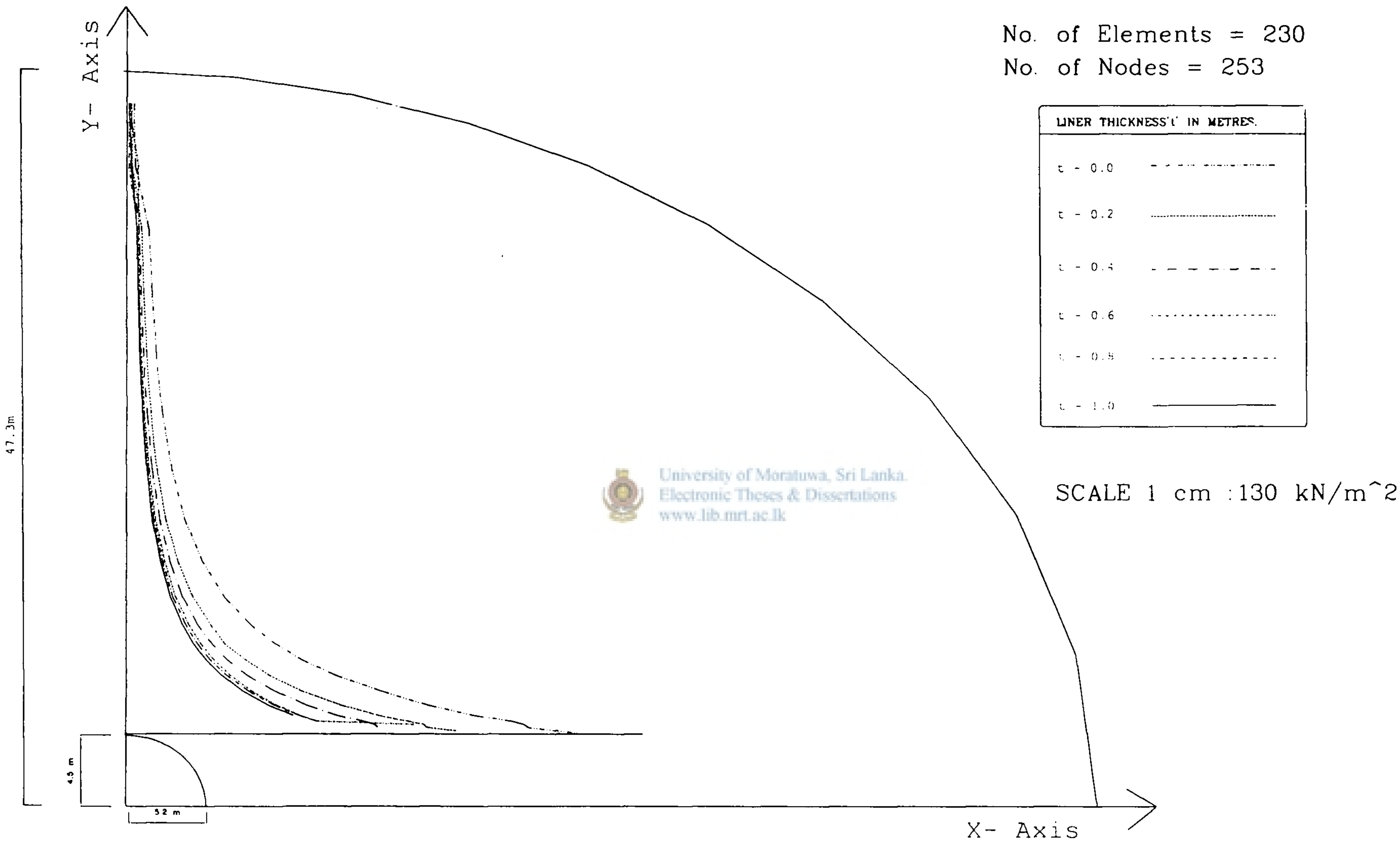

Figure 4.5 Variation of minor principal stress along radial line "AB"
(For elliptical tunnel-1, a/b = 1.156)

VARIATION OF MINOR PRINCIPAL STRESS ALONG RADIAL LINE "AB"
(FOR ELLIPTICAL TUNNEL-2, a/b = 1.156)

ELEMENT NUMBER	MINOR PRINCIPAL STRESSx(-1X10^3) (kN/m^2)					
	LINER THICKNESS (m)					
	t = 0.0	t = 0.2	t = 0.4	t = 0.6	t = 0.8	t =1.0
1	0.8843	0.8716	0.8697	0.8689	0.8707	0.8814
11	0.8352	0.6426	0.5798	0.6831	0.6743	0.7003
21	0.7821	0.5850	0.4900	0.4866	0.4657	0.5221
31	1.0440	0.7785	0.6427	0.5610	0.1633	1.7720
41	0.7503	0.5492	0.4606	0.3721	0.3744	0.4381
51	0.6872	0.4939	0.4142	0.3404	0.3388	0.3276
61	0.5891	0.4206	0.3530	0.2957	0.2909	0.2790
71	0.4951	0.3415	0.2896	0.2442	0.2375	0.2263
81	0.4086	0.2788	0.2346	0.2021	0.1948	0.1850
91	0.3426	0.2327	0.1960	0.1701	0.1629	0.1544
101	0.2923	0.1981	0.1671	0.1457	0.1389	0.1314
111	0.2423	0.1639	0.1384	0.1212	0.1150	0.1087
121	0.1907	0.1296	0.1096	0.0963	0.0909	0.0858
131	0.1480	0.1001	0.0847	0.0746	0.0702	0.0661
141	0.1134	0.0767	0.0649	0.0572	0.0537	0.0505
151	0.0881	0.0596	0.0504	0.0444	0.0416	0.0391
161	0.0697	0.0472	0.0399	0.0351	0.0329	0.0308
171	0.0573	0.0388	0.0328	0.0288	0.0269	0.0253
181	0.0492	0.0334	0.0281	0.0247	0.0231	0.0216
191	0.0435	0.0295	0.0249	0.0281	0.0204	0.0192
200	0.0171	0.0117	0.0082	0.0526	0.0048	0.0396
210	0.0143	0.0098	0.0070	0.0046	0.0042	0.0035

LINER ELEMENTS

Table 4.4

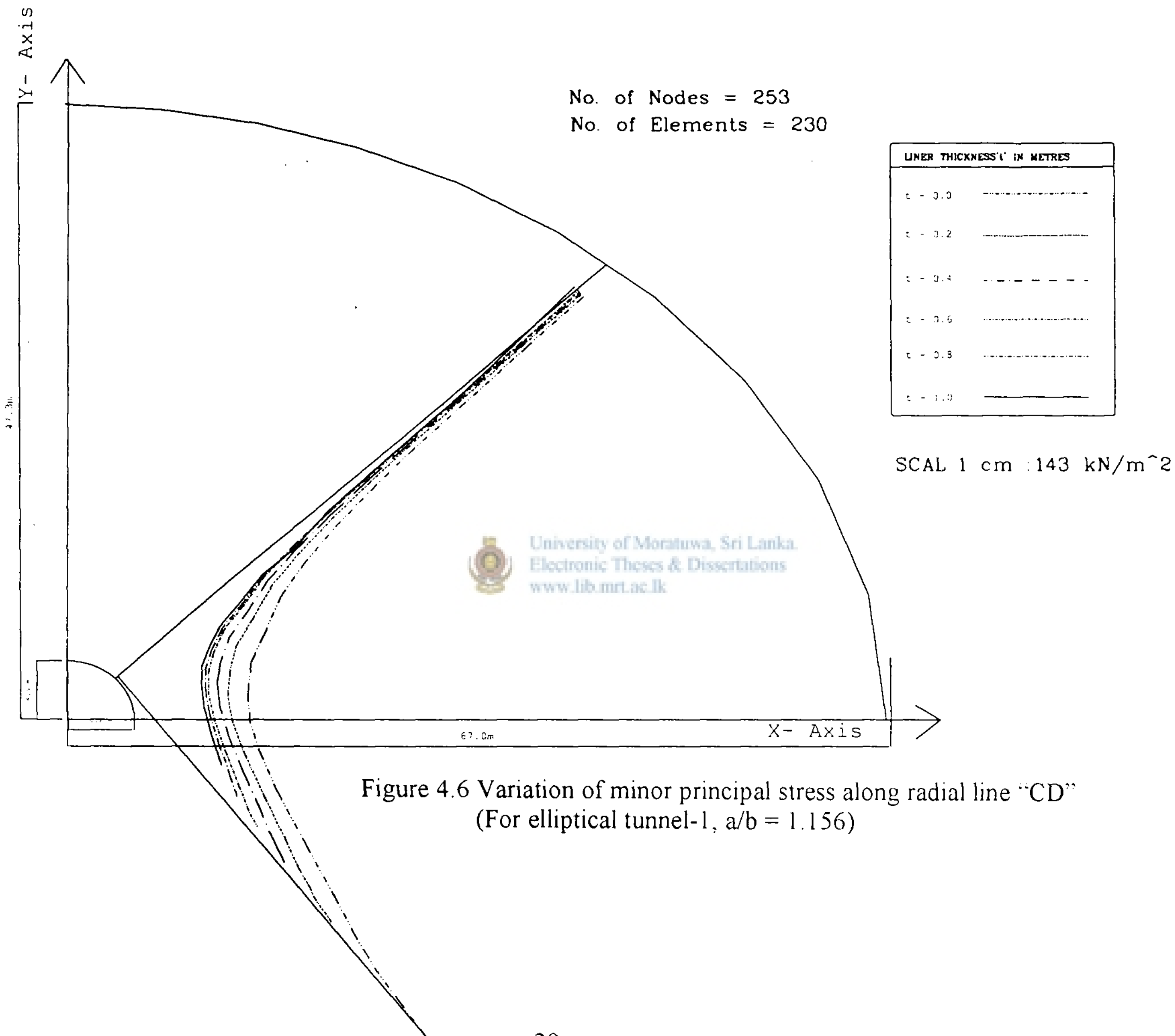

Figure 4.6 Variation of minor principal stress along radial line "CD"
(For elliptical tunnel-1, a/b = 1.156)

VARIATION OF MINOR PRINCIPAL STRESS ALONG RADIAL LINE "CD"
(FOR ELLIPTICAL TUNNEL-2, a/b = 1.156)

ELEMENT NUMBER	MINOR PRINCIPAL STRESSx($-1X10^3$) (kN/m^2)					
	LINER THICKNESS (m)					
	t = 0.0	t = 0.2	t = 0.4	t = 0.6	t = 0.8	t =1.0
6	1.0850	0.7854	0.8850	0.9362	0.9583	0.9813
16	0.9754	0.7463	0.7886	0.8078	0.8300	0.8445
26	0.8958	0.6783	0.5752	0.5255	0.5930	0.6218
36	0.8535	0.6600	0.5525	0.4731	0.5859	0.5866
46	0.7975	0.6058	0.5114	0.4286	0.3897	0.3768
56	0.7122	0.5381	0.4502	0.3748	0.3426	0.3126
66	0.5767	0.4319	0.3581	0.2949	0.2715	0.2461
76	0.4425	0.3268	0.2683	0.2191	0.2024	0.1836
86	0.3437	0.2506	0.2041	0.1657	0.1531	0.1388
96	0.2738	0.1973	0.1597	0.1290	0.1192	0.1081
106	0.2246	0.1604	0.1292	0.1041	0.0962	0.0872
116	0.1746	0.1234	0.0983	0.0784	0.0723	0.0653
126	0.1440	0.1013	0.0810	0.0656	0.0601	0.0545
136	0.1033	0.0719	0.0571	0.0456	0.0421	0.0381
146	0.0780	0.0540	0.0428	0.0341	0.0316	0.0386
156	0.0591	0.0407	0.0322	0.0256	0.0237	0.0214
166	0.0460	0.0316	0.0249	0.0197	0.0183	0.0165
176	0.0372	0.0255	0.0200	0.0158	0.0146	0.0132
186	0.0315	0.0215	0.0169	0.0133	0.0123	0.0112
196	0.0264	0.0181	0.0141	0.0122	0.0103	0.0931
206	0.0225	0.0154	0.0121	0.0951	0.0088	-0.0080
216	0.0204	0.0139	0.0109	0.0864	0.0080	-0.0072

LINER ELEMENTS

Table 4.5

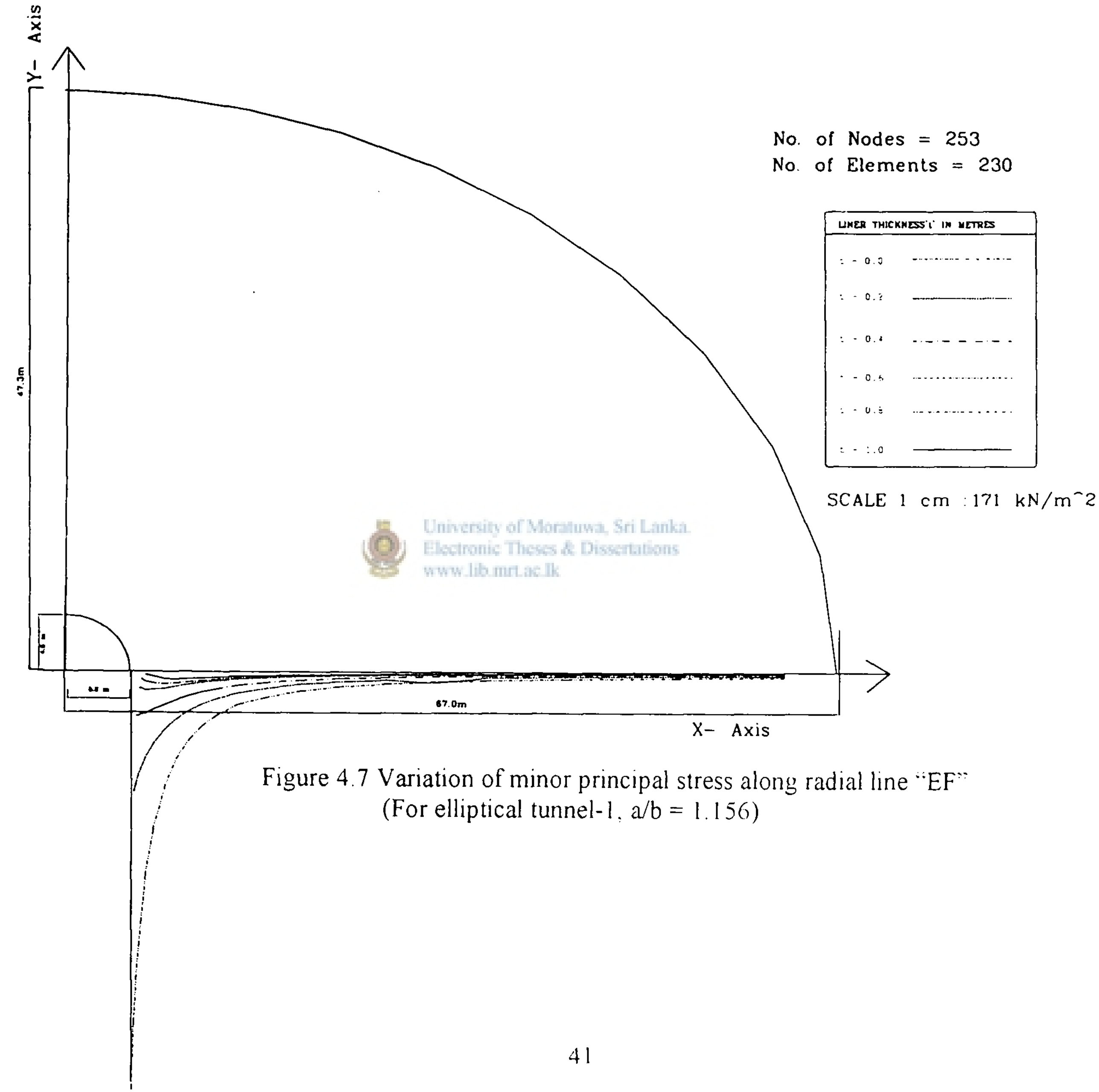

Figure 4.7 Variation of minor principal stress along radial line "EF"
(For elliptical tunnel-1, a/b = 1.156)

VARIATION OF MINOR PRINCIPAL STRESS ALONG RADIAL LINE "EF"
(FOR ELLIPTICAL TUNNEL-2, a/b = 1.156)

ELEMENT NUMBER	MINOR PRINCIPAL STRESSx(-1X10^3) (kN/m^2)					
	LINER THICKNESS (m)					
	t = 0.0	t = 0.2	t = 0.4	t = 0.6	t = 0.8	t =1.0
10	1.0210	0.4374	0.5375	0.6097	0.6674	0.7094
20	0.8463	0.2934	0.2371	0.3445	0.4156	0.4606
30	0.7394	0.2694	0.1086	0.1534	0.2413	0.2936
40	0.6619	0.2518	0.1086	0.0417	0.1270	0.1858
50	0.6055	0.2359	0.1040	0.0405	0.0177	0.0136
60	0.4984	0.2108	0.1034	0.0456	0.0241	0.0077
70	0.3824	0.1761	0.0927	0.0437	0.0279	0.0116
80	0.2787	0.1424	0.0810	0.0412	0.0304	0.0182
90	0.2092	0.1151	0.0684	0.0358	0.0282	0.0188
100	0.1653	0.0955	0.0582	0.0309	0.0252	0.0176
110	0.1339	0.0802	0.0498	0.0267	0.0223	0.0159
120	0.1071	0.0662	0.0419	0.0227	0.0193	0.0141
130	0.0819	0.0521	0.0334	0.0183	0.0158	0.0117
140	0.0621	0.0405	0.0264	0.0147	0.0129	0.0097
150	0.0470	0.0312	0.0206	0.0116	0.0103	0.0079
160	0.0363	0.0244	0.0163	0.0094	0.0084	0.0065
170	0.0288	0.0195	0.0132	0.0078	0.0067	0.0055
180	0.0238	0.0262	0.0111	0.0067	0.0061	0.0049
190	0.0205	0.0140	0.0097	0.0060	0.0054	0.0044
200	0.0171	0.0117	0.0082	0.0053	0.0048	0.0040
210	0.0143	0.0098	0.0070	0.0046	0.0042	0.0035
220	0.0122	0.0083	0.0060	0.0040	0.0037	0.0031

LINER ELEMENTS

Table 4.6

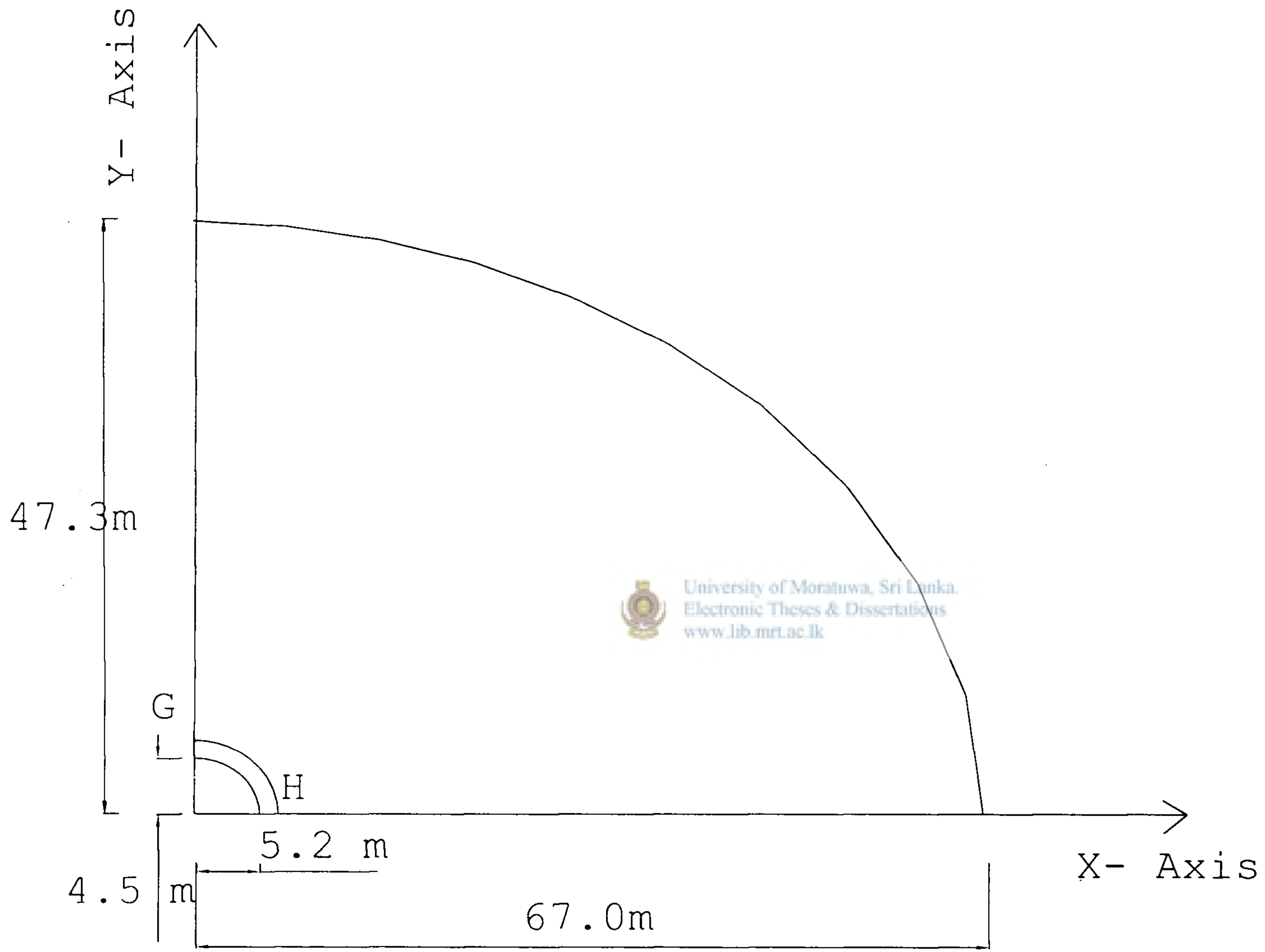

Figure 4.8 Circumferential lines (For elliptical tunnel-1, a/b = 1.156)

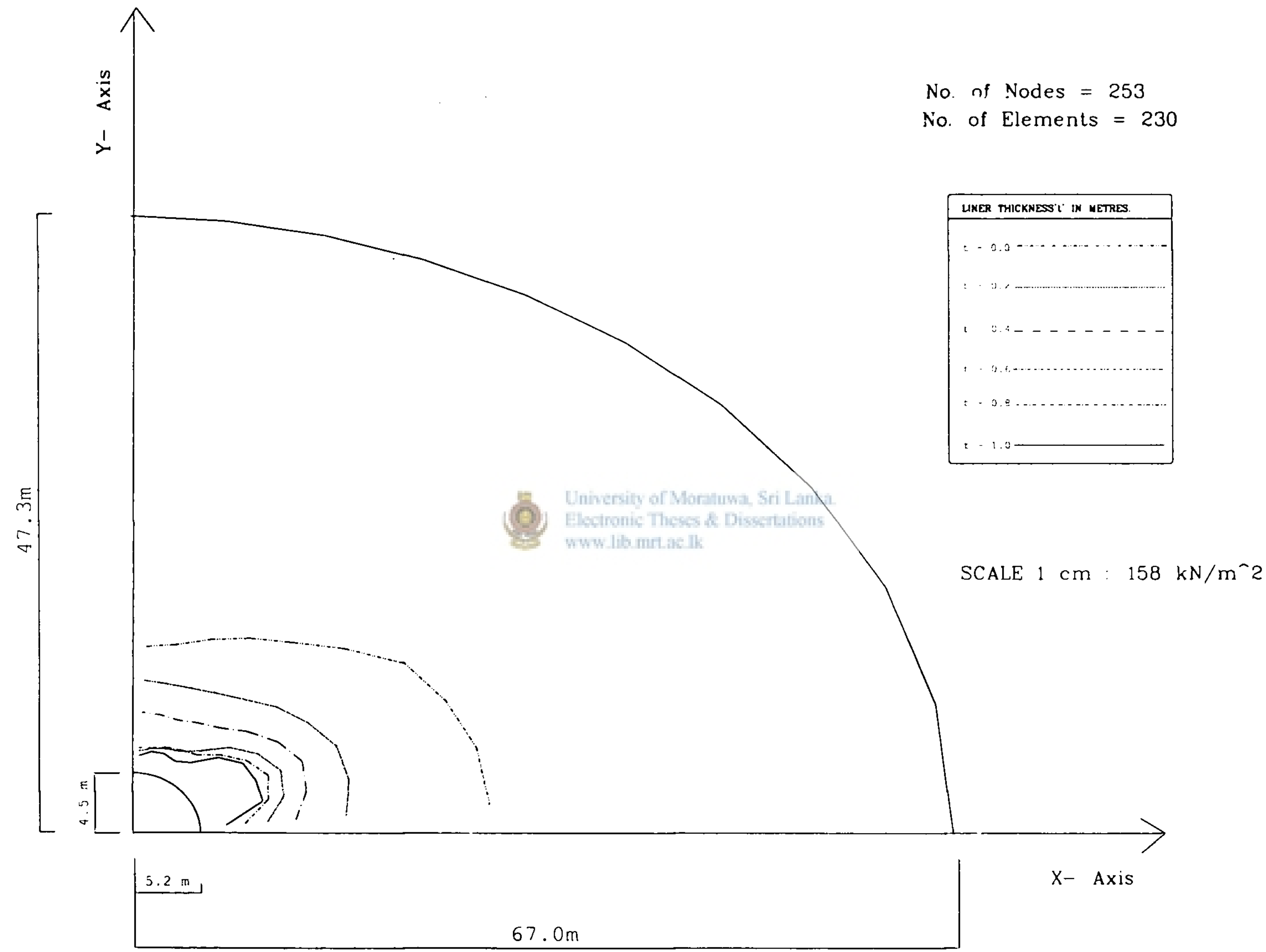

Figure 4.9 Variation of major principal stress along circumferential line "GH"
(For elliptical tunnel-1, a/b = 1.156)

VARIATION OF MAJOR PRINCIPAL STRESS ALONG CIRCUMFERENTIAL LINE "GH"
(FOR ELLIPTICAL TUNNEL-2, a/b = 1.156)

ELEMENT NUMBER	MAJOR PRINCIPAL STRESSx10^3 (kN/m^2)					
	LINER THICKNESS (m)					
	t = 0.0	t = 0.2	t = 0.4	t = 0.6	t = 0.8	t =1.0
51	0.4209	0.3437	0.2709	0.1840	0.1910	0.1727
52	0.4359	0.3443	0.2718	0.1929	0.1948	0.1867
53	0.4718	0.3517	0.2729	0.2027	0.2068	0.1916
54	0.5152	0.3681	0.2886	0.2128	0.2161	0.1876
55	0.5652	0.3945	0.3087	0.2409	0.2290	0.2060
56	0.6402	0.4358	0.3485	0.2936	0.2678	0.2597
57	0.7318	0.4730	0.3908	0.3385	0.3091	0.2980
58	0.7764	0.5081	0.4217	0.3684	0.3376	0.3072
59	0.8105	0.5115	0.4103	0.3557	0.3188	0.3065
60	0.8195	0.4909	0.3743	0.3095	0.2584	0.2151

Table 4.7

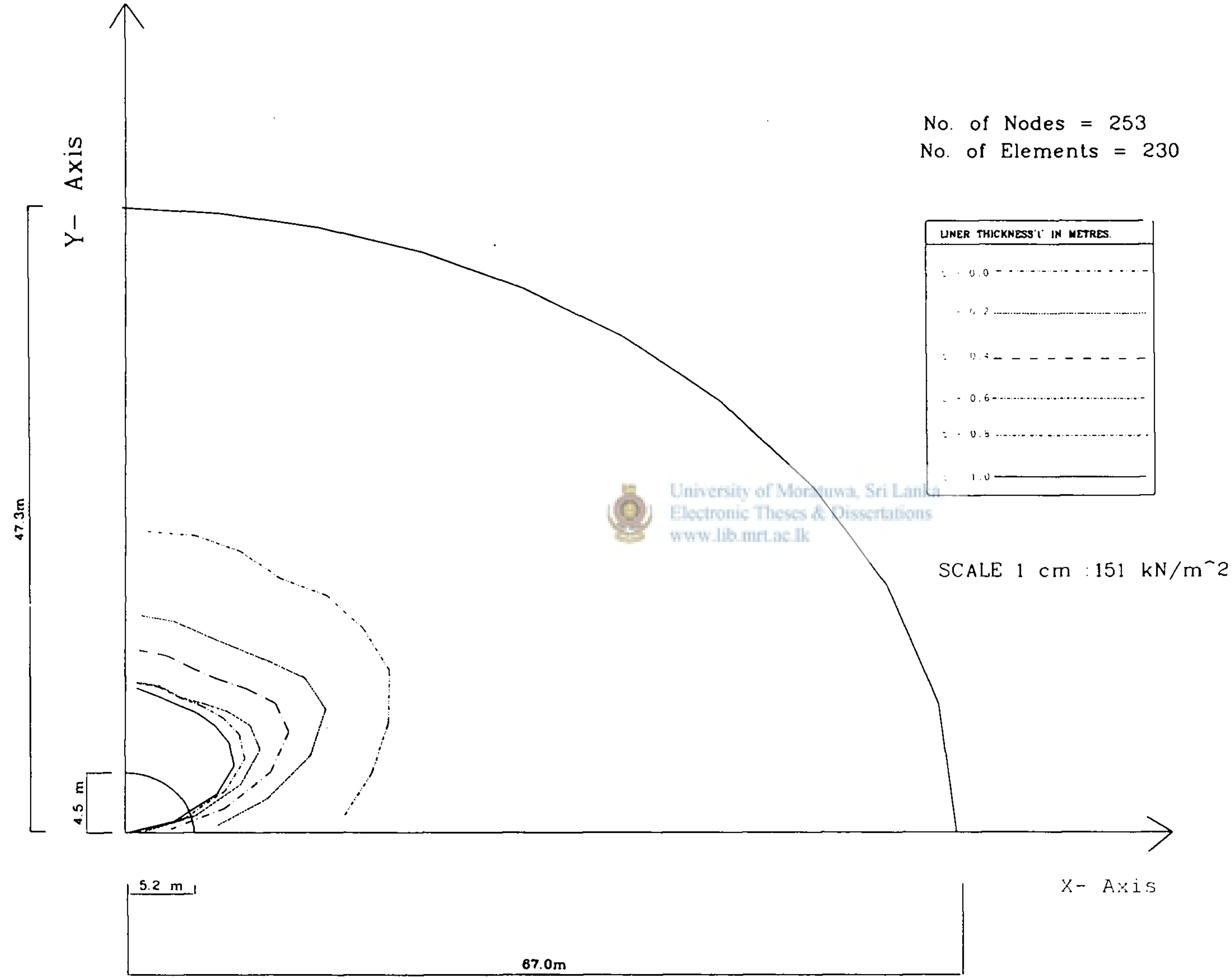

Figure 4.10 Variation of minor principal stress along circumferential line "GH"
(For elliptical tunnel-1, a/b = 1.156)

VARIATION OF MINOR PRINCIPAL STRESS ALONG CIRCUMFERENTIAL LINE "GH"
(FOR ELLIPTICAL TUNNEL-2, a/b = 1.156)

ELEMENT NUMBER	MINOR PRINCIPAL STRESSx($-1X10^3$) (kN/m^2)					
	LINER THICKNESS (m)					
	t = 0.0	t = 0.2	t = 0.4	t = 0.6	t = 0.8	t =1.0
51	0.6872	0.4939	0.4142	0.3404	0.3388	0.3276
52	0.6945	0.4925	0.4123	0.3412	0.3379	0.3174
53	0.6922	0.4835	0.4019	0.3313	0.3298	0.3134
54	0.6779	0.4897	0.4060	0.3421	0.3355	0.3162
55	0.7084	0.5081	0.4272	0.3603	0.3427	0.3174
56	0.7122	0.5381	0.4504	0.3748	0.3426	0.3126
57	0.7030	0.5350	0.4368	0.3598	0.3187	0.2899
58	0.6452	0.4558	0.3568	0.2835	0.2454	0.2244
59	0.5732	0.3336	0.2311	0.1663	0.1399	0.1139
60	0.4984	0.2108	0.1034	0.0456	0.0241	0.0077

Table 4.8

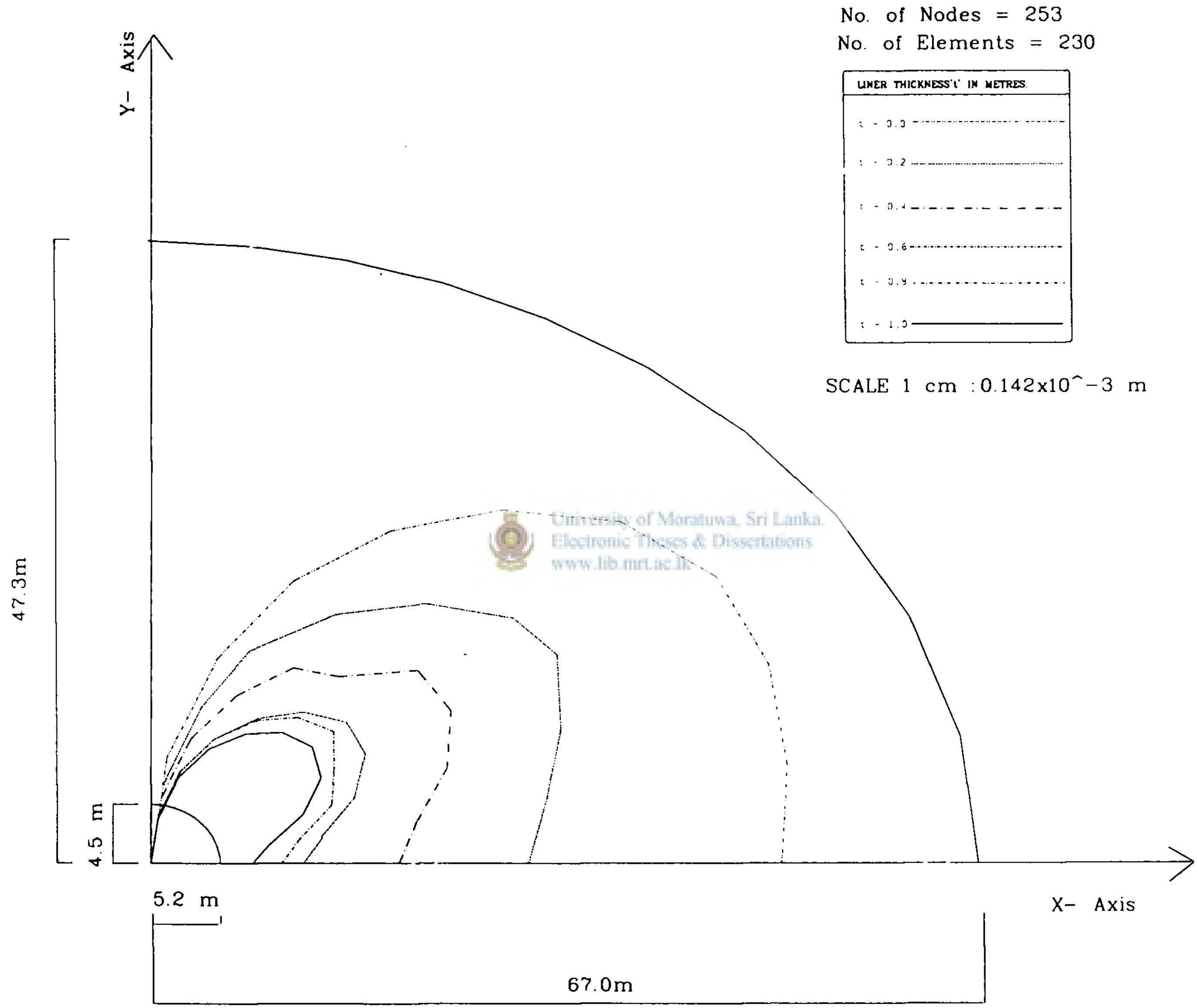

Figure 4.11 Variation of "x" displacement along circumferential line "GH"
(For elliptical tunnel-1, a/b = 1.156)

VARIATION OF "X' DISPLACEMENT ALONG CIRCUMFERENTIAL LINE "GH"
(FOR ELLIPTICAL TUNNEL-2, a/b = 1.156)

NODE NUMBER	"X' DISPLACEMENT X 10^{-3} (m)					
	LINER THICKNESS (m)					
	t = 0.0	t = 0.2	t = 0.4	t = 0.6	t = 0.8	t =1.0
67	0.0000	0.0000	0.0000	0.0000	0.0000	0.0000
68	0.2452	0.1895	0.1518	0.1111	0.1124	0.1047
69	0.4907	0.3751	0.2996	0.2202	0.2216	0.2052
70	0.7205	0.5434	0.4316	0.3184	0.3182	0.2935
71	0.9324	0.6986	0.5518	0.4082	0.4026	0.3660
72	1.1340	0.8465	0.6036	0.4889	0.4712	0.4221
73	1.3180	0.9735	0.7500	0.5482	0.5124	0.4525
74	1.4360	1.0220	0.7646	0.5472	0.4964	0.4324
75	1.4690	0.9851	0.7061	0.4838	0.4290	0.3606
76	1.4560	0.9032	0.6101	0.3897	0.3376	0.2702
77	1.4240	0.8542	0.5615	0.3446	0.2951	0.2299

Table 4.9

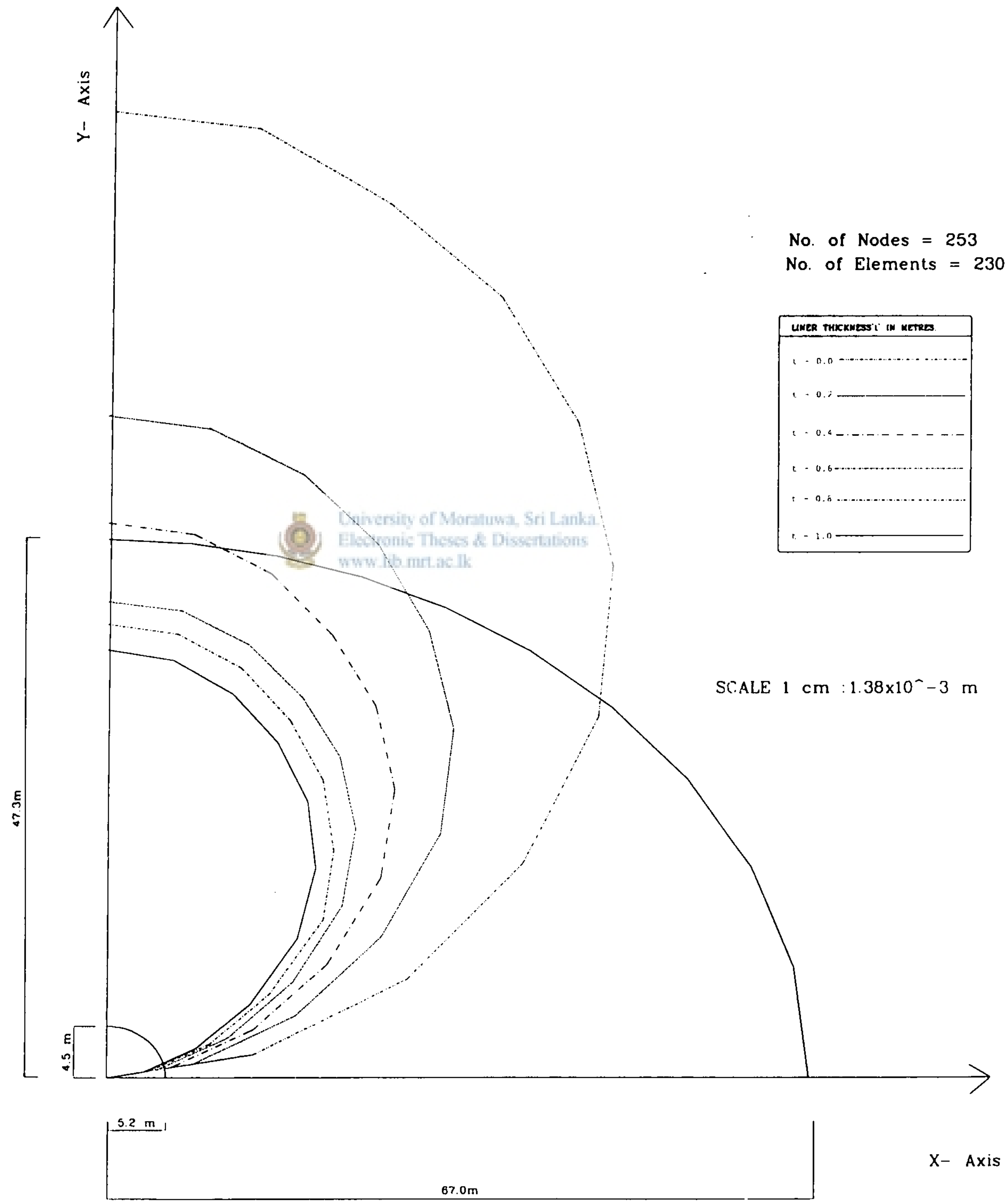

Figure 4.12 Variation of "y" displacement along circumferential line "GH"
(For elliptical tunnel-1, a/b = 1.156)

VARIATION OF "Y' DISPLACEMENT ALONG CIRCUMFERENTIAL LINE "GH"
(FOR ELLIPTICAL TUNNEL-2, a/b = 1.156)

NODE NUMBER	"Y" DISPLACEMENT X 10^{-3} (m)					
	LINER THICKNESS (m)					
	t = 0.0	t = 0.2	t = 0.4	t = 0.6	t = 0.8	t =1.0
67	2.5480	1.7460	1.4630	1.2560	1.1970	1.1300
68	2.5330	1.7330	1.4510	1.2480	1.1860	1.1160
69	2.4210	1.6730	1.3980	1.2030	1.1390	1.0670
70	2.3100	1.5790	1.3120	1.1320	1.0630	0.9944
71	2.1370	1.4570	1.2130	1.0490	0.9730	0.9041
72	1.9110	1.3040	1.0810	0.9321	0.8498	0.7823
73	1.6230	1.0980	0.8987	0.7705	0.9880	0.9238
74	1.2450	0.8178	0.6533	0.5525	0.4821	0.4293
75	0.8410	0.5256	0.4060	0.3358	0.2863	0.2464
76	0.3936	0.2303	0.1706	0.1370	0.1136	0.9314
77	0.0000	0.0000	0.0000	0.0000	0.0000	0.0000

Table 4.10

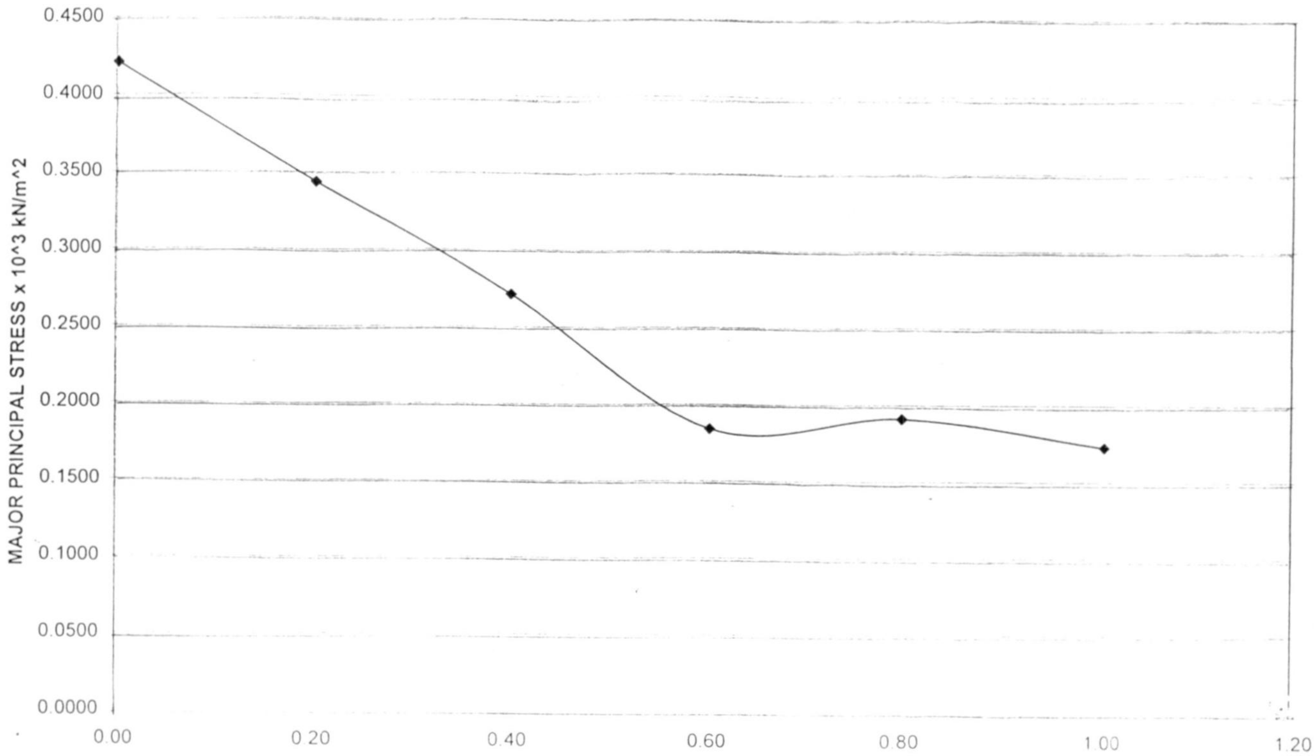

Figure 4.13 Variation of major principal stress with liner thickness
(For element number 51)

LINER THICKNESS(m)	STRESS x10^3 kN/m^2
0.00	0.4209
0.20	0.3437
0.40	0.2709
0.60	0.1840
0.80	0.1910
1.00	0.1727

Table 4.11

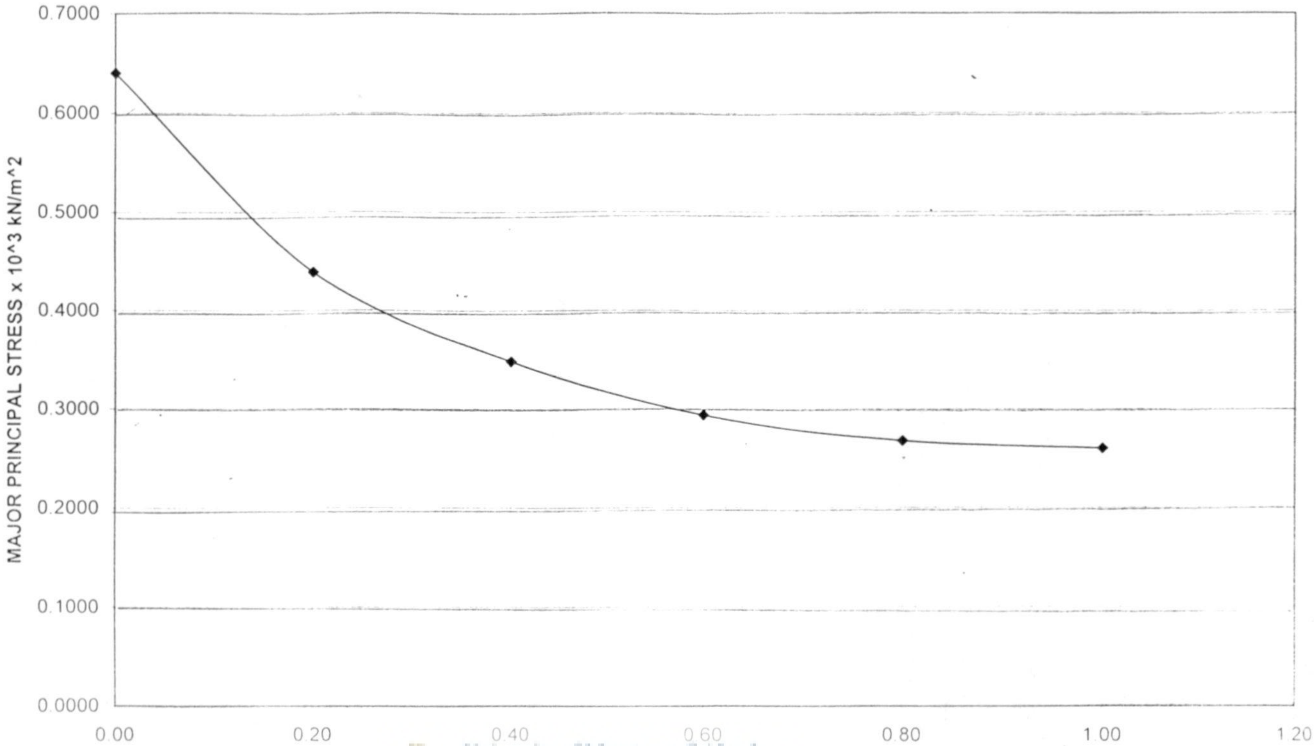

Figure 4.14 Variation of major principal stress with liner thickness
(For element number 56)

LINER THICKNESS(m)	STRESS $x10^3$ kN/m^2
0.00	0.6402
0.20	0.4385
0.40	0.3485
0.60	0.2936
0.80	0.2678
1.00	0.2597

Table 4.12

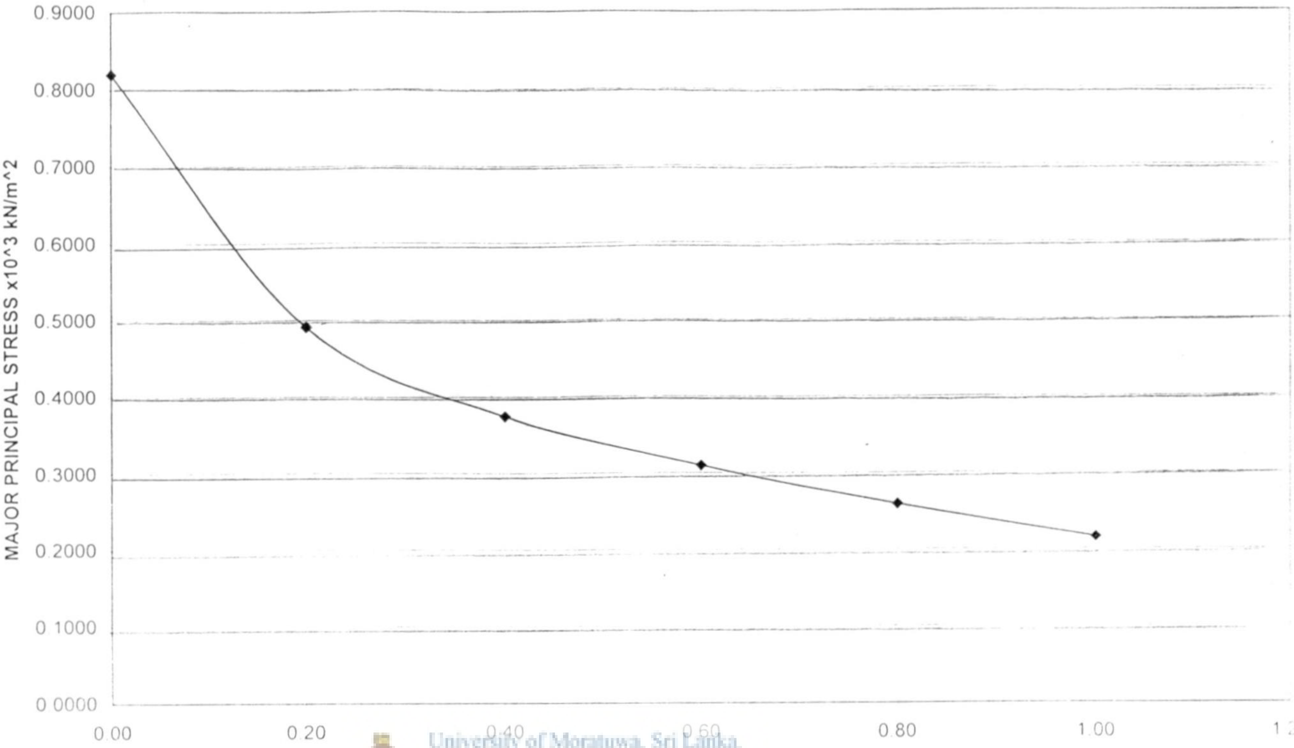

Figure 4.15 Variation of major principal stress with liner thickness
(For element number 60)

LINER THICKNESS(m)	STRESS x10^3 kN/m^2
0.00	0.8195
0.20	0.4909
0.40	0.3743
0.60	0.3095
0.80	0.2584
1.00	0.2151

Table 4.13

CHAPTER 5.0

RESULTS FOR ELLIPTICAL TUNNEL a/b = 1.358

5.1. Influence of Liner Thickness on Stress and Deformation in Rock Around Tunnel

Principal stresses were investigated along three radial lines AB, CD and EF, shown in figure 5.1 radiating from the center of the tunnel. For the tunnel with *a/b* = 1.358, variation of the major principal stress along the radial line AB for different liner thicknesses is shown in figure 5.2, and the variation of the minor principal stress along the same line for different liner thicknesses is shown in figure 5.5. Corresponding results for the same tunnel along line CD are shown in figures 5.3 and 5.6, respectively. Figures 5.4 and 5.7, respectively, show the corresponding results for the same tunnel along line EF.

Figure 5.8 shows the circumferential line considered for analysis Figure 5.9 shows the variation of principal tensile stress along an elliptical (circumferential) line of a shape similar to that of the tunnel opening, but at some distance inside the rock mass from the tunnel face, as the liner thickness is varied, for the tunnel with *a/b* = 1.358. The circumferential line along which the stresses shown in figure 5.9 are evaluated is similar to the line GH shown on figure 5.8.

For the elliptical tunnel with *a/b* = 1.358, influence of the concrete liner thickness on displacement at points inside the rock mass are illustrated by figures 5.10 and 5.11. Figures 5.10 and 5.11 show displacements at points inside the rock mass located along an elliptical (circumferential) line GH, which is shown on the scaled diagram of 5.8.

Figure 5.2, 5.3 & 5.4 are shows the variation of major principal stress along radical line AB,CD &EF respectively.

In the case of line AB (figure 5.2), for the tunnel a/b=1.358 principal tensile stress at a point inside the rock(element number 21) when there is no lining, which is 547.8kPa decreases by 20.44% when a liner of thickness of 0.2m is introduced. The corresponding reductions are 38.9% for a liner thickness of 0.4m thickness and 65.5% for a liner of 1.0m.

In the case of line CD (figure 5.3), for the tunnel a/b=1.358 principal stress at a point inside the rock(element number 26) reduce by 28.3% when a liner of thickness of 0.2m is introduced as compared to the stresses in the case of unlined tunnel. The corresponding reductions are 40.0% for a liner thickness of 0.4m thickness and 55.5% for a liner of 1.0m.

In the case of line EF (figure 5.4, for the tunnel a/b=1.358 major principal stress at a point inside the rock(element number 26) reduce by 28.3% when a liner of thickness of 0.2m is introduced as compared to the stresses in the case of unlined tunnel. The corresponding reductions are 40.0% for a liner thickness of 0.4m thickness and 55.5% for a liner of 1.0m.

The numerical results and the comparison of figures 5.2, 5.3 & 5.4 show that the line EF is the critical line along which maximum principal tensile stresses occurred.

Figures 5.5, 5.6 and 5.7 show the influence of concrete liner thickness on the compressive principal stress around the tunnel with *a/b* = 1.358. According to figure 5.5, the minor principal stress at a point inside the rock closure to point A reduces by 16.5% when a 0.2 m thick concrete is introduced to the originally unlined tunnel; this reduction is 26.53% for a 0.4 m thick liner and 40.8% for a 1.0 m thick liner. Figure 5.6 shows similar behavior of the minor principal stress along the line CD. Figure 5.7 shows that large percentage stress reductions occur in the case of the minor principal stress along line EF. This stress reduces at a point inside the rock closure to point E by 52.5% when a 0.2 m thick liner is introduced to the unlined tunnel; the corresponding reduction is 79.2% for a 0.4 m thick liner, and 91.1% for a 1.0 m thick liner.

Figures 5.9 & 5.10 show the variation of major principal stress and minor principal stress along circumferential line GH respectively, which is in rock.

The major principal stress reduction is 19.18% when 0.2m liner is introduced as compared to the stress in the case of unlined tunnel closure to point A. Where as reduction is 27.6% at point E when 0.2m liner is introduced as compared to the stress in the case of an unlined tunnel.

Figure 5.10 shows the minor principal stress variation along line GH. It also shows the same pattern of reduction as in the major principal stress mentioned above.

According to these results in figures 5.11 and 5.12, the percentage reduction of x-displacement and y-displacement over the rock domain varies with the location. Figure 5.11 shows relatively large percentage reductions in the x-displacement at the x-axis as the tunnel liner thickness is increased (this is 42.92% when a 0.2 m thick liner is introduced on the unlined tunnel; and about 94.57% for a 1.0 m thick liner).

Figures 4.13.4.14 & 4.15 are shows the variation of major principal stress with the introduction of concrete liner on three elements close to point A,C & E respectively.

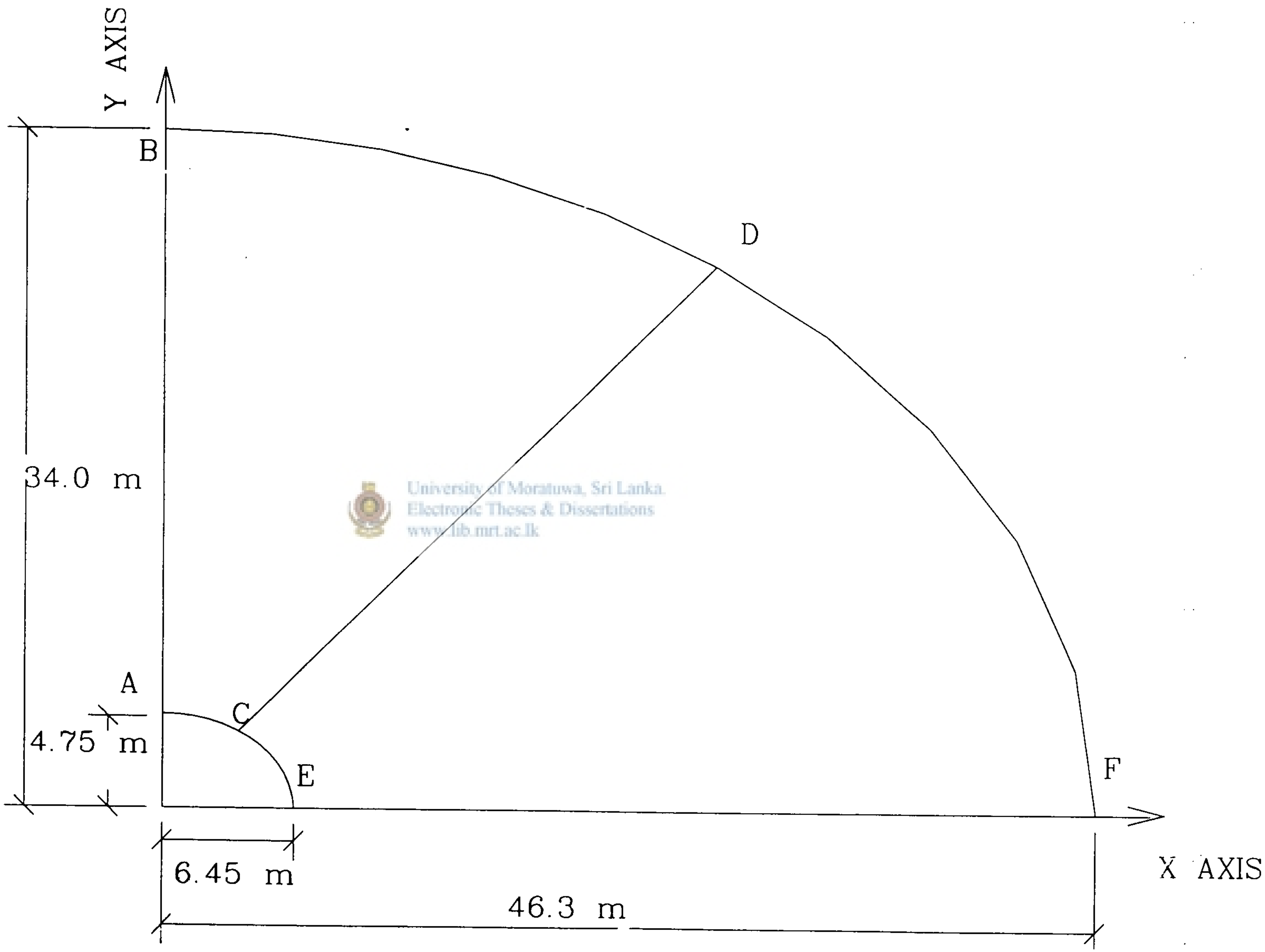

Figure 5.1 Radial lines (For elliptical tunnel-2, a/b = 1.358)

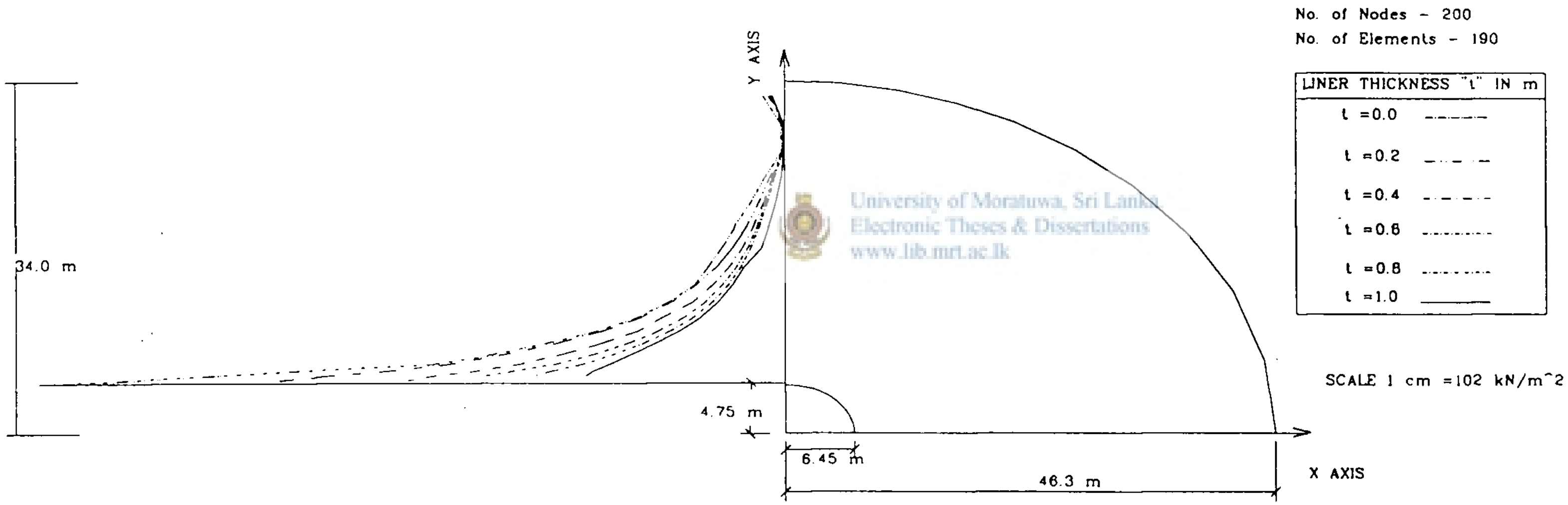

Figure 5.2 Variation of major principal stress along radial line "AB"
(For elliptical tunnel-2, a/b = 1.358)

VARIATION OF MAJOR PRINCIPAL STRESS ALONG RADIAL LINE "AB"
(FOR ELLIPTICAL TUNNEL -2,a/b = 1.356)

ELEMENT NUMBER	MAJOR PRINCIPAL STRESS $*10^3$ (kN/m^2)						
	LINER THICKNESS (m)						
	t =0.0	t =0.2	t =0.4	t =0.6	t =0.8	t =1.0	
1	0.7122	7.2430	5.6360	4.7630	3.8850	3.1840	LINER ELEMENTS
11	0.6343	0.4818	0.3591	4.5450	3.8260	3.1370	
21	0.5478	0.4358	0.3345	0.2848	0.2379	0.1891	
31	0.4672	0.3776	0.2944	0.2574	0.2210	0.1814	
41	0.3978	0.3191	0.2518	0.1274	0.1918	0.1660	
51	0.3346	0.2643	0.2109	0.1806	0.1616	0.1450	
61	0.2758	0.2145	0.1725	0.1477	0.1331	0.1215	
71	0.2247	0.1730	0.1398	0.1200	0.1086	0.0998	
81	0.1803	0.1378	0.1170	0.0963	0.0874	0.0806	
91	0.1418	0.1079	0.0877	0.0759	0.0690	0.0637	
101	0.1110	0.0844	0.0687	0.0597	0.0543	0.0503	
111	0.0860	0.0653	0.0533	0.0464	0.0423	0.0392	
121	0.0651	0.0495	0.0404	0.0354	0.0323	0.0299	
131	0.0475	0.0361	0.0296	0.0260	0.0237	0.0220	
141	0.0324	0.0246	0.0202	0.0177	0.0162	0.0151	
151	0.0192	0.0146	0.0119	0.0105	0.0095	0.0088	
161	0.0081	0.0060	0.0049	0.0041	0.0037	0.0034	
171	0.0033	0.0024	0.0019	0.0017	0.0016	0.0015	
181	0.0197	0.0159	0.0139	0.0131	0.0124	0.0118	

Table 5.1

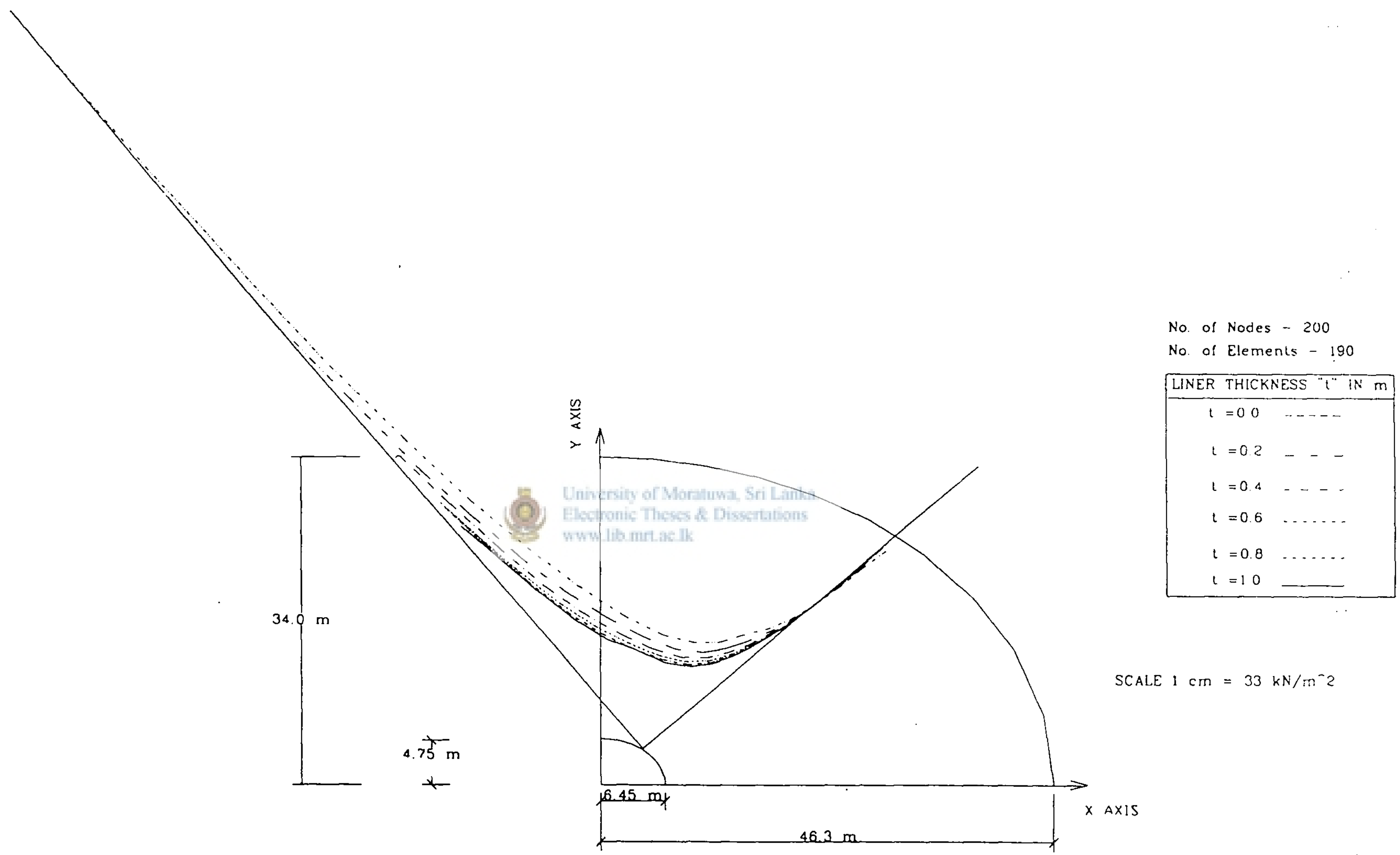

Figure 5.3 Variation of major principal stress along radial line "CD"
(For elliptical tunnel-2, a/b = 1.358)

VARIATION OF MAJOR PRINCIPAL STRESS ALONG RADIAL LINE "CD"
(FOR ELLIPTICAL TUNNEL -2,a/b = 1.356)

ELEMENT NUMBER	MAJOR PRINCIPAL STRESS*10^3 (kN/m^2) LINER THICKNESS (m)						
	t =0.0	t =0.2	t =0.4	t =0.6	t =0.8	t =1.0	
6	0.9991	7.7680	5.3120	4.4850	3.9790	3.5370	LINER ELEMENTS
16	0.7849	0.5535	0.3944	4.1330	3.7910	3.2930	
26	0.6593	0.4726	0.3947	0.3288	0.3220	0.2964	
36	0.5088	0.3684	0.3231	0.2764	0.2650	0.2560	
46	0.4056	0.2998	0.2524	0.2211	0.2072	0.1986	
56	0.3075	0.2303	0.1901	0.1677	0.1551	0.1465	
66	0.2323	0.1752	0.1428	0.1260	0.1159	0.0904	
76	0.1704	0.1288	0.1041	0.0917	0.0840	0.0783	
86	0.1169	0.0882	0.0708	0.0621	0.0567	0.0526	
96	0.0756	0.0567	0.0450	0.0393	0.0356	0.0329	
106	0.0490	0.0365	0.0288	0.0249	0.0225	0.0207	
116	0.0322	0.0237	0.0185	0.0158	0.0141	0.0129	
126	0.0203	0.0148	0.0112	0.0094	0.0083	0.0075	
136	0.0109	0.0077	0.0057	0.0046	0.0040	0.0036	
146	0.0035	0.0023	0.0014	0.0009	0.0007	0.0005	
156	-0.0006	-0.0007	-0.0007	-0.0008	-0.0008	-0.0007	
166	-0.0032	-0.0024	-0.0019	-0.0017	-0.0015	-0.0013	
176	-0.0036	-0.0025	-0.0019	-0.0015	-0.0012	-0.0010	
186	-0.0056	-0.0004	-0.0011	-0.0007	-0.0005	-0.0004	

Table 5.2

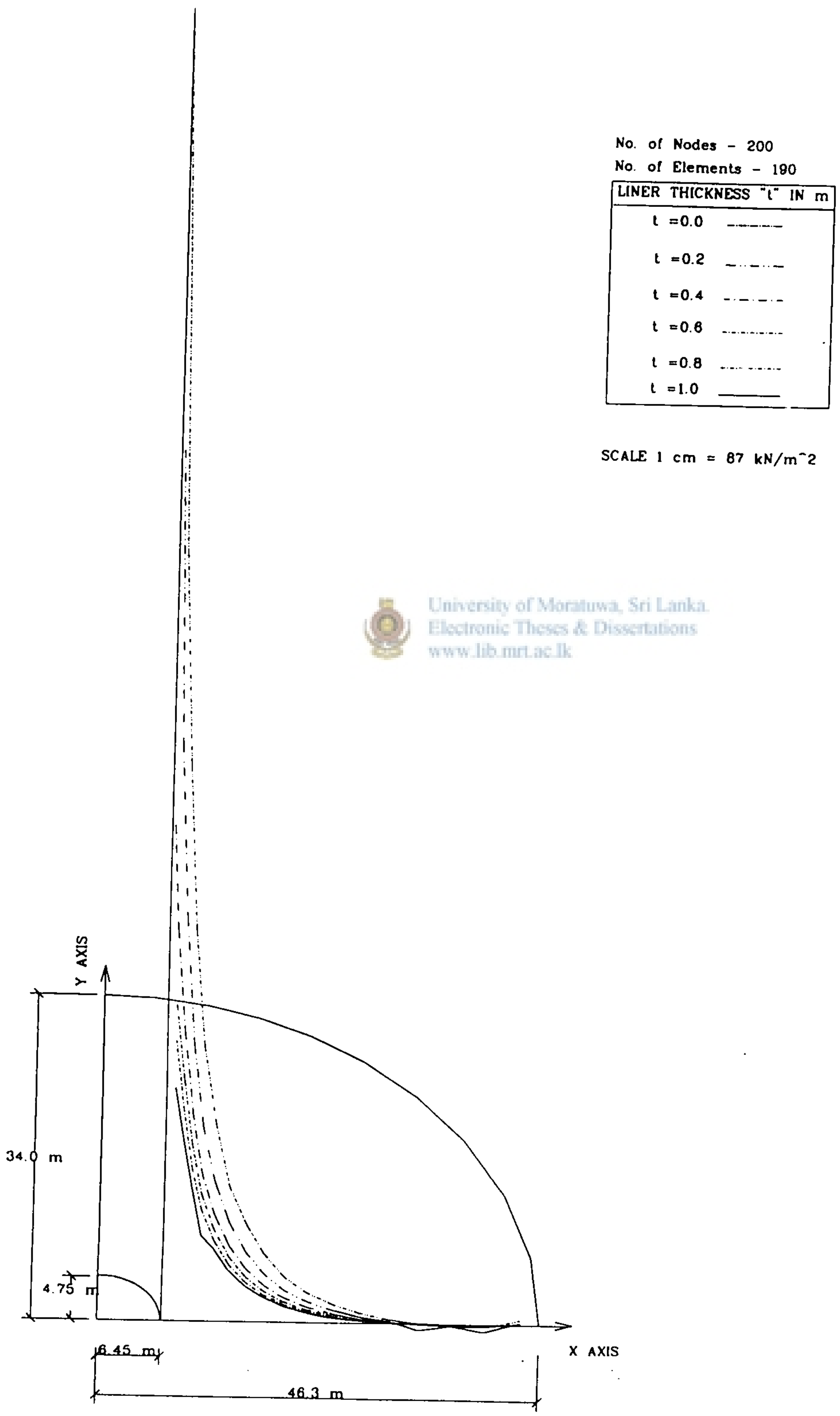

Figure 5.4 Variation of major principal stress along radial line "EF"
(For elliptical tunnel-2, a/b = 1.358)

VARIATION OF MAJOR PRINCIPAL STRESS ALONG RADIAL LINE "EF"
(FOR ELLIPTICAL TUNNEL -2,a/b = 1.356)

ELEMENT NUMBER	MAJOR PRINCIPAL STRESS *10^3 (kN/m^2)						
	LINER THICKNESS (m)						
	t =0.0	t =0.2	t =0.4	t =0.6	t =0.8	t =1.0	
10	1.3670	11.3203	7.4210	6.2540	5.7130	5.2690	LINER ELEMENTS
20	1.0950	0.9083	0.5184	4.6120	4.0780	3.4660	
30	0.8015	0.6006	0.4074	0.3313	0.2942	0.2447	
40	0.5815	0.4209	0.3016	0.2527	0.2218	0.1936	
50	0.4075	0.2907	0.2163	0.1846	0.1616	0.1425	
60	0.2887	0.2053	0.1560	0.1336	0.1175	0.0904	
70	0.2065	0.1470	0.1127	0.0964	0.0850	0.0759	
80	0.1458	0.1037	0.0797	0.0679	0.0598	0.0535	
90	0.1024	0.0728	0.0559	0.0473	0.0416	0.0372	
100	0.0711	0.0504	0.0384	0.0323	0.0283	0.0254	
110	0.0482	0.0340	0.0257	0.0213	0.0186	0.0164	
120	0.0316	0.0221	0.0164	0.0134	0.0115	0.0101	
130	0.0198	0.0135	0.0098	0.0078	0.0066	0.0057	
140	0.0112	0.0074	0.0051	0.0039	0.0031	0.0026	
150	0.0050	0.0030	0.0018	0.0017	0.0008	0.0005	
160	0.0005	-0.0067	-0.0004	-0.0006	0.0007	-0.0008	
170	-0.0025	-0.0021	-0.0018	-0.0017	-0.0001	-0.0015	
180	-0.0026	-0.0021	-0.0075	-0.0016	-0.0001	-0.0014	
190	0.0054	0.0013	0.0019	0.0013	0.0007	0.0004	

Table 5.3

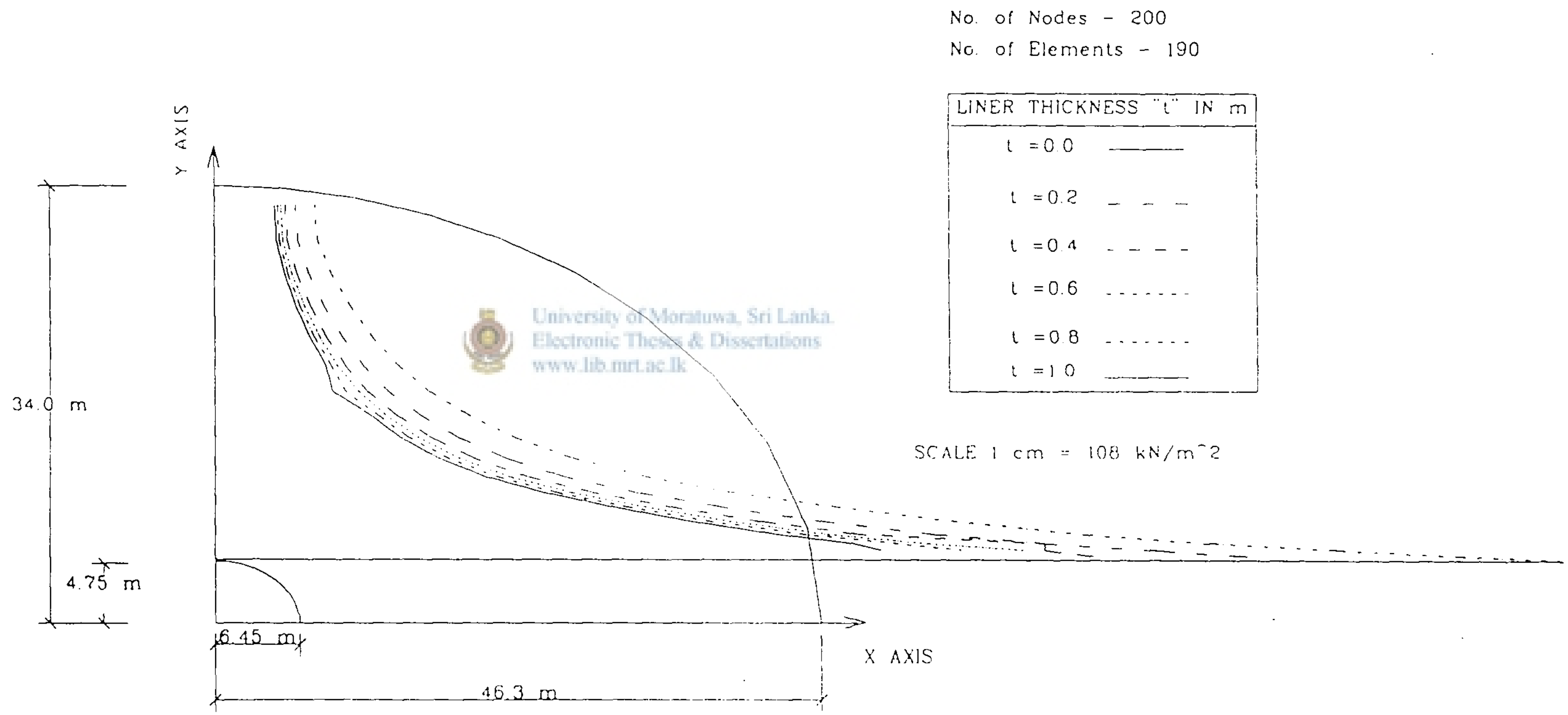

Figure 5.5 Variation of minor principal stress along radial line "AB"
(For elliptical tunnel-2, a/b = 1.358)

VARIATION OF MINOR PRINCIPAL STRESS ALONG RADIAL LINE "AB"
(FOR ELLIPTICAL TUNNEL -2,a/b = 1.356)

ELEMENT NUMBER	MINOR PRINCIPAL STRESS $(kN/m^2)*10^3$						
	LINER THICKNESS (m)						
	t =0.0	t =0.2	t =0.4	t =0.6	t =0.8	t =1.0	
1	-1.0320	-0.9726	-0.8671	-0.9171	-0.9288	-0.9387	LINER ELEMENTS
11	-0.9541	-0.7891	-0.6717	-0.7394	-0.7157	-0.6605	
21	-0.8603	-0.7181	-0.6321	-0.6169	-0.5697	-0.5089	
31	-0.7609	-0.6343	-0.5640	-0.5439	-0.5195	-0.4865	
41	-0.6642	-0.5496	-0.4924	-0.4686	-0.4497	-0.4289	
51	-0.5643	-0.4631	-0.4161	-0.3938	-0.3782	-0.3631	
61	-0.4750	-0.3876	-0.3483	-0.3290	-0.3157	-0.3036	
71	-0.3961	-0.3221	-0.2888	-0.2726	-0.2613	-0.2511	
81	-0.3288	-0.2668	-0.2385	-0.2250	-0.2153	-0.2066	
91	-0.2733	-0.2216	-0.1974	-0.1862	-0.1779	-0.1704	
101	-0.2285	-0.1852	-0.1644	-0.1550	-0.1478	-0.1414	
111	-0.1931	-0.1565	-0.1384	-0.1304	-0.1242	-0.1187	
121	-0.1638	-0.1328	-0.1171	-0.1102	-0.1005	-0.0950	
131	-0.1405	-0.1138	-0.1001	-0.0942	-0.0895	-0.0854	
141	-0.1208	-0.0979	-0.0859	-0.0808	-0.0767	-0.0731	
151	-0.1041	-0.0843	-0.0738	-0.0694	-0.0659	-0.0627	
161	-0.0898	-0.0727	-0.0636	-0.0598	-0.0567	-0.0540	
171	-0.0791	-0.0640	-0.0560	-0.0526	-0.0500	-0.0475	
181	-0.0769	-0.0623	-0.0544	-0.0511	-0.0485	-0.0461	

Table 5.4

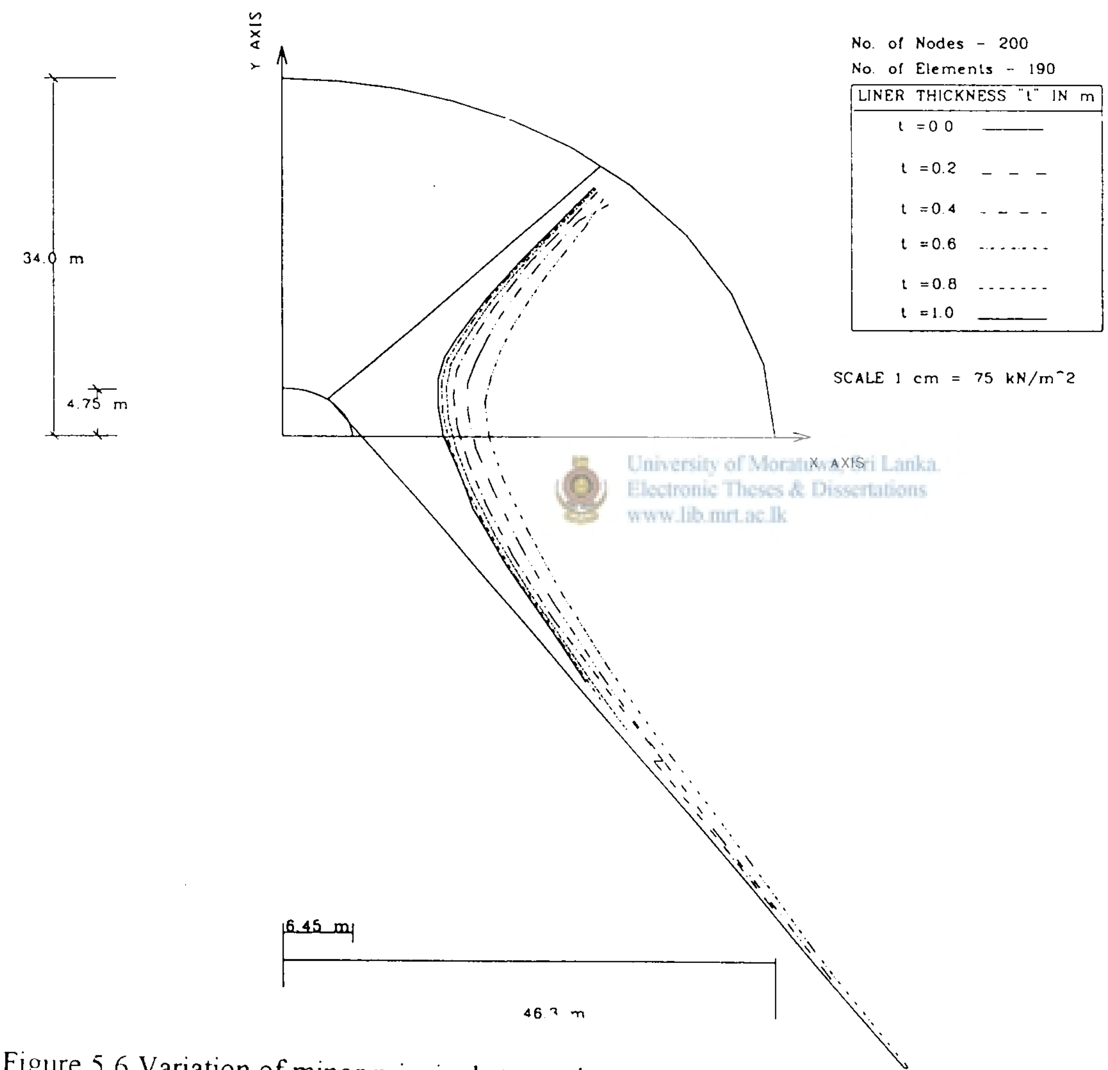

Figure 5.6 Variation of minor principal stress along radial line "CD"
(For elliptical tunnel-2, a/b = 1.358)

VARIATION OF MINOR PRINCIPAL STRESS ALONG RADIAL LINE "CD"
(FOR ELLIPTICAL TUNNEL -2,a/b = 1.356)

ELEMENT NUMBER	MINOR PRINCIPAL STRESS $(kN/m^2)*10^3$						
	LINER THICKNESS (m)						
	t =0.0	t =0.2	t =0.4	t =0.6	t =0.8	t =1.0	
6	-0.8335	-0.4562	-0.6347	-0.6632	-0.6885	-0.7096	LINER ELEMENTS
16	-0.8354	-0.7242	-0.6399	-0.5000	-0.4903	-0.4717	
26	-0.6888	-0.5519	-0.4629	-0.4246	-0.3872	-0.3651	
36	-0.5920	-0.4761	-0.4696	-0.3479	-0.3230	-0.3107	
46	-0.4716	-0.3758	-0.3019	-0.2667	-0.2447	-0.2308	
56	-0.3661	-0.2896	-0.2300	-0.2024	-0.1845	-0.1719	
66	-0.2875	-0.2246	-0.1768	-0.1548	-0.1403	-0.1297	
76	-0.2218	-0.1713	-0.1345	-0.1172	-0.1059	-0.0975	
86	-0.1674	-0.1279	-0.1004	-0.0871	-0.0786	-0.0721	
96	-0.1272	-0.0959	-0.0749	-0.0645	-0.0579	-0.0529	
106	-0.0987	-0.0738	-0.0577	-0.0495	-0.0443	-0.0404	
116	-0.0843	-0.0628	-0.0490	-0.0420	-0.0375	-0.0341	
126	-0.0716	-0.0532	-0.0415	-0.0355	-0.0317	-0.0288	
136	-0.0607	-0.0449	-0.0350	-0.0298	-0.0265	-0.0241	
146	-0.0528	-0.0390	-0.0304	-0.0259	-0.0231	-0.0209	
156	-0.0453	-0.0333	-0.0250	-0.0220	-0.0196	-0.0177	
166	-0.0396	-0.0292	-0.0227	-0.0193	-0.0172	-0.0156	
176	-0.0337	-0.0247	-0.0191	-0.0161	-0.0142	-0.0128	
186	-0.0240	-0.0319	-0.0161	-0.0134	-0.0125	-0.0106	

Table 5.5

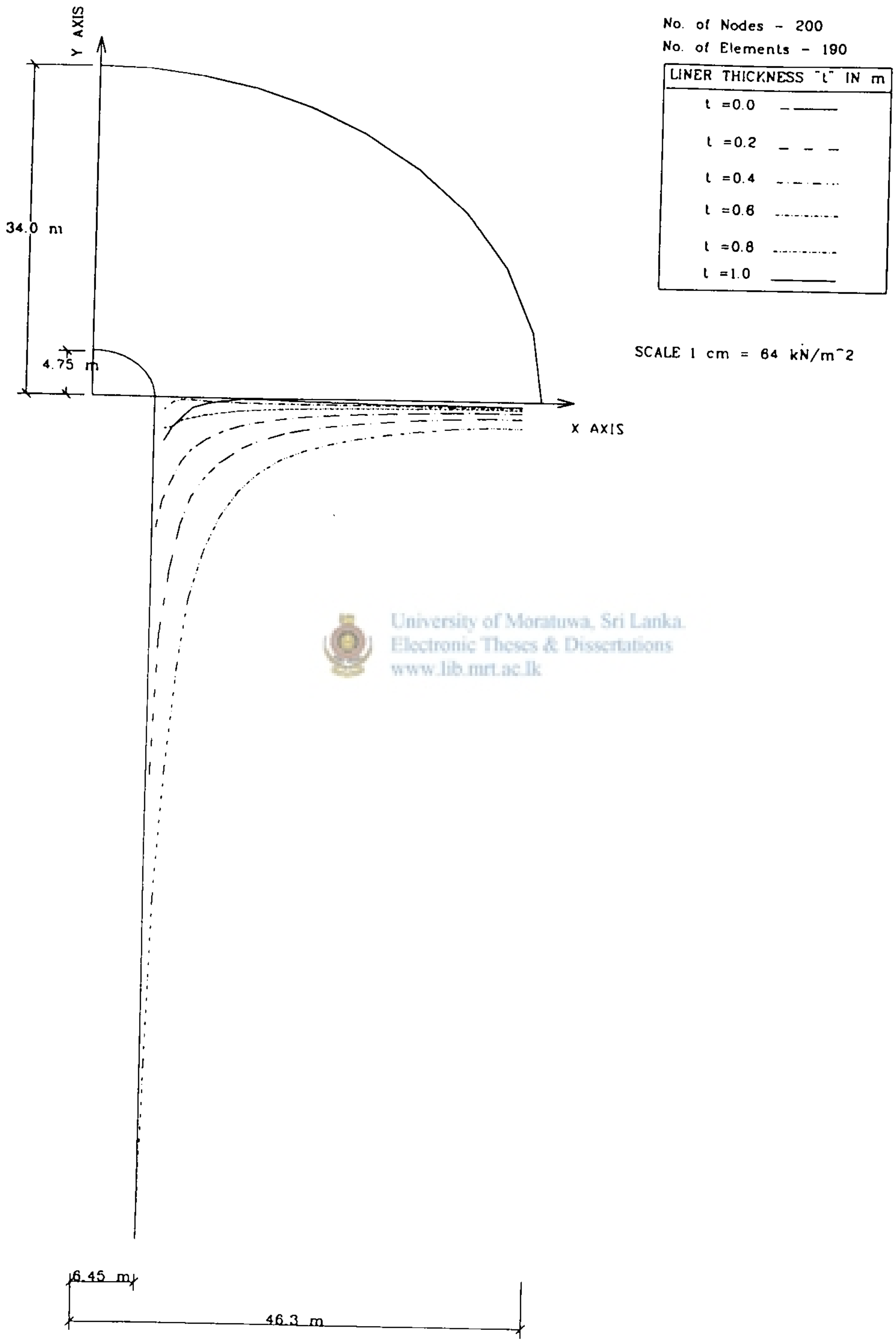

Figure 5.7 Variation of minor principal stress along radial line "EF"
(For elliptical tunnel-2, a/b = 1.358)

VARIATION OF MINOR PRINCIPAL STRESS ALONG RADIAL LINE "EF"
(FOR ELLIPTICAL TUNNEL -2,a/b = 1.356)

ELEMENT NUMBER	MINOR PRINCIPAL STRESS $(kN/m^2)*10^3$						
	LINER THICKNESS (m)						
	t =0.0	t =0.2	t =0.4	t =0.6	t =0.8	t =1.0	
10	-0.8696	-0.6431	-0.4378	-0.4961	-0.5459	-0.5739	LINER ELEMENTS
20	-0.6887	-0.3898	-0.1358	-0.1480	-0.0640	-0.8474	
30	-0.5173	-0.2458	-0.1075	-0.0323	-0.0128	0.0458	
40	-0.3816	-0.1784	-0.0860	-0.0305	0.0048	0.0299	
50	-0.2799	-0.1322	-0.0657	-0.0233	0.0023	0.0199	
60	-0.2074	-0.1028	-0.0531	-0.0208	-0.0022	0.0103	
70	-0.1595	-0.0820	-0.0431	-0.0177	-0.0035	0.0060	
80	-0.1233	-0.0657	-0.0350	-0.0151	-0.0042	0.0031	
90	-0.0971	-0.0534	-0.0289	-0.0131	-0.0046	0.0010	
100	-0.0783	-0.0442	-0.0245	-0.0118	-0.0050	-0.0005	
110	-0.0642	-0.0371	-0.0210	-0.0107	-0.0051	-0.0015	
120	-0.0542	-0.0321	-0.0186	-0.0100	-0.0054	-0.0024	
130	-0.0467	-0.0281	-0.0167	-0.0095	-0.0056	-0.0031	
140	-0.0409	-0.0251	-0.0153	-0.0092	-0.0059	-0.0037	
150	-0.0362	-0.0226	-0.0141	-0.0089	-0.0060	-0.0046	
160	-0.0324	-0.0205	-0.0131	-0.0085	-0.0060	-0.0043	
170	-0.0289	-0.0186	-0.0121	-0.0081	-0.0006	-0.0043	
180	-0.0267	-0.0173	-0.0115	-0.0079	-0.0006	-0.0045	
190	-0.0270	-0.0177	-0.0118	-0.0083	-0.0006	-0.0049	

Table 5.6

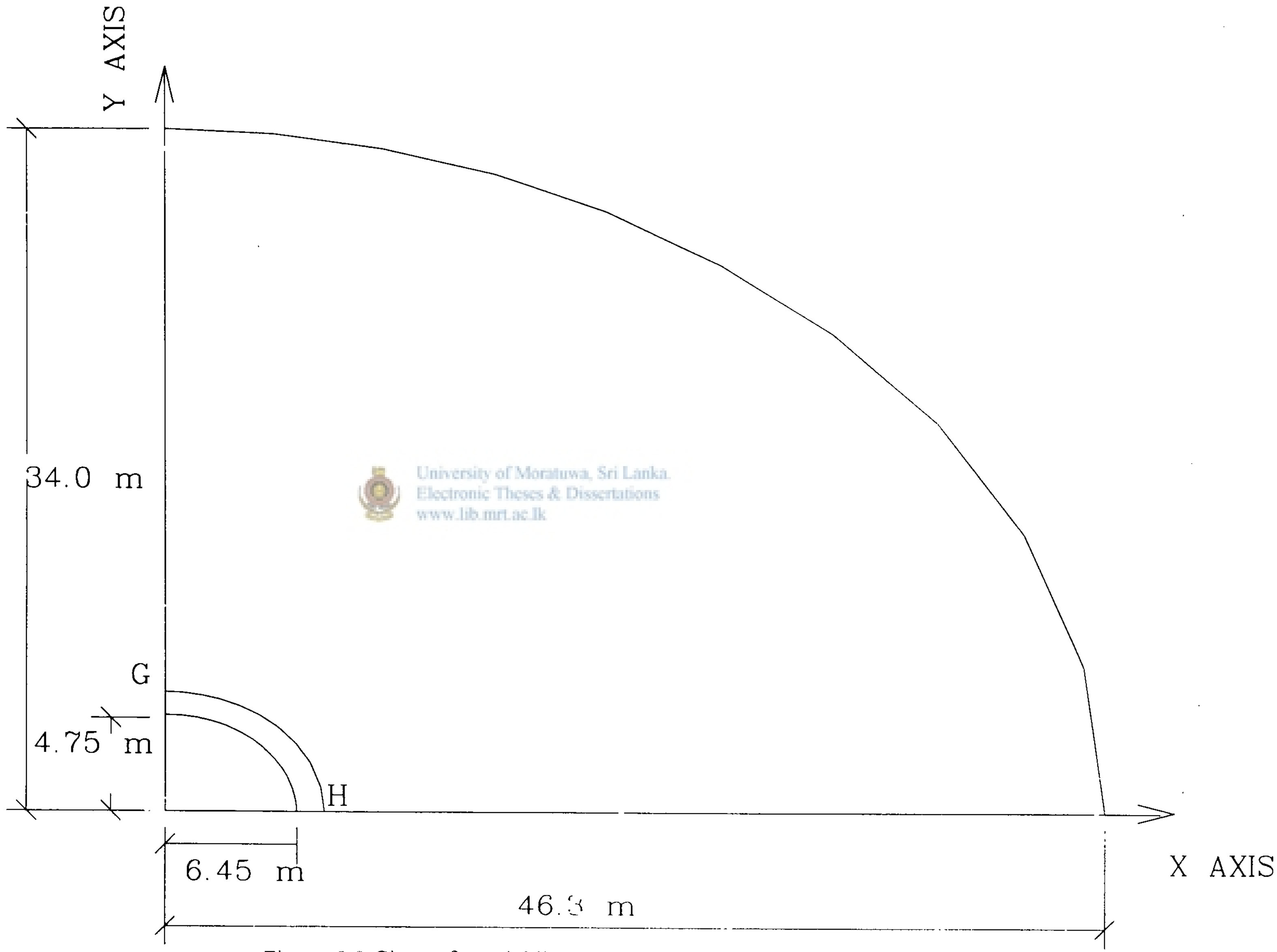

Figure 5.8 Circumferential lines (For elliptical tunnel-2, a/b = 1.358)

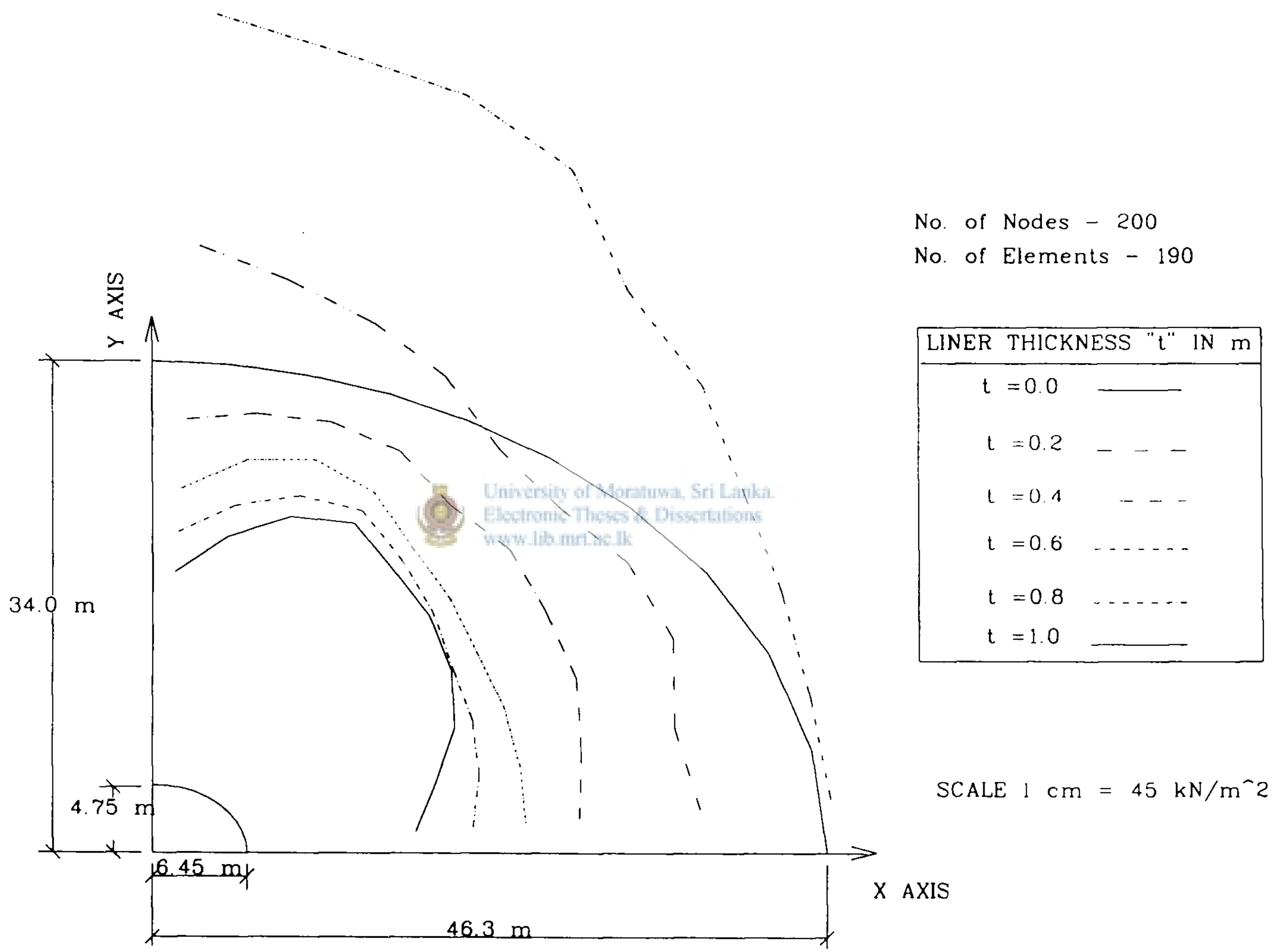

Figure 5.9 Variation of major principal stress along circumferential line "GH"
(For elliptical tunnel-2, a/b = 1.358)

VARIATION OF MAJOR PRINCIPAL STRESS ALONG CIRCUMFERENTIAL LINE "GH"
(FOR ELLIPTICAL TUNNEL -2,a/b = 1.356)

ELEMENT NUMBER	MAJOR PRINCIPAL STRESS*10^3 (kN/m^2)					
	LINER THICKNESS (m)					
	t =0.0	t =0.2	t =0.4	t =0.6	t =0.8	t =1.0
31	0.4672	0.3776	0.2945	0.2574	0.2210	0.1814
32	0.4646	0.3190	0.3032	0.2598	0.2309	0.1993
33	0.4685	0.3873	0.3157	0.2618	0.2383	0.2250
34	0.4771	0.3835	0.3178	0.2626	0.2427	0.2414
35	0.4982	0.3834	0.3231	0.2697	0.2545	0.2510
36	0.5088	0.3684	0.3164	0.2764	0.2650	0.2560
37	0.5551	0.3871	0.3270	0.2928	0.2774	0.2670
38	0.5679	0.3978	0.3235	0.2951	0.2674	0.2514
39	0.5691	0.4074	0.3132	0.2800	0.2470	0.2242
40	0.5815	0.4209	0.3016	0.2527	0.2218	0.1936

Table 5.7

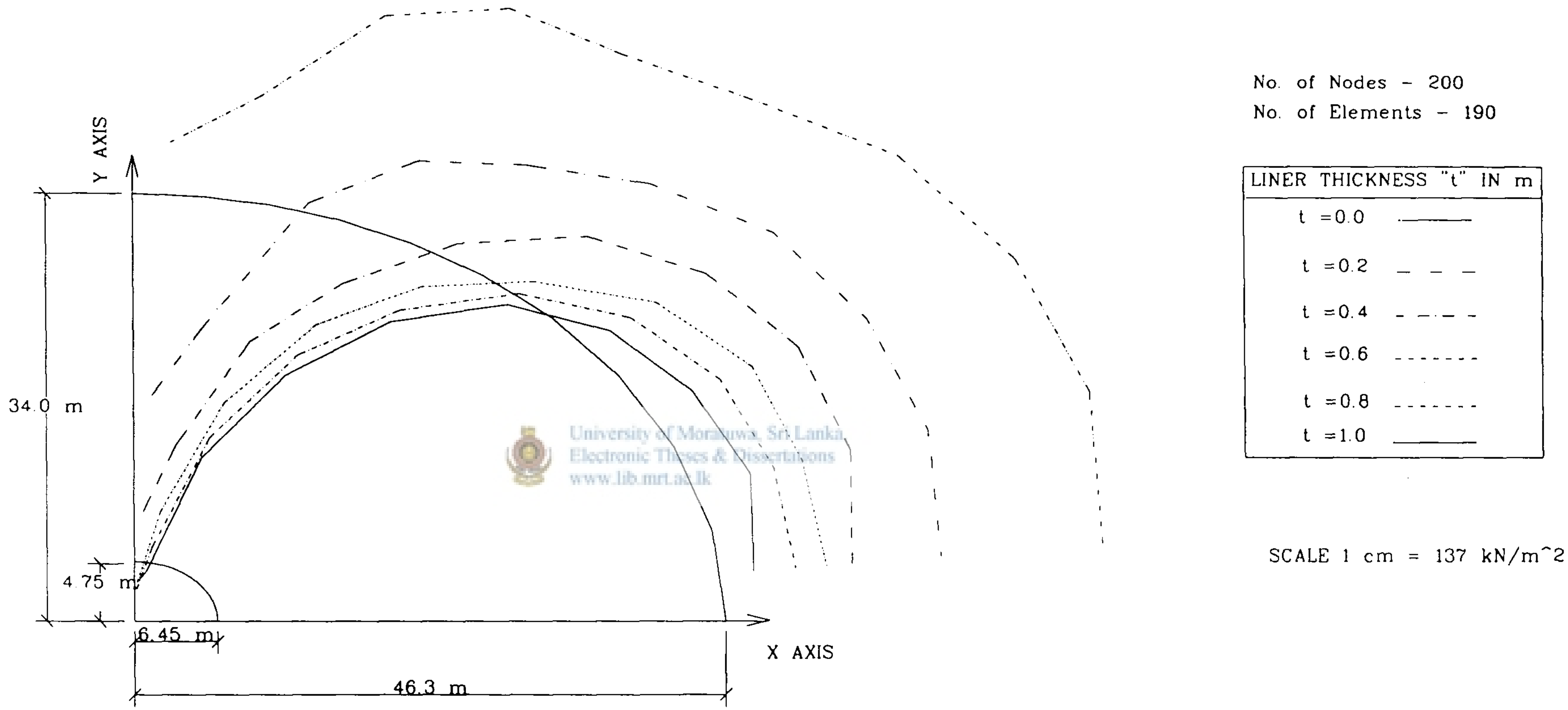

Figure 5.10 Variation of minor principal stress along circumferential line "GH"
(For elliptical tunnel-2, a/b = 1.358)

VARIATION OF MINOR PRINCIPAL STRESS ALONG CIRCUMFERENTIAL "GH"
(FOR ELLIPTICAL TUNNEL -2,a/b = 1.356)

ELEMENT NUMBER	MINOR PRINCIPAL STRESS $(kN/m^2)*10^3$					
	LINER THICKNESS (m)					
	t =0.0	t =0.2	t =0.4	t =0.6	t =0.8	t =1.0
31	-0.7609	-0.6343	-0.5640	-0.5439	-0.5195	-0.4865
32	-0.7703	-0.6405	-0.5773	-0.5384	-0.5154	-0.4964
33	-0.7488	-0.6224	-0.5640	-0.5244	-0.4975	-0.474
34	-0.7055	-0.5889	-0.5266	-0.4813	-0.4579	-0.4385
35	-0.6377	-0.5348	-0.4696	-0.4137	-0.3954	-0.3849
36	-0.5920	-0.4761	-0.3937	-0.3479	-0.3230	-0.3107
37	-0.5693	-0.4287	-0.3133	-0.2743	-0.2460	-0.2276
38	-0.5197	-0.3595	-0.2385	-0.1867	-0.1568	-0.1390
39	-0.4280	-0.2404	-0.1428	-0.0888	-0.0591	-0.0398
40	-0.3816	-0.1784	-0.0860	-0.0305	-0.0248	-0.0299

Table 5.8

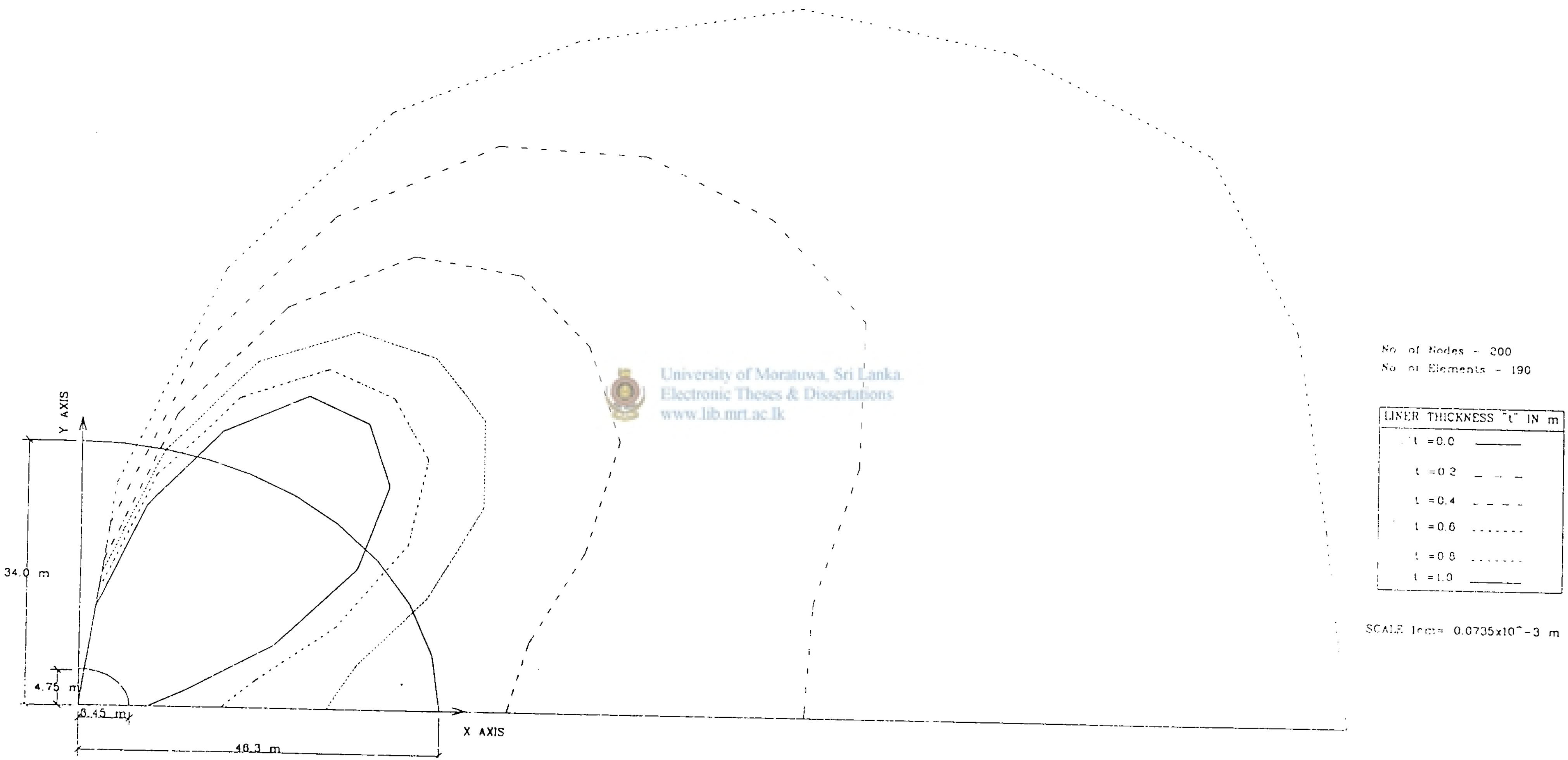

Figure 5.11 Variation of "x" displacement along circumferential line "GH"
(For elliptical tunnel-2, a/b = 1.358)

VARIATION OF "X" DISPLACEMENTS CIRCUMFERENTIAL LINE "GH"
(FOR ELLIPTICAL TUNNEL -2,a/b = 1.356)

NODE NUMBER	"X" DISPLACEMENT $*10^{-3}$(m)					
	LINER THICKNESS (m)					
	t =0.0	t =0.2	t =0.4	t =0.6	t =0.8	t =1.0
34	0.0000	0.0000	0.0000	0.0000	0.0000	0.0000
35	0.2909	0.2374	0.1915	0.1734	0.1524	0.1294
36	0.5913	0.4867	0.3958	0.3505	0.3135	0.2710
37	0.8622	0.7100	0.5775	0.4984	0.4459	0.3987
38	1.1070	0.9001	0.7199	0.5985	0.5377	0.4953
39	1.2910	1.0160	0.7919	0.6397	0.5651	0.5204
40	1.4640	1.0870	0.8018	0.6379	0.5492	0.4889
41	1.6120	1.1210	0.7735	0.5794	0.4715	0.3984
42	1.6310	1.0440	0.6807	0.4673	0.3459	0.2617
43	1.6100	0.9485	0.5836	0.3600	0.2309	0.1396
44	1.6240	0.9270	0.5487	0.3180	0.1824	0.0882

Table 5.9

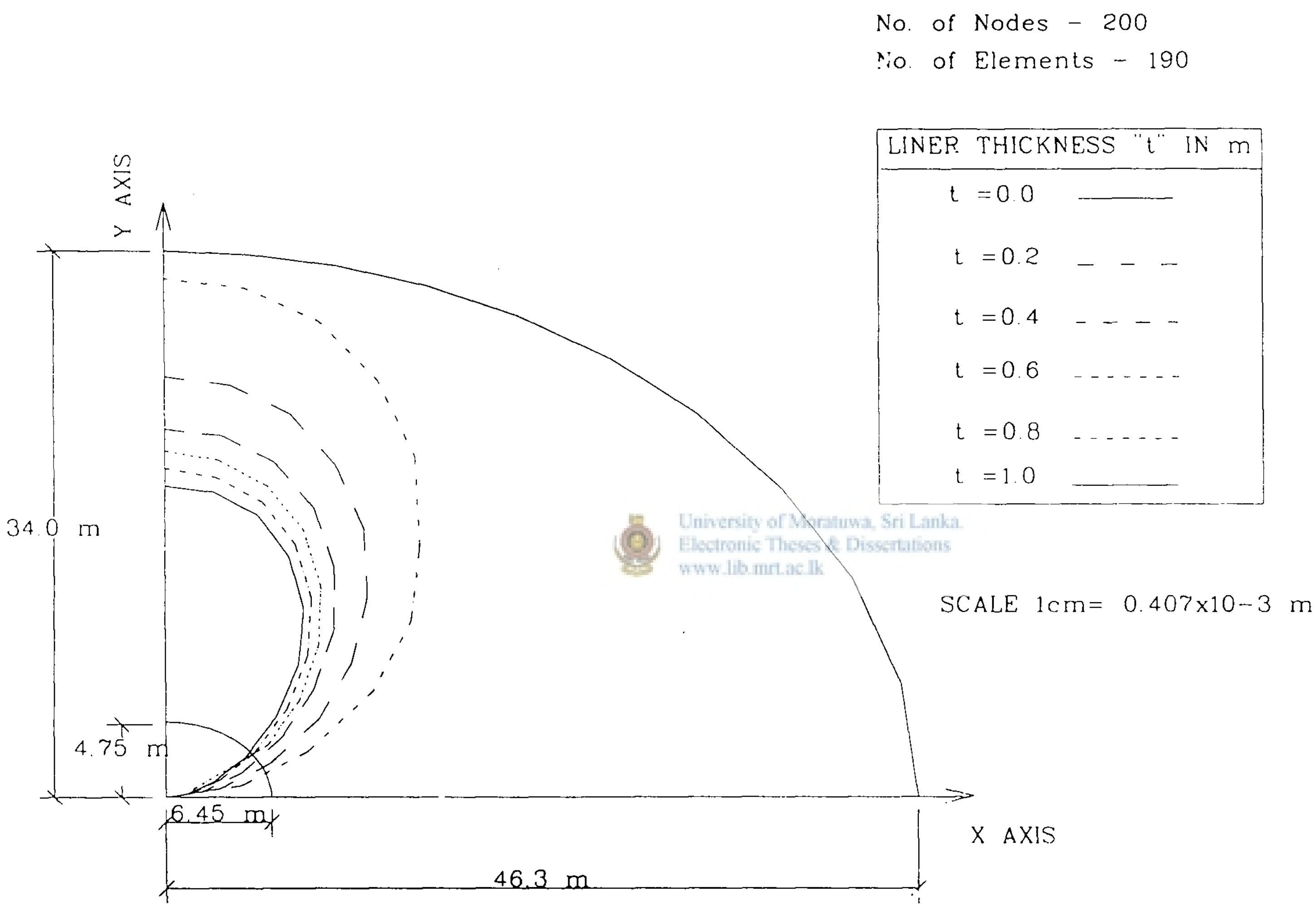

Figure 5.12 Variation of "y" displacement along circumferential line "GH"
(For elliptical tunnel-2, a/b = 1.358)

VARIATION OF "Y' DISPLACEMENT CIRCUMFERENTIAL LINE "GH"
(FOR ELLIPTICAL TUNNEL -2,a/b = 1.356)

NODE NUMBER	"Y" DISPLACEMENT (m)*10^{-3}					
	LINER THICKNESS (m)					
	t =0.0	t =0.2	t =0.4	t =0.6	t =0.8	t =1.0
34	3.2260	2.6200	2.3060	2.1700	2.0640	1.9550
35	3.2070	2.6010	2.2900	2.1420	2.0350	1.9420
36	3.1150	2.5180	2.2160	2.0570	1.9530	1.8650
37	2.9160	2.3400	2.0430	1.8910	1.7840	1.6970
38	2.6380	2.0950	1.7960	1.6450	1.5480	1.4660
39	2.2268	1.7740	1.4830	1.3490	1.2510	1.1710
40	1.8810	1.4330	1.1400	1.0310	0.9341	0.8553
41	1.4440	1.0750	0.8068	0.7100	0.6221	0.5520
42	0.9429	0.6801	0.4863	0.1813	0.3499	0.2993
43	0.4729	0.3309	0.2268	0.1613	0.1543	0.1291
44	0.0000	0.0000	0.0000	0.0000	0.0000	0.0000

Table 5.10

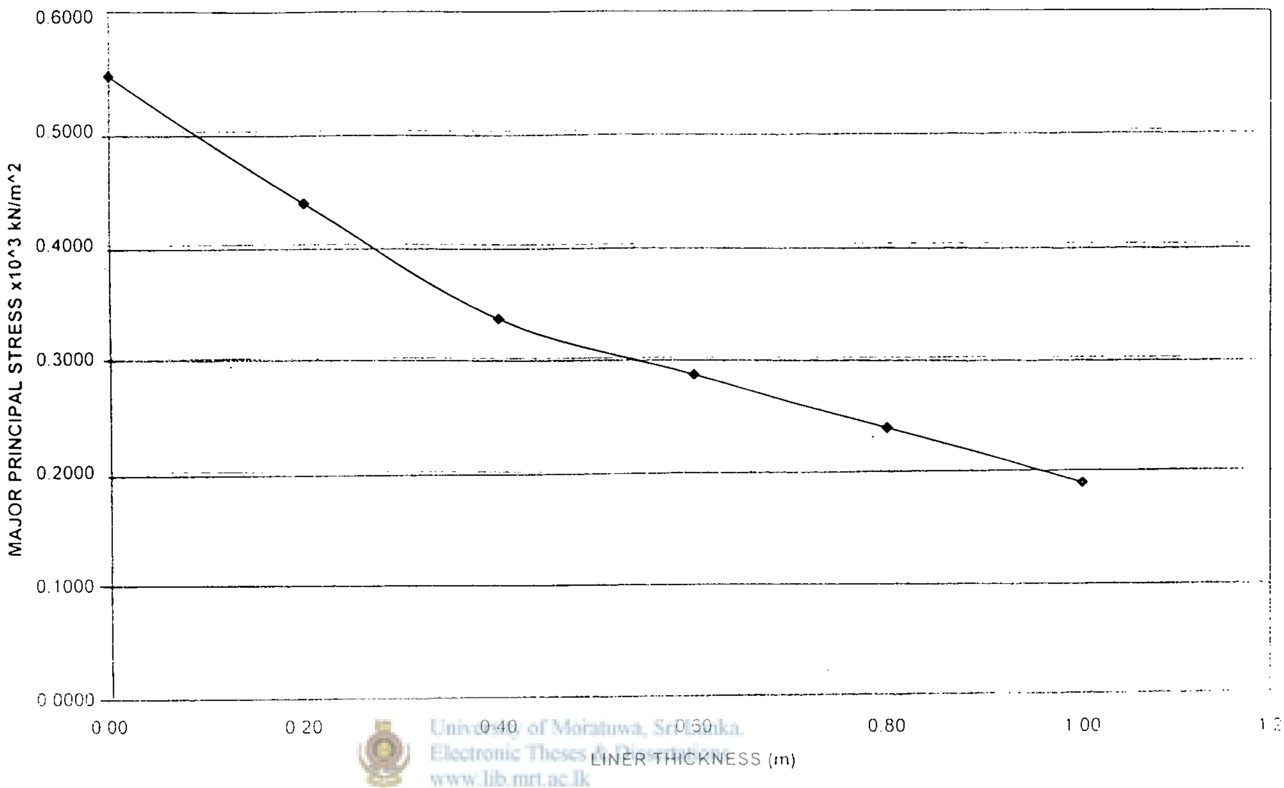

Figure 5.13 Variation of major principal stress with liner thickness
(For element number 21)

LINER THICKNESS(m)	STRESS x10^3 kN/m^2
0.00	0.5478
0.20	0.4358
0.40	0.3345
0.60	0.2848
0.80	0.2379
1.00	0.1891

Table 5.11

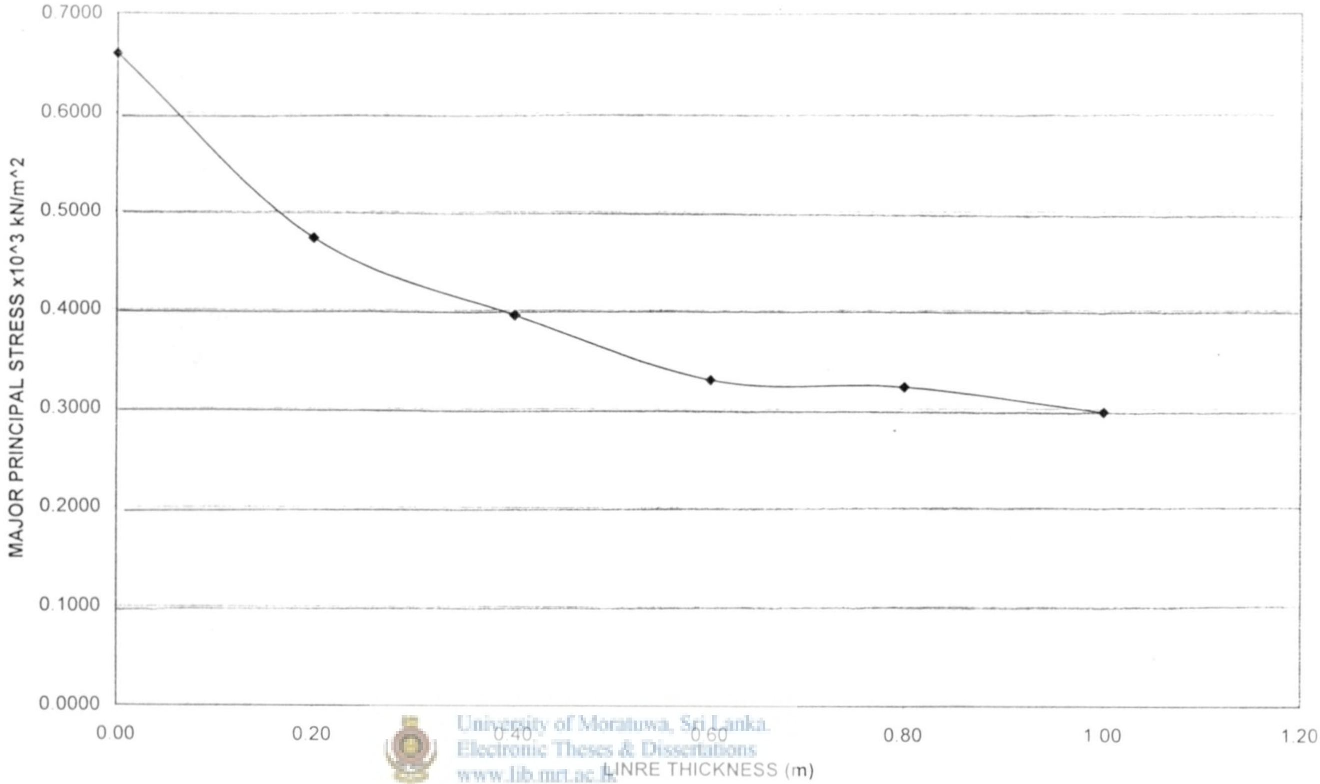

Figure 5.14 Variation of major principal stress with liner thickness
(For element number 26)

LINER THICKNESS(m)	STRESS x10^3 kN/m^2
0.00	0.6593
0.20	0.4726
0.40	0.3947
0.60	0.3288
0.80	0.3220
1.00	0.2964

Table 5.12

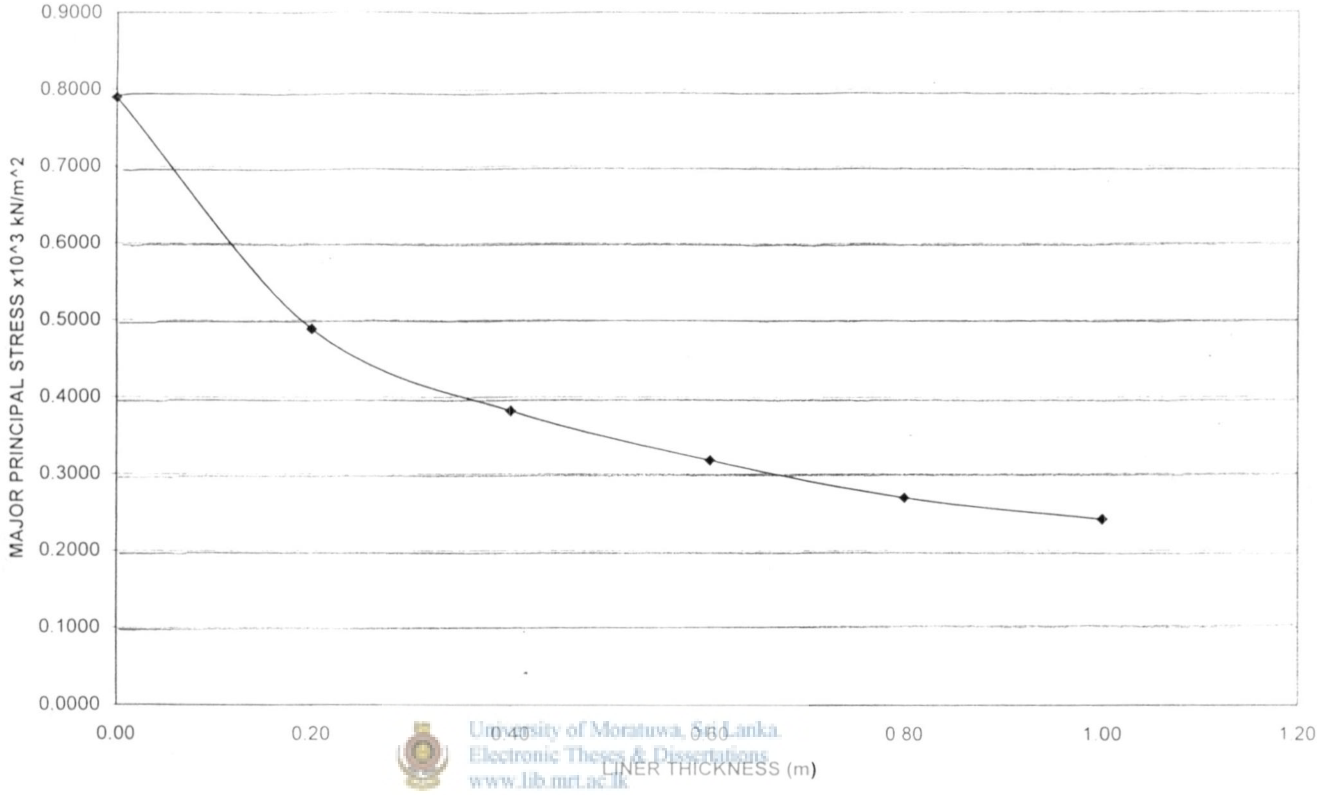

Figure 5.15 Variation of major principal stress with liner thickness
(For element number 36)

LINER THICKNESS(m)	STRESS x10^3 kN/m^2
0.00	0.8015
0.20	0.6006
0.40	0.4074
0.60	0.3313
0.80	0.2942
1.00	0.2447

Table 5.13

CHPTER 6.0

RESULTS FOR ELLIPTICAL TUNNEL a/b =1.500

6.1. Influence of Liner Thickness on Stress and Deformation in Rock Around Tunnel

Principal stresses were investigated along three radial lines AB, CD and EF, shown in figure 6.1 radiating from the center of the tunnel. For the tunnel with a/b = 1.500, variation of the major principal stress along the radial line AB for different liner thicknesses is shown in figure 6.2, and the variation of the minor principal stress along the same line for different liner thicknesses is shown in figure 6.5. Corresponding results for the same tunnel along line CD are shown in figures 6.3 and 6.6, respectively. Figures 6.4 and 6.7, respectively, show the corresponding results for the same tunnel along line EF.

Figure 6.8 shows the circumferential line considered for analysis. Figure 6.9 shows the variation of major principal stress along an elliptical (circumferential) line of a shape similar to that of the tunnel opening, but at some distance inside the rock mass from the tunnel face, as the liner thickness is varied, for the tunnel with a/b = 1.500. The circumferential line along which the stresses shown in figure 6.9 are evaluated is similar to the line GH shown on figure 6.8.

For the elliptical tunnel with a/b = 1.500, influence of the concrete liner thickness on displacement at points inside the rock mass are illustrated by figures 6.10 and 6.11. Figures 6.10 and 6.11 show displacements at points inside the rock mass located along an elliptical (circumferential) line GH, which is shown on the scaled diagram of 6.8.

Figure 6.2, 6.3 & 6.4 show the variation of major principal stress along radical line AB, CD & EF respectively.

In the case of line AB (figure 6.2), for the tunnel a/b=1.500 tensile stress at a point inside the rock(element number 51) when there is no lining, which is 343.4kPa decreases by 14.78% when a liner of thickness of 0.2m is introduced. The corresponding reductions are 29.24% for a liner thickness of 0.4m thickness and 47.26% for a liner of 1.0m.

In the case of line CD (figure 6.3), for the tunnel a/b=1.500 principal stress at a point inside the rock(element number 56) reduce by 24.17% when a liner of thickness of 0.2m is introduced as compared to the stresses in the case of unlined tunnel. The corresponding reductions are 38.48% for a liner thickness of 0.4m thickness and 51.64% for a liner of 1.0m.

In the case of line EF (figure 6.4), for the tunnel a/b=1.500 principal stress at a point inside the rock(element number 60) reduce by38.17% when a liner of thickness of 0.2m is introduced as compared to the stresses in the case of unlined tunnel. The corresponding reductions are 51.69% for a liner thickness of 0.4m thickness and 69.58% for a liner of 1.0m.

The numerical results and the comparison of figures 6.2, 6.3 & 6.4 show that the line EF is the critical line along which maximum major principal stresses occurred.

Figures 6.5, 6.6 and 6.7 show the influence of concrete liner thickness on the compressive principal stress around the tunnel with *a/b* = 1.500. According to Figure (6.8), the compressive principal stress at a point inside the rock closure to point A reduces by 13.52% when a 0.2 m thick concrete is introduced to the originally unlined tunnel; this reduction is 19.33% for a 0.4 m thick liner and 24.66% for a 1.0 m thick liner. Figure 6.6 shows similar behavior of the compressive principal stress along the line CD. Figure 6.7 shows that large percentage stress reductions occur in the case of the compressive principal stress along line EF. This stress reduces at point E by 67.68% when a 0.2 m thick liner is introduced to the unlined tunnel; the corresponding reduction is 71.72% for a 0.4 m thick liner, and 75.26% for a 1.0 m thick liner.

Figures 6.9 & 6.10 shows the variation of major principal stress and minor principal stress along circumferential line GH respectively, which is in rock.

The major principal stress reduction is 14.68% when 0.2m liner is introduced as compared to the stress in the case of unlined tunnel closure to point A. Where as reduction is 28.28% at point E when 0.2m liner is introduced as compared to the stress in the case of an unlined tunnel.

Figure 6.10 shows the minor principal stress variation along line GH. It also shows the same pattern of reduction as in the major principal stress mentioned above.

According to these results in figures 6.11 and 6.12 the percentage reduction of x-displacement and y-displacement over the rock domain varies with the location. figure 6.11 shows relatively large percentage reductions in the x-displacement at the x-axis as the tunnel liner thickness is increased (this is 51.8% when a 0.2 m thick liner is introduced on the unlined tunnel; and about 99% for a 1.0 m thick liner).

Figures 4.13, 4.14 & 4.15 are shows the variation of major principal stress with the introduction of concrete liner on three elements close to point A,C & E respectively.

A further analysis of strain set up in the concrete liner as predicted by the finite element is given in Appendix B.

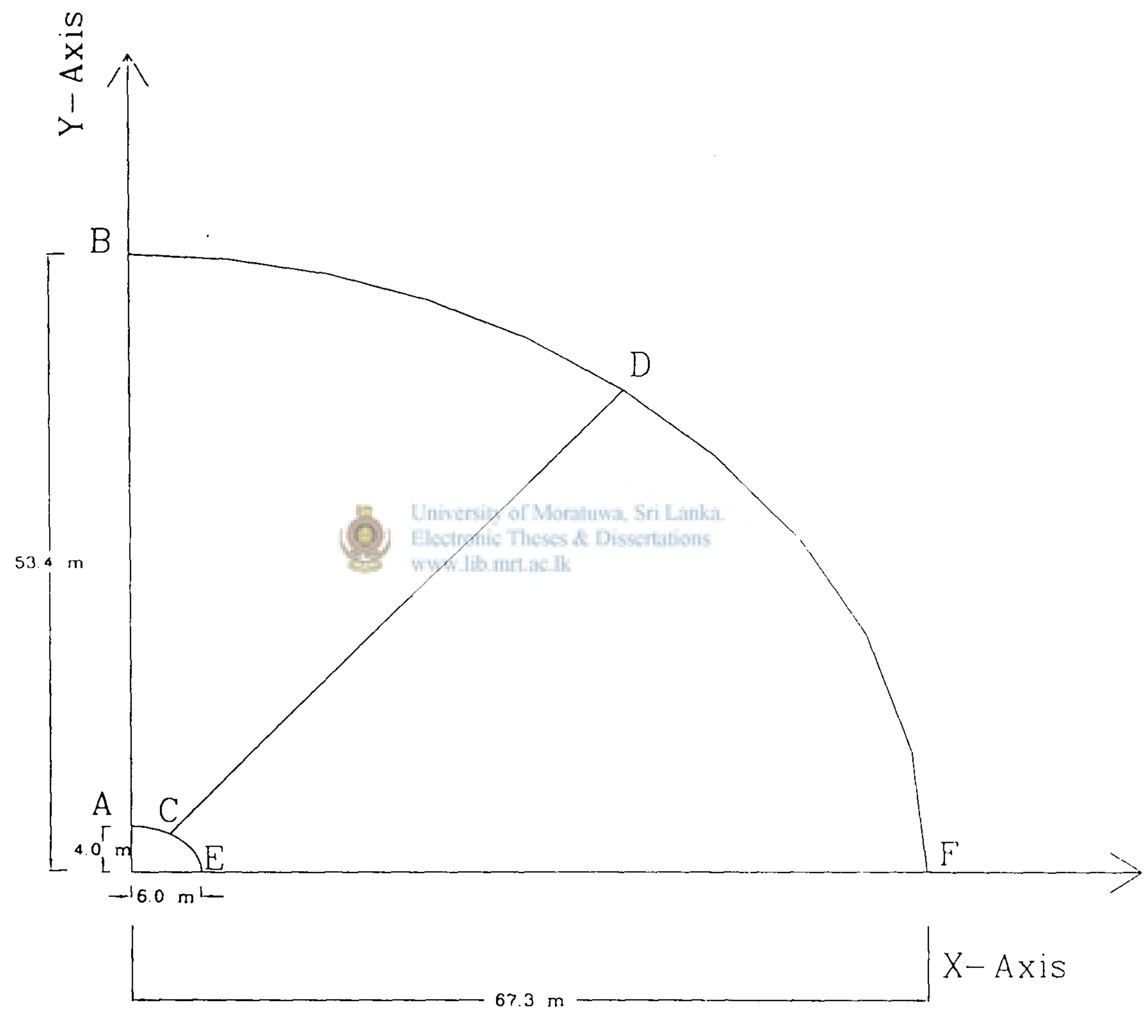

Figure 6.1 Radial lines (For elliptical tunnel-3, a/b = 1.500)

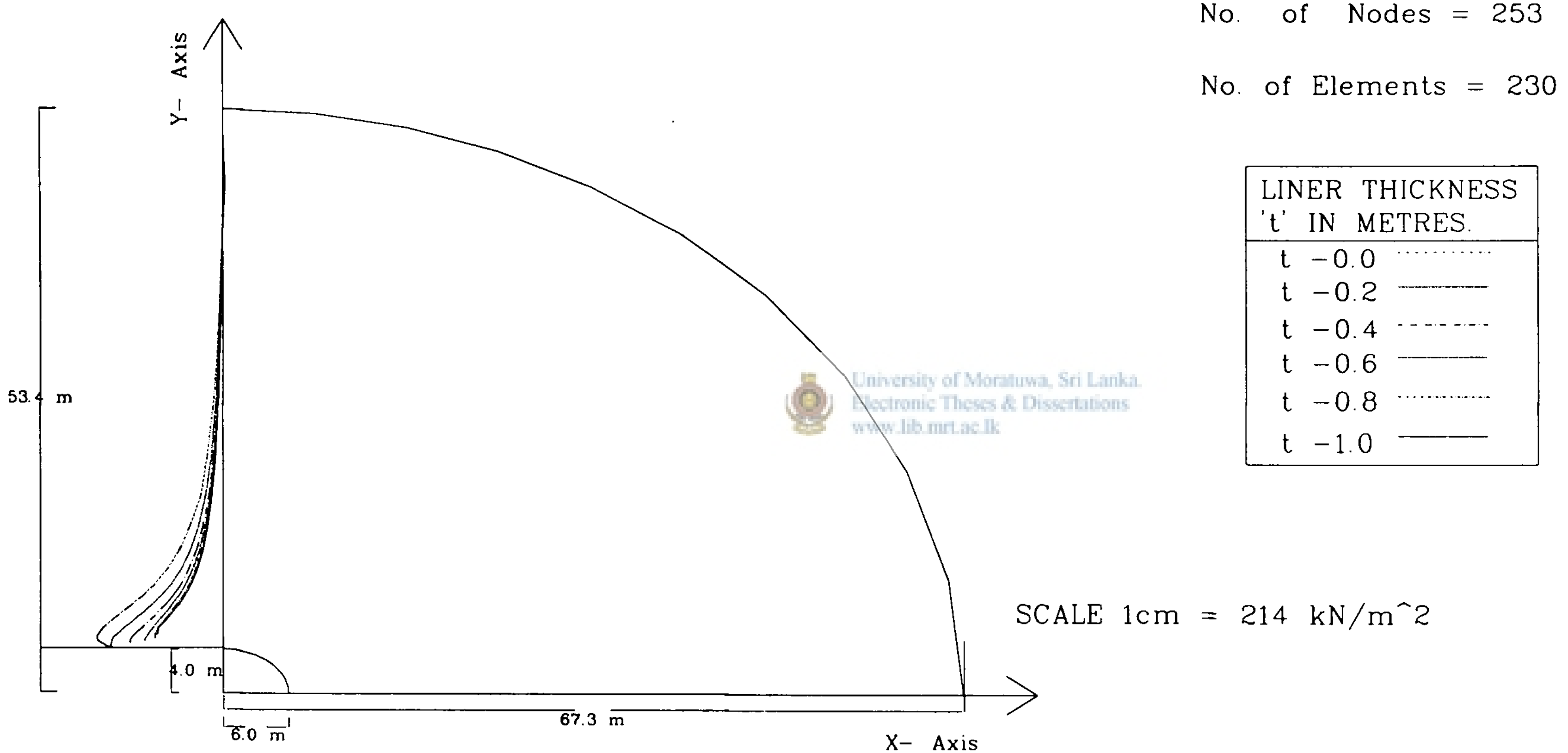

Figure 6.2 Variation of major principal stress along radial line "AB"
(For elliptical tunnel-3, a/b = 1.500)

VARIATION OF MAJOR PRINCIPAL STRESS ALONG RADIAL LINE "AB"
(FOR ELLIPTICAL TUNNEL-3, a/b = 1.500)

ELEMENT NUMBER	MAJOR PRINCIPAL STRESSx10^3 (kN/m^2)						
	LINER THICKNESS (m)						
	t = 0.0	t = 0.2	t = 0.4	t = 0.6	t = 0.8	t =1.0	
1	0.3002	5.0010	3.8490	2.8670	2.2010	1.6880	LINER ELEMENTS
11	0.3212	0.3080	4.2840	3.3230	2.6370	2.1850	
21	0.3308	0.3056	0.2540	3.9600	2.9630	2.5640	
31	0.3409	0.3061	0.2570	0.2162	3.3140	2.9570	
41	0.3449	0.3031	0.2536	0.2132	0.1868	3.1780	
51	0.3434	0.2930	0.2436	0.2069	0.1878	0.1811	
61	0.3300	0.2712	0.2231	0.1928	0.1788	0.1769	
71	0.2967	0.2365	0.1929	0.1690	0.1561	0.1509	
81	0.2579	0.2011	0.1634	0.1443	0.1322	0.1258	
91	0.2213	0.1698	0.1379	0.1220	0.1112	0.1051	
101	0.1891	0.1434	0.1165	0.1032	0.0936	0.0882	
111	0.1564	0.1174	0.0956	0.0848	0.0767	0.0721	
121	0.1209	0.0899	0.0734	0.0651	0.0588	0.0552	
131	0.0904	0.0668	0.0547	0.0486	0.0439	0.0411	
141	0.0645	0.0476	0.0392	0.0349	0.0315	0.0295	
151	0.0441	0.0325	0.0269	0.0241	0.0218	0.0204	
161	0.0273	0.0202	0.0168	0.0151	0.0137	0.0129	
171	0.0163	0.0122	0.0103	0.0093	0.0085	0.0080	
181	0.0086	0.0064	0.0055	0.0055	0.0046	0.0043	
191	0.0027	0.0020	0.0017	0.0017	0.0014	0.0014	
200	0.0002	-0.0713	-0.0006	-0.0006	-0.0023	0.0004	
210	-0.0018	-0.0013	-0.0009	-0.0009	-0.0006	-0.0003	

Table 6.1

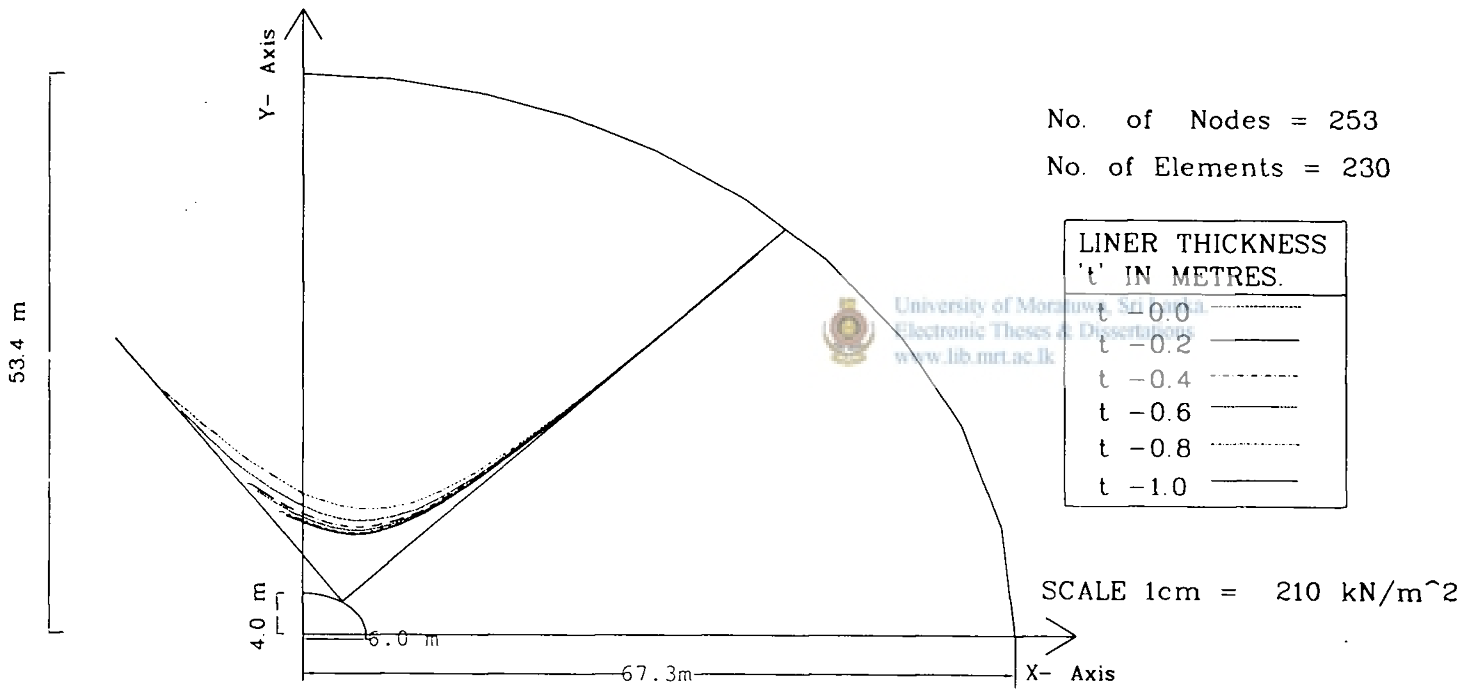

Figure 6.3 Variation of major principal stress along radial line "CD"
(For elliptical tunnel-3, a/b = 1.500)

VARIATION OF MAJOR PRINCIPAL STRESS ALONG RADIAL LINE "CD"
(FOR ELLIPTICAL TUNNEL-3, a/b = 1.500)

ELEMENT NUMBER	MAJOR PRINCIPAL STRESS$\times 10^3$ (kN/m^2)						
	LINER THICKNESS (m)						
	t = 0.0	t = 0.2	t = 0.4	t = 0.6	t = 0.8	t =1.0	
6	0.7990	9.9410	6.2190	5.0880	4.1000	3.5880	LINER ELEMENTS
16	0.7842	0.7144	5.8550	4.8480	3.8690	3.4300	
26	0.7369	0.6181	0.4356	4.7030	3.6670	3.2850	
36	0.7100	0.5635	0.4290	0.4017	3.6440	3.2930	
46	0.6500	0.5134	0.4085	0.3827	0.3137	3.2090	
56	0.6048	0.4586	0.3721	0.3453	0.3064	0.2925	
66	0.5004	0.3737	0.3101	0.2859	0.2646	0.2535	
76	0.4048	0.3012	0.2518	0.2301	0.2128	0.2038	
86	0.3182	0.2353	0.1982	0.1809	0.1674	0.1601	
96	0.2582	0.1902	0.1603	0.1457	0.1343	0.1280	
106	0.2108	0.1550	0.1307	0.1187	0.1093	0.1040	
116	0.1688	0.1241	0.1047	0.0950	0.0873	0.0829	
126	0.1242	0.0921	0.0770	0.0698	0.0641	0.0608	
136	0.0874	0.0630	0.0538	0.0486	0.0445	0.0421	
146	0.0606	0.0443	0.0372	0.0336	0.0307	0.0290	
156	0.0387	0.0282	0.0235	0.0211	0.0193	0.0182	
166	0.0224	0.0161	0.0133	0.0119	0.0108	0.0101	
176	0.0119	0.0085	0.0069	0.0062	0.0055	0.0052	
186	0.0056	0.0039	0.0031	0.0027	0.0024	0.0023	
196	0.0012	0.0008	0.0006	0.0005	0.0004	0.0004	
206	-0.0016	-0.0011	-0.0009	-0.0008	-0.0007	-0.0006	
216	-0.0027	-0.0018	-0.0013	-0.0011	-0.0009	-0.0007	

Table 6.2

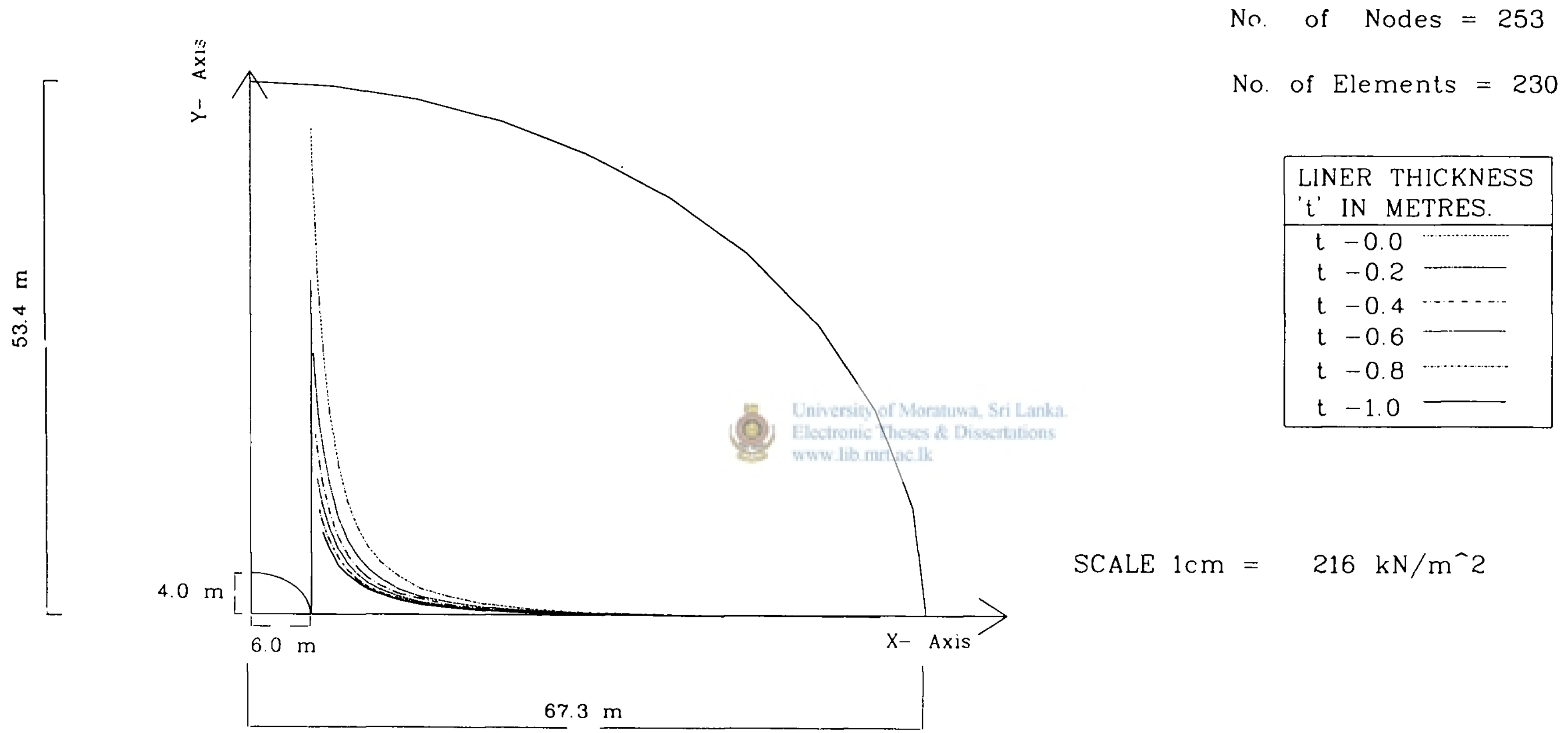

Figure 6.4 Variation of major principal stress along radial line "EF"
(For elliptical tunnel-3, a/b = 1.500)

VARIATION OF MAJOR PRINCIPAL STRESS ALONG RADIAL LINE "EF"
(FOR ELLIPTICAL TUNNEL-3, a/b = 1.500)

ELEMENT NUMBER	MAJOR PRINCIPAL STRESSx10^3 (kN/m^2)						
	LINER THICKNESS (m)						
	t = 0.0	t = 0.2	t = 0.4	t = 0.6	t = 0.8	t =1.0	
10	1.4620	1.0500	7.9680	6.9480	6.3130	5.9540	LINER ELEMENTS
20	1.3050	0.7786	6.4570	5.5680	5.0830	4.8010	
30	1.1610	0.6947	0.5317	4.3630	4.0380	3.8260	
40	1.0290	0.6245	0.4843	0.3970	3.1400	2.9980	
50	0.9317	0.5675	0.4404	0.3626	0.3048	2.2000	
60	0.7897	0.4883	0.3815	0.3176	0.2683	0.2402	
70	0.6048	0.3815	0.2999	0.2526	0.2149	0.1918	
80	0.4372	0.2829	0.2240	0.1909	0.1643	0.1481	
90	0.3243	0.2141	0.1701	0.1459	0.1264	0.1147	
100	0.2493	0.1672	0.1333	0.1150	0.1002	0.0915	
110	0.1982	0.1342	0.1071	0.0926	0.0809	0.0741	
120	0.1534	0.1048	0.0837	0.0726	0.0636	0.0584	
130	0.1121	0.0770	0.0614	0.0532	0.0466	0.0428	
140	0.0751	0.0520	0.0458	0.0362	0.0320	0.0296	
150	0.0530	0.0366	0.0290	0.0251	0.0221	0.0204	
160	0.0320	0.0221	0.0173	0.0149	0.0130	0.0120	
170	0.0178	0.0122	0.0093	0.0079	0.0068	0.0063	
180	0.0089	0.0059	0.0043	0.0036	0.0031	0.0030	
190	0.0038	0.0024	0.0016	0.0013	0.0012	0.0014	
200	0.0002	-0.0713	-0.0002	-0.0002	-0.0023	0.0004	
210	-0.0018	-0.0013	-0.0001	-0.0008	-0.0006	-0.0003	
220	-0.0022	-0.0014	-0.0009	-0.0006	-0.0004	-0.0003	

Table 6.3

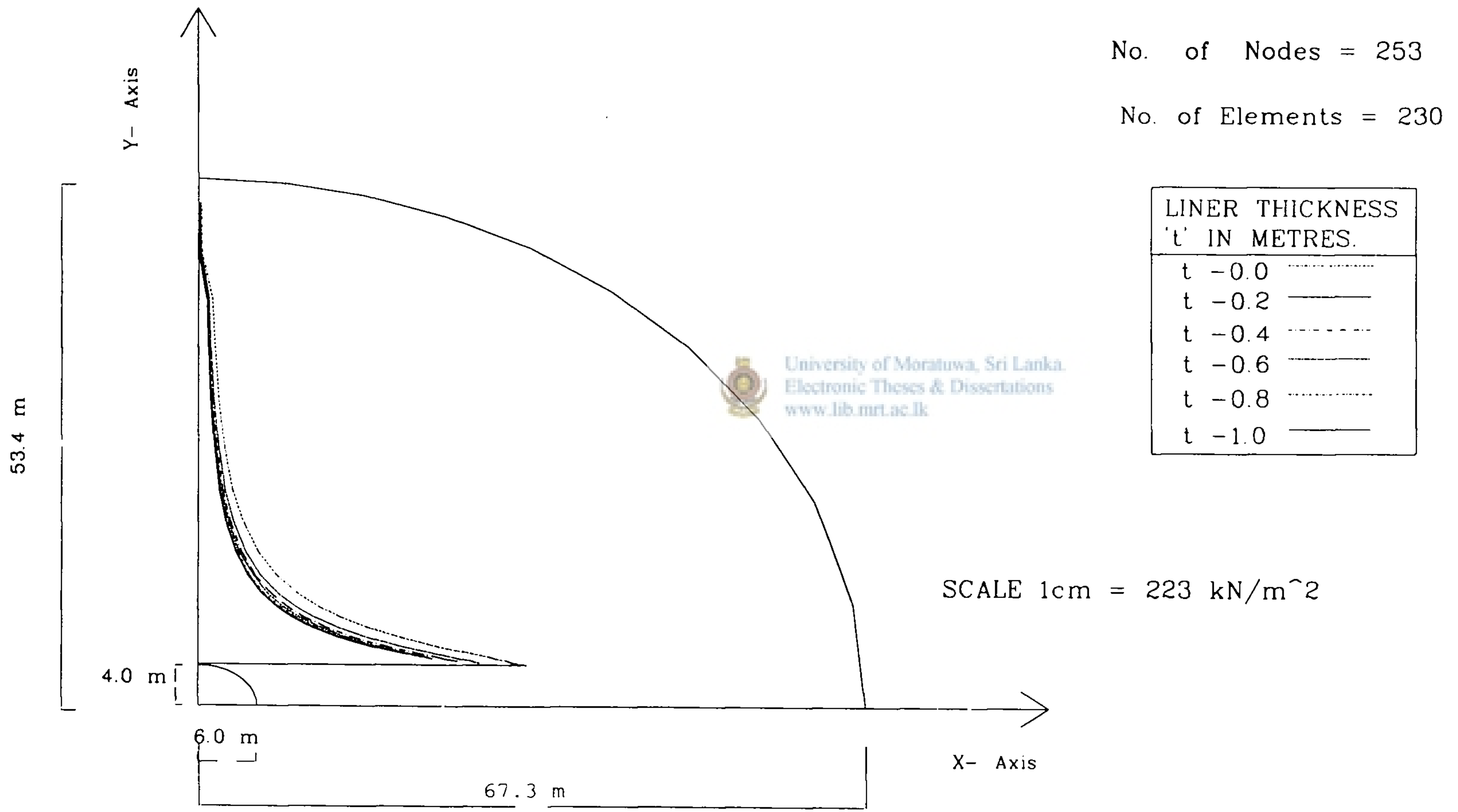

Figure 6.5 Variation of minor principal stress along radial line "AB"
(For elliptical tunnel-3, a/b = 1.500)

VARIATION OF MINOR PRINCIPAL STRESS ALONG RADIAL LINE "AB"
(FOR ELLIPTICAL TUNNEL-3, a/b = 1.500)

ELEMENT NUMBER	MINOR PRINCIPAL STRESSx(-1X10^3) (kN/m^2)						
	LINER THICKNESS (m)						
	t = 0.0	t = 0.2	t = 0.4	t = 0.6	t = 0.8	t =1.0	
1	1.0020	1.0890	1.1130	1.0970	1.1070	1.1230	LINER ELEMENTS
11	0.9551	0.8537	0.8046	0.8160	0.8523	0.8685	
21	0.9380	0.8319	0.7890	0.8180	0.8821	0.9187	
31	0.9046	0.7956	0.7500	0.7132	0.7444	0.7869	
41	0.8850	0.7740	0.7278	0.6921	0.6824	0.7912	
51	0.8310	0.7187	0.6704	0.6369	0.6284	0.6261	
61	0.7307	0.6211	0.5748	0.5498	0.5364	0.5284	
71	0.6190	0.5172	0.4757	0.4551	0.4403	0.4290	
81	0.5181	0.4268	0.3912	0.3738	0.3594	0.3485	
91	0.4364	0.3554	0.3253	0.3102	0.2970	0.2873	
101	0.3711	0.2997	0.2740	0.2609	0.2490	0.2405	
111	0.3059	0.2452	0.2240	0.2129	0.2027	0.1955	
121	0.2407	0.1915	0.1748	0.1695	0.1575	0.1517	
131	0.1848	0.1461	0.1333	0.1262	0.1195	0.1150	
141	0.1419	0.1116	0.1017	0.0961	0.0909	0.0873	
151	0.1049	0.0822	0.0748	0.0705	0.0666	0.0639	
161	0.0794	0.0620	0.0563	0.0531	0.0500	0.0479	
171	0.0619	0.0482	0.0437	0.0411	0.0387	0.0371	
181	0.0513	0.0398	0.0361	0.0339	0.0319	0.0305	
191	0.0440	0.0341	0.0309	0.0290	0.0272	0.0260	
200	0.0121	0.0068	0.0033	0.0017	0.0007	0.0005	
210	0.0106	0.0062	0.0034	0.0018	0.0011	0.0008	

Table 6.4

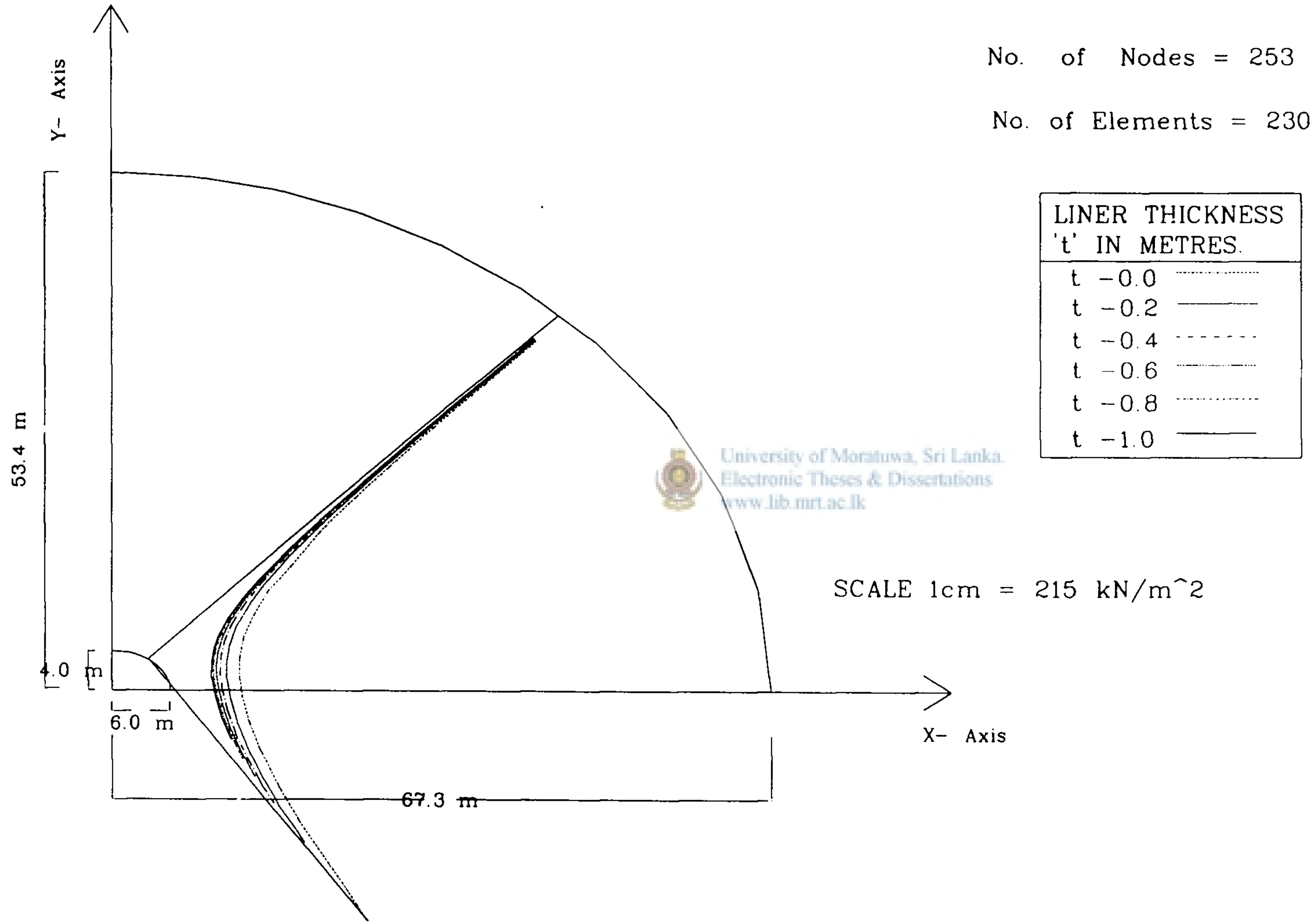

Figure 6.6 Variation of minor principal stress along radial line "CD"
(For elliptical tunnel-3, a/b = 1.500)

VARIATION OF MINOR PRINCIPAL STRESS ALONG RADIAL LINE "CD"
(FOR ELLIPTICAL TUNNEL-3, a/b = 1.500)

ELEMENT NUMBER	MINOR PRINCIPAL STRESSx($-1X10^3$) (kN/m^2)						
	LINER THICKNESS (m)						
	t = 0.0	t = 0.2	t = 0.4	t = 0.6	t = 0.8	t =1.0	
6	1.0450	0.6004	0.7902	0.8159	0.8749	0.8976	LINER ELEMENTS
16	0.9792	0.7335	0.7847	0.7441	0.8044	0.8139	
26	0.9285	0.6893	0.5849	0.6354	0.7079	0.7237	
36	0.8046	0.6005	0.5231	0.4845	0.3844	0.4132	
46	0.7772	0.5749	0.4922	0.4533	0.4216	0.3934	
56	0.6766	0.5036	0.4345	0.4002	0.3732	0.3538	
66	0.5571	0.4129	0.3529	0.3217	0.2974	0.2824	
76	0.4367	0.3250	0.2780	0.2526	0.2334	0.2221	
86	0.3439	0.2542	0.2150	0.1938	0.1775	0.1638	
96	0.2752	0.2029	0.1710	0.1538	0.1405	0.1329	
106	0.2285	0.1675	0.1403	0.1257	0.1144	0.1079	
116	0.1837	0.1338	0.1113	0.0993	0.0900	0.0847	
126	0.1390	0.1011	0.0840	0.0749	0.0679	0.0638	
136	0.1070	0.0776	0.0632	0.0560	0.0503	0.0471	
146	0.0799	0.0576	0.0473	0.0419	0.0377	0.0352	
156	0.0970	0.0427	0.0347	0.0306	0.0273	0.0255	
166	0.0443	0.0316	0.0255	0.0223	0.0198	0.0184	
176	0.0345	0.0245	0.0196	0.0171	0.0152	0.0140	
186	0.0285	0.0201	0.0161	0.0140	0.0123	0.0114	
196	0.0338	0.0168	0.0133	0.0115	0.0102	0.0094	
206	0.0205	0.0145	0.0115	0.0099	0.0087	0.0080	
216	0.0183	0.0129	0.0102	0.0089	0.0078	0.0071	

Table 6.5

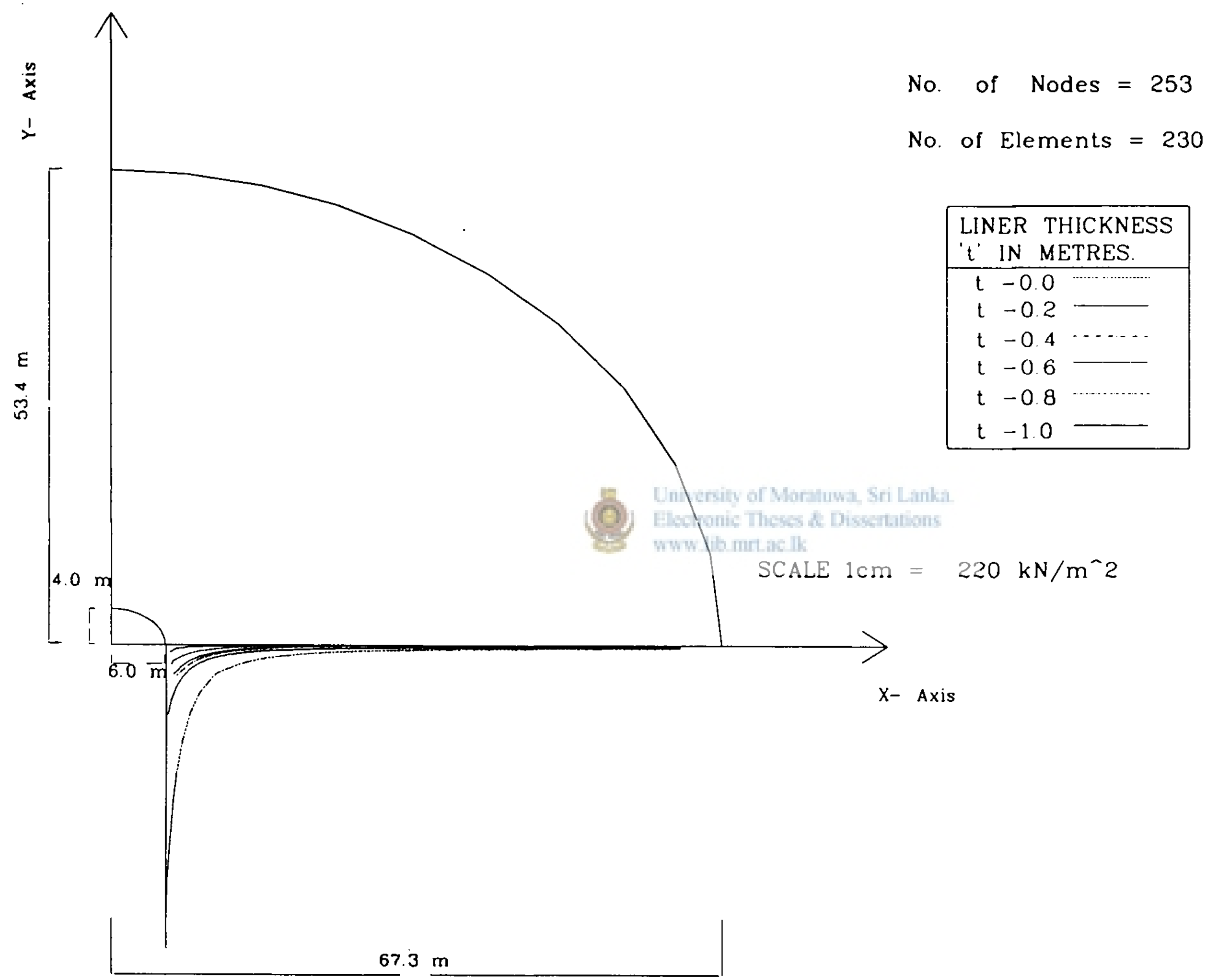

Figure 6.7 Variation of minor principal stress along radial line "EF"
(For elliptical tunnel-3, a/b = 1.500)

VARIATION OF MINOR PRINCIPAL STRESS ALONG RADIAL LINE "EF"
(FOR ELLIPTICAL TUNNEL-3, a/b = 1.500)

ELEMENT NUMBER	MINOR PRINCIPAL STRESSx($-1X10^3$) (kN/m^2)						
	LINER THICKNESS (m)						
	t = 0.0	t = 0.2	t = 0.4	t = 0.6	t = 0.8	t =1.0	
10	0.9234	0.4399	0.5236	0.5765	0.6123	0.6339	LINER ELEMENTS
20	0.7544	0.2300	0.1588	0.2711	0.3332	0.3679	
30	0.6593	0.2029	0.0239	0.0370	0.1163	0.1614	
40	0.5925	0.1774	0.0109	0.0653	0.1639	0.1045	
50	0.5103	0.1629	0.0177	0.0524	0.0988	0.7631	
60	0.4243	0.1374	0.0120	0.0483	0.0892	0.1035	
70	0.3129	0.1075	0.0098	0.0369	0.0692	0.0837	
80	0.2184	0.0792	0.0064	0.0278	0.0516	0.0627	
90	0.1584	0.0608	0.0055	0.0202	0.0382	0.0467	
100	0.1215	0.0480	0.0039	0.0165	0.0307	0.0372	
110	0.0972	0.0398	0.0039	0.0126	0.0242	0.0295	
120	0.0770	0.0325	0.0037	0.0096	0.0189	0.0231	
130	0.0584	0.0255	0.0034	0.0068	0.0138	0.0171	
140	0.0436	0.0195	0.0029	0.0047	0.0099	0.0122	
150	0.0339	0.0162	0.0039	0.0018	0.0056	0.0074	
160	0.0254	0.0123	0.0030	0.0013	0.0043	0.0056	
170	0.0197	0.0099	0.0030	0.0002	0.0024	0.0033	
180	0.0161	0.0084	0.0031	0.0006	0.0010	0.0016	
190	0.0140	0.0076	0.0032	0.0012	0.0001	0.0004	
200	0.0121	0.0068	0.0033	0.0016	0.0007	0.0005	
210	0.0106	0.0062	0.0034	0.0020	0.0011	0.0008	
220	0.0095	0.0057	0.0033	0.0021	0.0012	0.0008	

Table 6.6

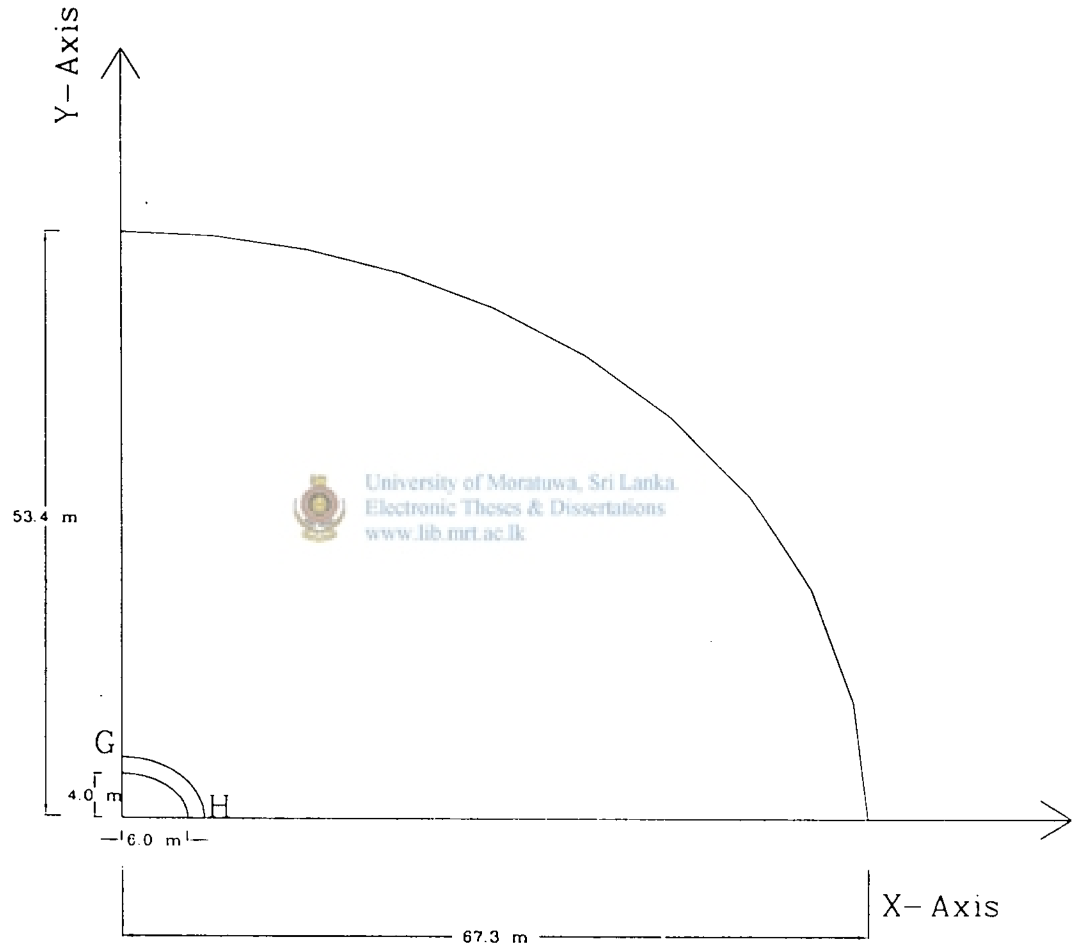

Figure 6.8 Circumferential lines (For elliptical tunnel-3, a/b = 1.500)

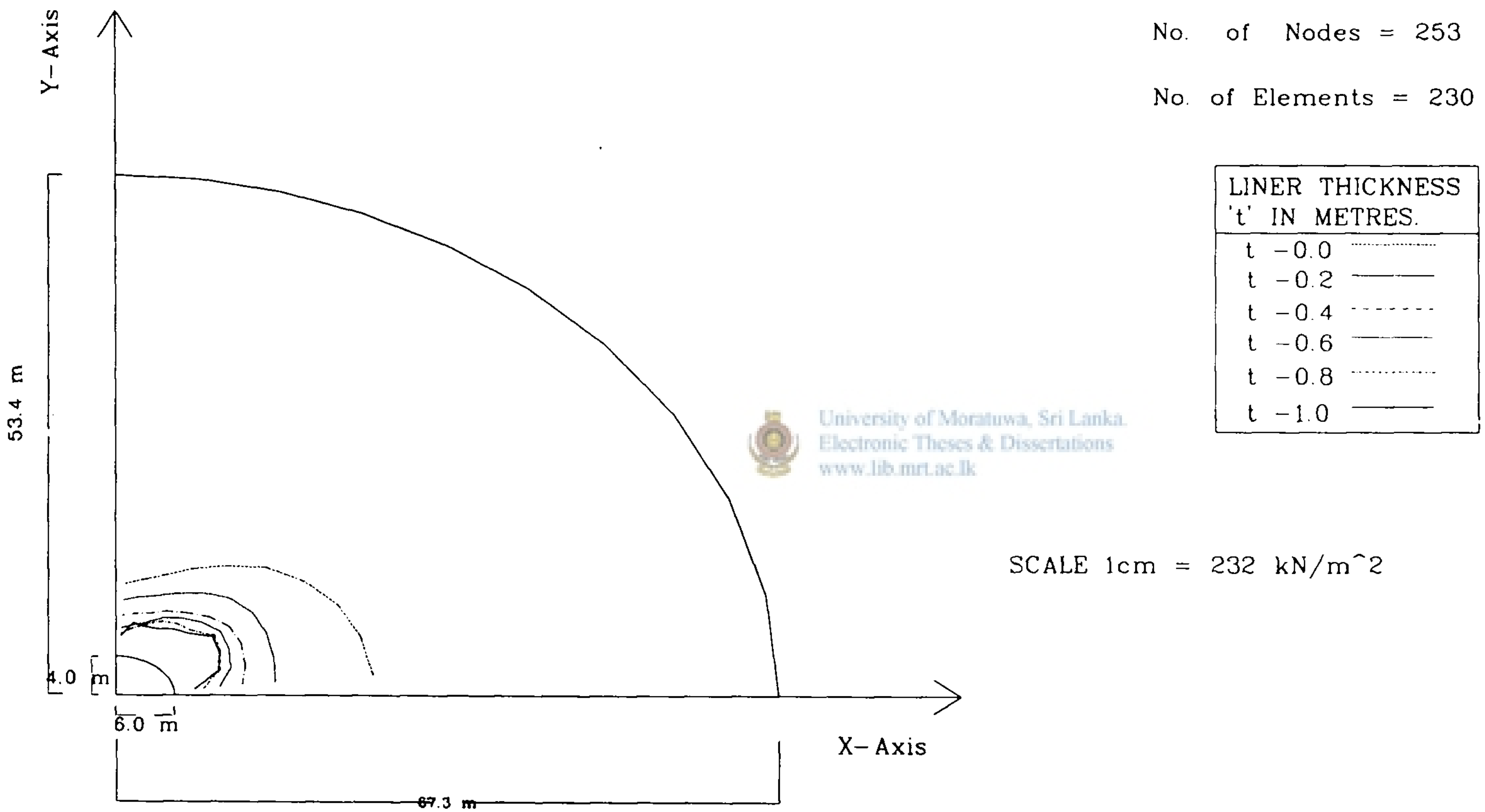

Figure 6.9 Variation of major principal stress along circumferential line "GH"
(For elliptical tunnel-3, a/b = 1.500)

VARIATION OF MAJOR PRINCIPAL STRESS ALONG CIRCUMFERENTIAL LINE "GH"
(FOR ELLIPTICAL TUNNEL3, a/b = 1.500)

ELEMENT NUMBER	MAJOR PRINCIPAL STRESSx10^3 (kN/m^2)					
	LINER THICKNESS (m)					
	t = 0.0	t = 0.2	t = 0.4	t = 0.6	t = 0.8	t =1.0
51	0.3434	0.2930	0.2463	0.2069	0.1878	0.1811
52	0.3671	0.3110	0.2583	0.2218	0.2110	0.2293
53	0.3998	0.3317	0.2735	0.2426	0.2353	0.2288
54	0.4566	0.3711	0.3027	0.2784	0.2667	0.2430
55	0.5223	0.4133	0.3335	0.3109	0.2880	0.2672
56	0.6048	0.4586	0.3721	0.3453	0.3064	0.2925
57	0.6736	0.4881	0.4059	0.3737	0.3534	0.3460
58	0.7336	0.4978	0.4149	0.3741	0.3467	0.3418
59	0.7699	0.4972	0.4060	0.3601	0.3262	0.3200
60	0.7897	0.4883	0.3815	0.3176	0.2683	0.2402

Table 6.7

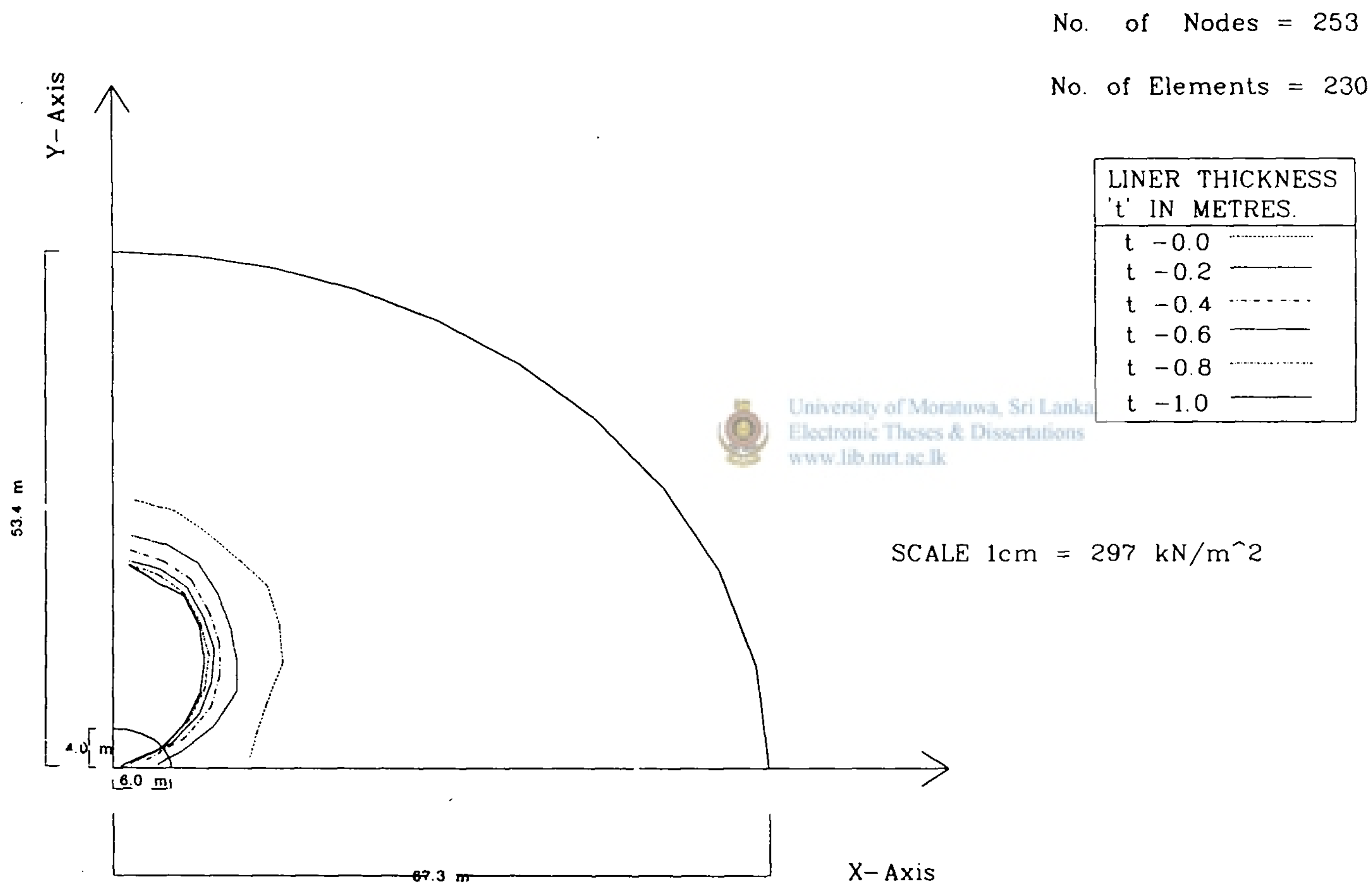

Figure 6.10 Variation of minor principal stress along circumferential line "GH"
(For elliptical tunnel-3, a/b = 1.500)

VARIATION OF MINOR PRINCIPAL STRESS ALONG CIRCUMFERENTIAL LINE "GH"
(FOR ELLIPTICAL TUNNEL3, a/b = 1.500)

ELEMENT NUMBER	MINOR PRINCIPAL STRESSx10^3 (kN/m^2)					
	LINER THICKNESS (m)					
	t = 0.0	t = 0.2	t = 0.4	t = 0.6	t = 0.8	t =1.0
51	0.8310	0.7187	0.6704	0.6396	0.6284	0.6261
52	0.8176	0.7080	0.6561	0.6294	0.6109	0.5864
53	0.7951	0.6844	0.6279	0.6002	0.5797	0.5738
54	0.7501	0.6247	0.5659	0.5391	0.5198	0.5097
55	0.7358	0.5611	0.5067	0.4814	0.4567	0.4345
56	0.6766	0.5030	0.4345	0.4002	0.3732	0.3538
57	0.6148	0.4492	0.3537	0.3116	0.2713	0.2567
58	0.5132	0.3395	0.2406	0.1956	0.1674	0.1586
59	0.4562	0.2184	0.1058	0.0541	0.0231	0.0196
60	0.4243	0.1374	0.0120	0.0483	0.0892	0.1035

Table 6.8

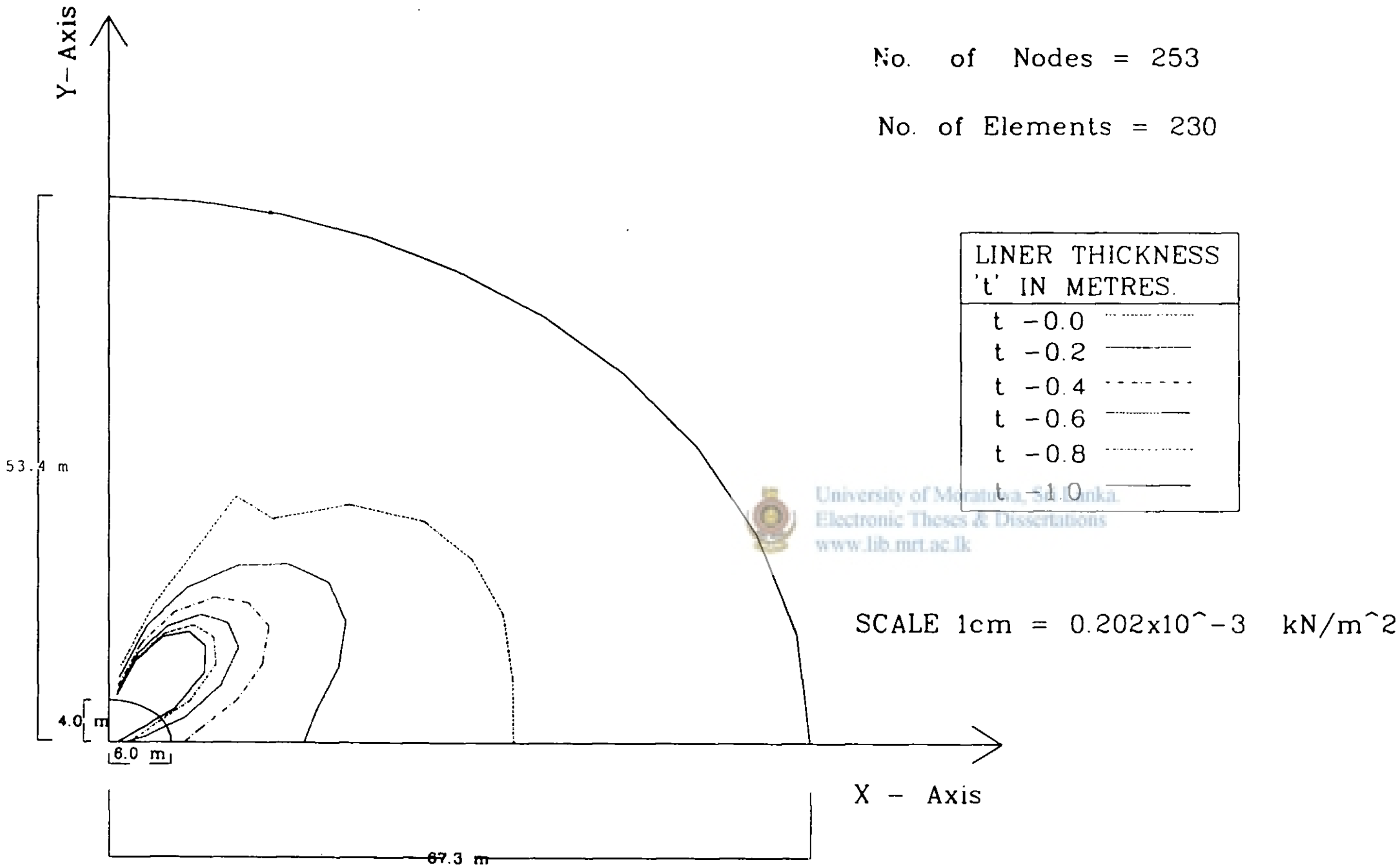

Figure 6.11 Variation of "x" displacement along circumferential line "GH"
(For elliptical tunnel-3, a/b = 1.500)

VARIATION OF "X" DISPLACEMENT ALONG CIRCUMFERENTIAL LINE "GH"
(FOR ELLIPTICAL TUNNEL3, a/b = 1.500)

NODE NUMBER	DISPLACEMEN x 10^{-3} (m)					
	LINER THICKNESS (m)					
	t = 0.0	t = 0.2	t = 0.4	t = 0.6	t = 0.8	t =1.0
67	0.0000	0.0000	0.0000	0.0000	0.0000	0.0000
68	0.2210	0.1862	0.1606	0.1438	0.1361	0.1350
69	0.4154	0.3476	0.2967	0.2654	0.2497	0.2440
70	0.6156	0.5027	0.4201	0.3737	0.3484	0.3379
71	0.8069	0.6352	0.5155	0.4535	0.4145	0.3927
72	0.9831	0.7326	0.5679	0.4850	0.4262	0.3918
73	1.1110	0.7872	0.5687	0.4617	0.3806	0.3386
74	1.1780	0.7694	0.4959	0.3622	0.2614	0.2115
75	1.1980	0.6995	0.3852	0.2308	0.1171	0.0607
76	1.1810	0.6084	0.2706	0.1065	-0.0135	-0.0754
77	1.1690	0.5635	0.2175	0.0497	-0.0723	-0.0137

Table 6.9

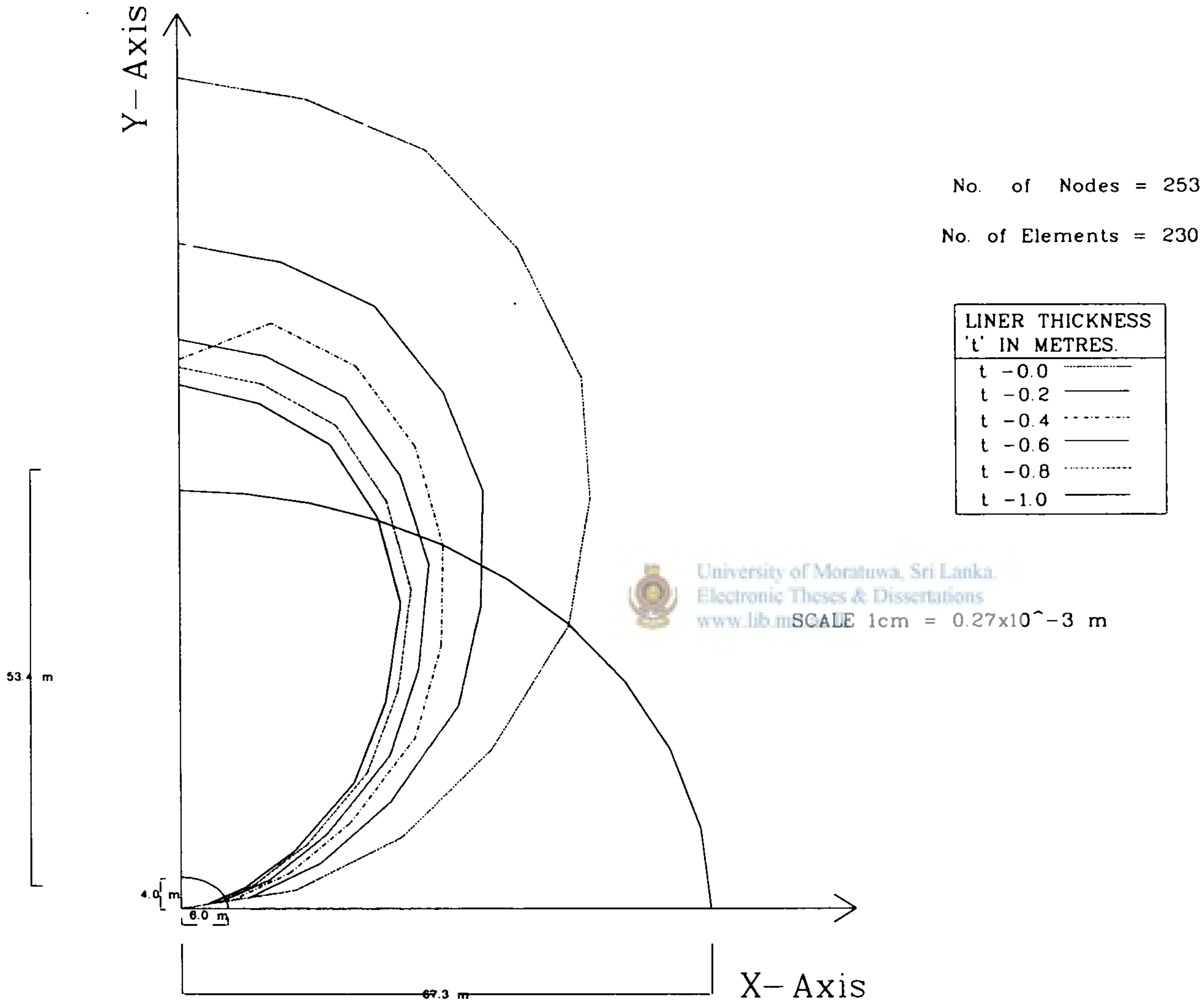

Figure 6.12 Variation of "y" displacement along circumferential line "GH"
(For elliptical tunnel-3, a/b = 1.500)

VARIATION OF "Y" DISPLACEMENT CIRCUMFERENTIAL LINE "GH"
(FOR ELLIPTICAL TUNNEL3, a/b = 1.500)

NODE NUMBER	"Y" DISPLACEMENT X10^{-3} (m)					
	LINER THICKNESS (m)					
	t = 0.0	t = 0.2	t = 0.4	t = 0.6	t = 0.8	t =1.0
67	3.2030	2.5640	2.3230	2.1930	2.0850	2.0170
68	3.1650	2.5260	2.2850	2.1550	2.0450	1.9670
69	0.3080	2.4410	2.1980	2.0690	1.9530	1.8740
70	2.8600	2.2310	1.9930	1.8650	1.7490	1.6750
71	2.6040	1.9790	1.7500	1.6230	1.5060	1.1438
72	2.2220	1.6300	1.4170	1.2910	1.1810	1.1120
73	1.8510	1.3160	1.1110	0.9906	0.0886	0.8241
74	1.3340	0.9020	0.7312	0.6296	0.5434	0.4980
75	0.8911	0.5657	0.4381	0.3624	0.2991	0.2572
76	0.4476	0.2672	0.1980	0.1574	0.1242	0.1001
77	0.0000	0.0000	0.0000	0.0000	0.0000	0.0000

Table 6.10

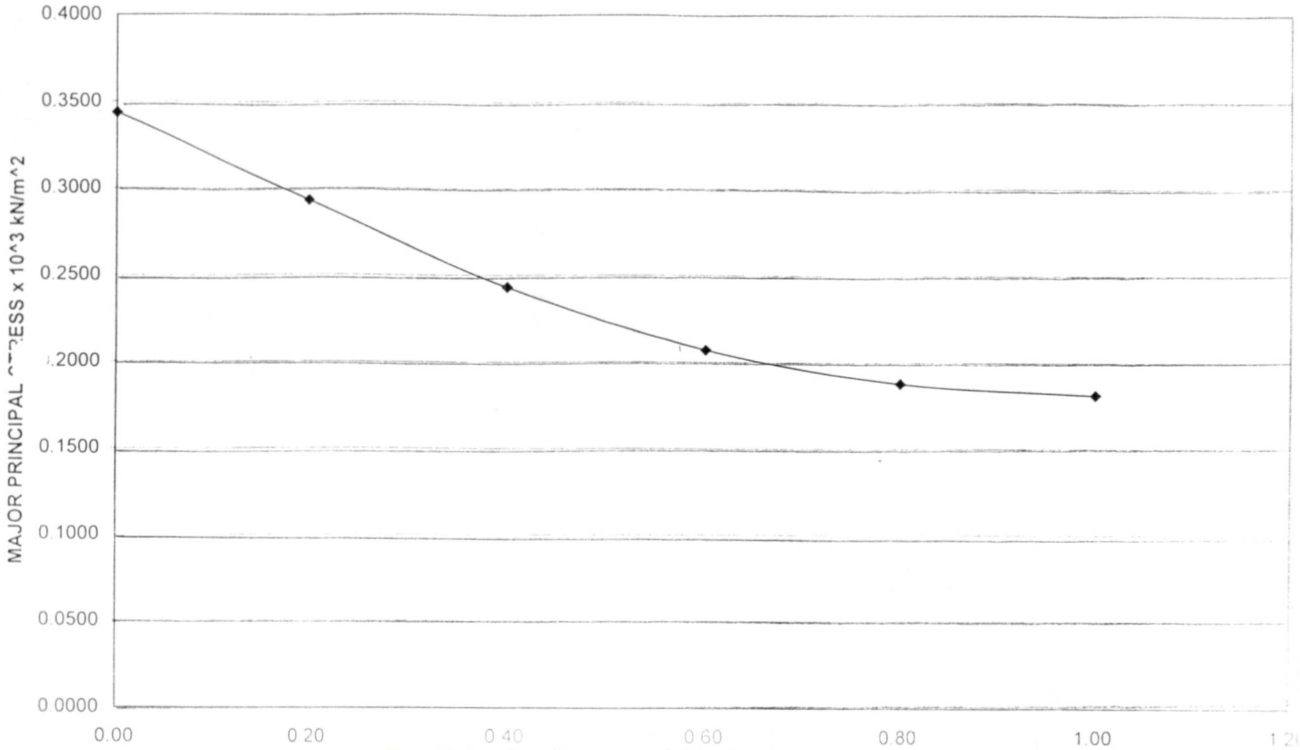

Figure 6.13 Variation of major principal stress with liner thickness
(For element number 51)

LINER THICKNESS(m)	STRESS x10^3 kN/m^2
0.00	0.3434
0.20	0.2930
0.40	0.2430
0.60	0.2069
0.80	0.1878
1.00	0.1811

Table 6.11

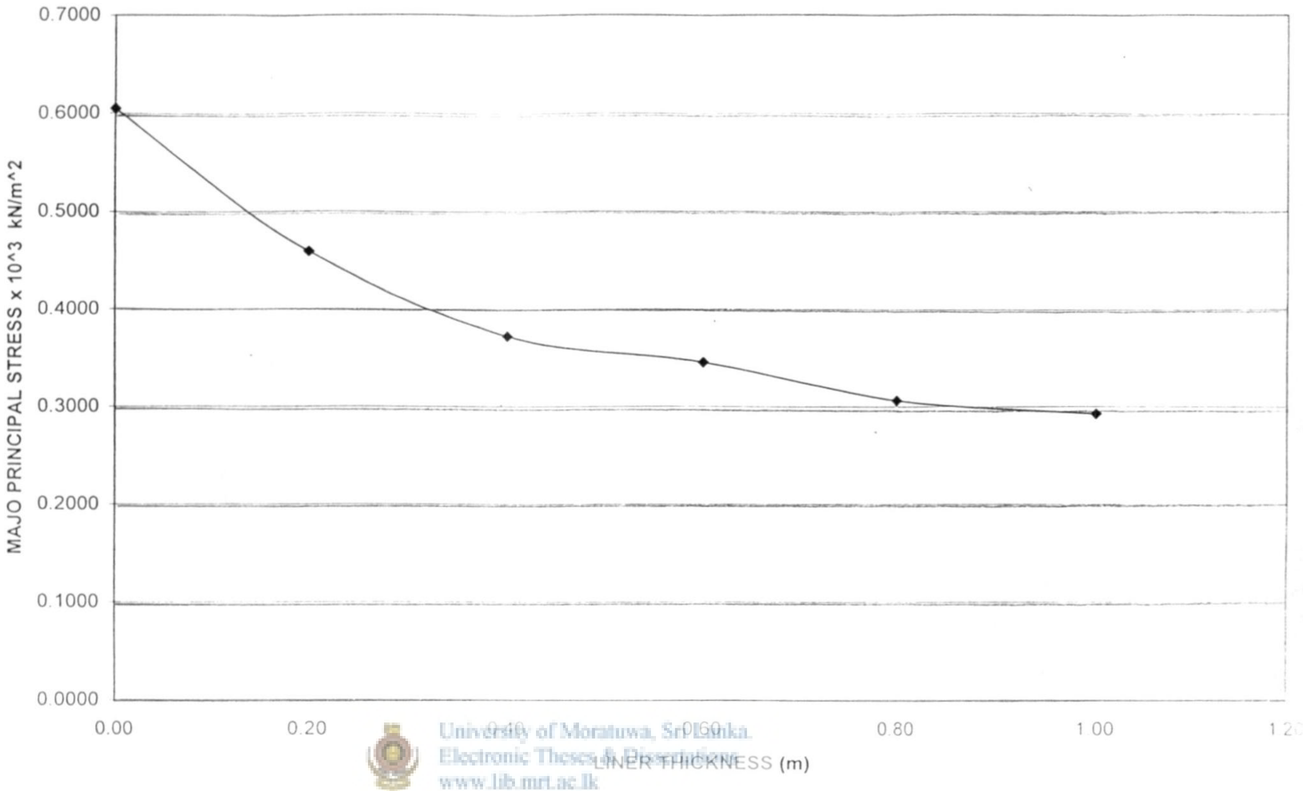

Figure 6.14 Variation of major principal stress with liner thickness
(For element number 56)

LINER THICKNESS(m)	STRESS x10^3 kN/m^2
0.00	0.6048
0.20	0.4586
0.40	0.3721
0.60	0.3453
0.80	0.3064
1.00	0.2925

Table 6.12

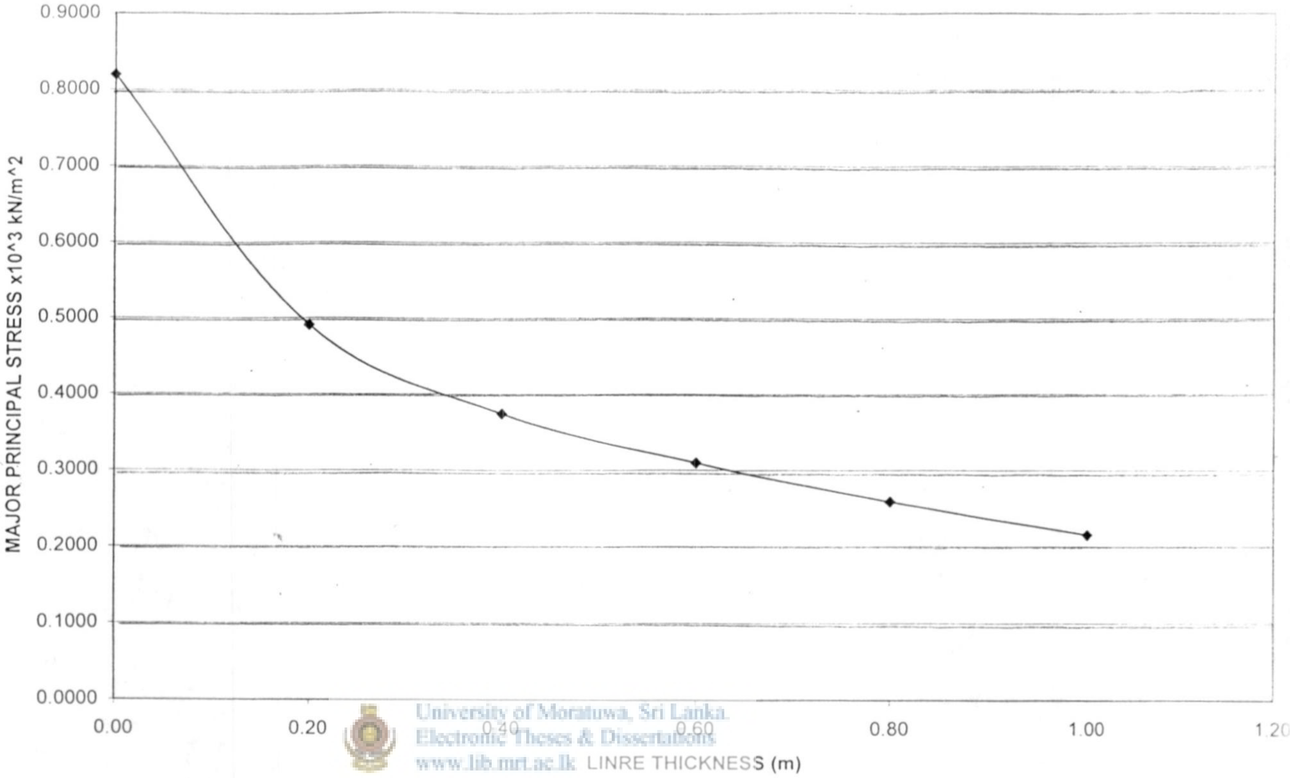

Figure 6.15 Variation of major principal stress with liner thickness
(For element number 60)

LINER THICKNESS(m)	STRESS x10^3 kN/m^2
0.00	0.7897
0.20	0.4883
0.40	0.3815
0.60	0.3176
0.80	0.2683
1.00	0.2402

Table 6.13

CHAPTER 7.0

INFLUENCE OF TUNNEL GEOMETRY ON STRESS IN ROCK AROUND ELLIPTICAL TUNNELS

Figures 7.1 to 7.12 indicate the influence of the tunnel geometry (the *a/b* ratio) on the principal stress distribution in the rock mass, for different liner thicknesses. A distinct feature that can be seen from these figures is that the minimum stresses along the line CD are indicated for the tunnel with *a/b* = 1.156. In most cases, the maximum stress is indicated for the tunnel with *a/b* = 1.358, while tunnel with *a/b* = 1.500 indicates intermediate values.

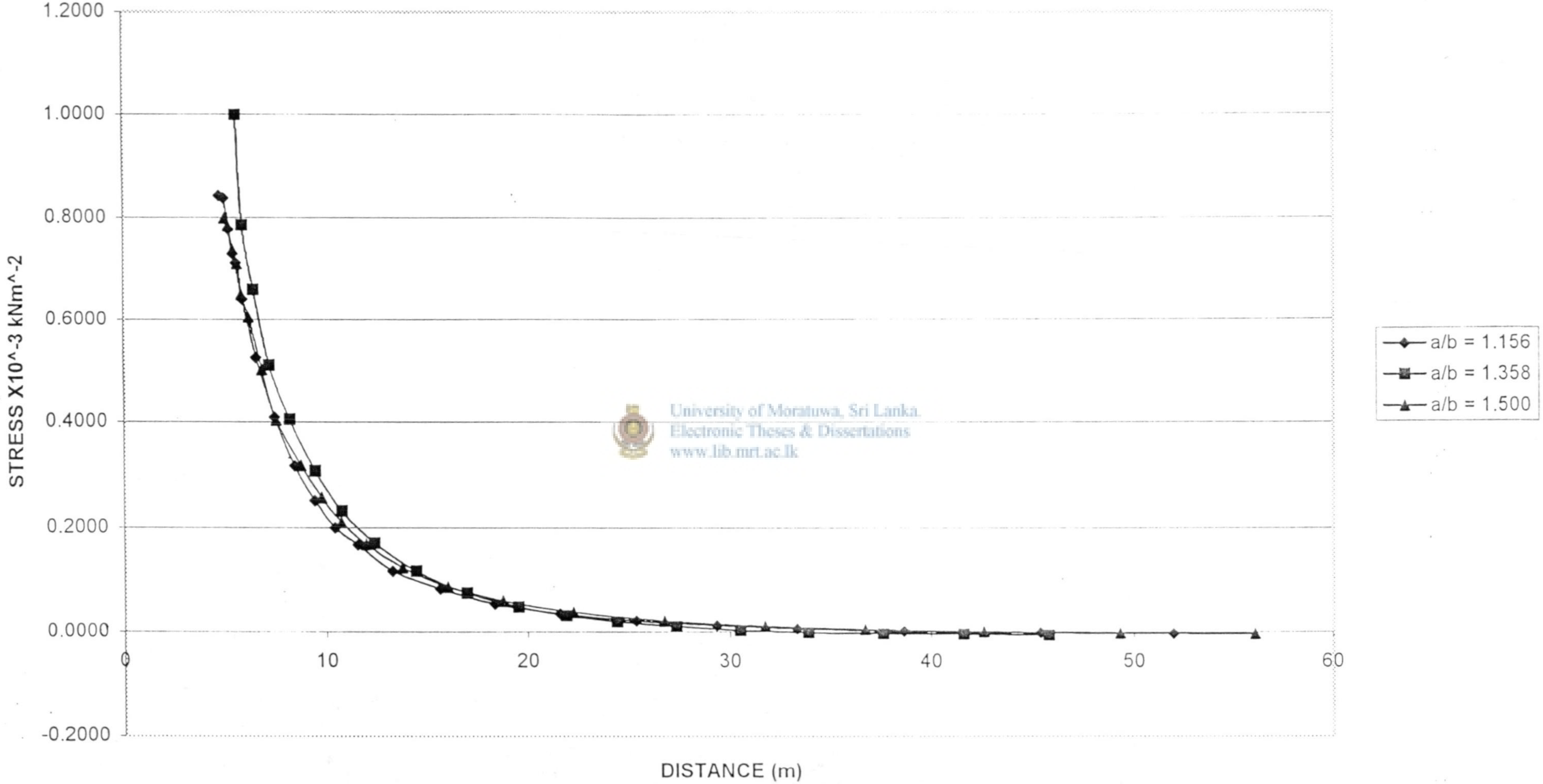

Figure 7.1 Variation of major principal stress along radial line "CD"
(Without liner)

VARIATION OF MAJOR PRINCIPAL STRESS ALONG RADIAL LINE "CD"
(FOR LINER THICKNESS t =0.0)

ELEMENT NUMBER	MAJOR PRINCIPAL STRESSx10^3 (kN/m^2)		
	RATIO OF a/b		
	a/b = 1.156	a/b = 1.358	a/b = 1.500
6	0.8419	0.9991	0.7990
16	0.8378	0.7849	0.7842
26	0.7772	0.6593	0.7369
36	0.7279	0.5088	0.7100
46	0.7105	0.4056	0.6500
56	0.6402	0.3075	0.6048
66	0.5236	0.2323	0.5004
76	0.4089	0.1704	0.4048
86	0.3174	0.1169	0.3182
96	0.2519	0.0756	0.2582
106	0.2004	0.0490	0.2108
116	0.1677	0.0322	0.1688
126	0.1169	0.0203	0.1242
136	0.0830	0.0109	0.0874
146	0.0055	0.0035	0.0606
156	0.0359	-0.0006	0.0387
166	0.0218	-0.0032	0.0224
176	0.0128	-0.0036	0.0119
186	0.0070	-0.0056	0.0056

Table 7.1

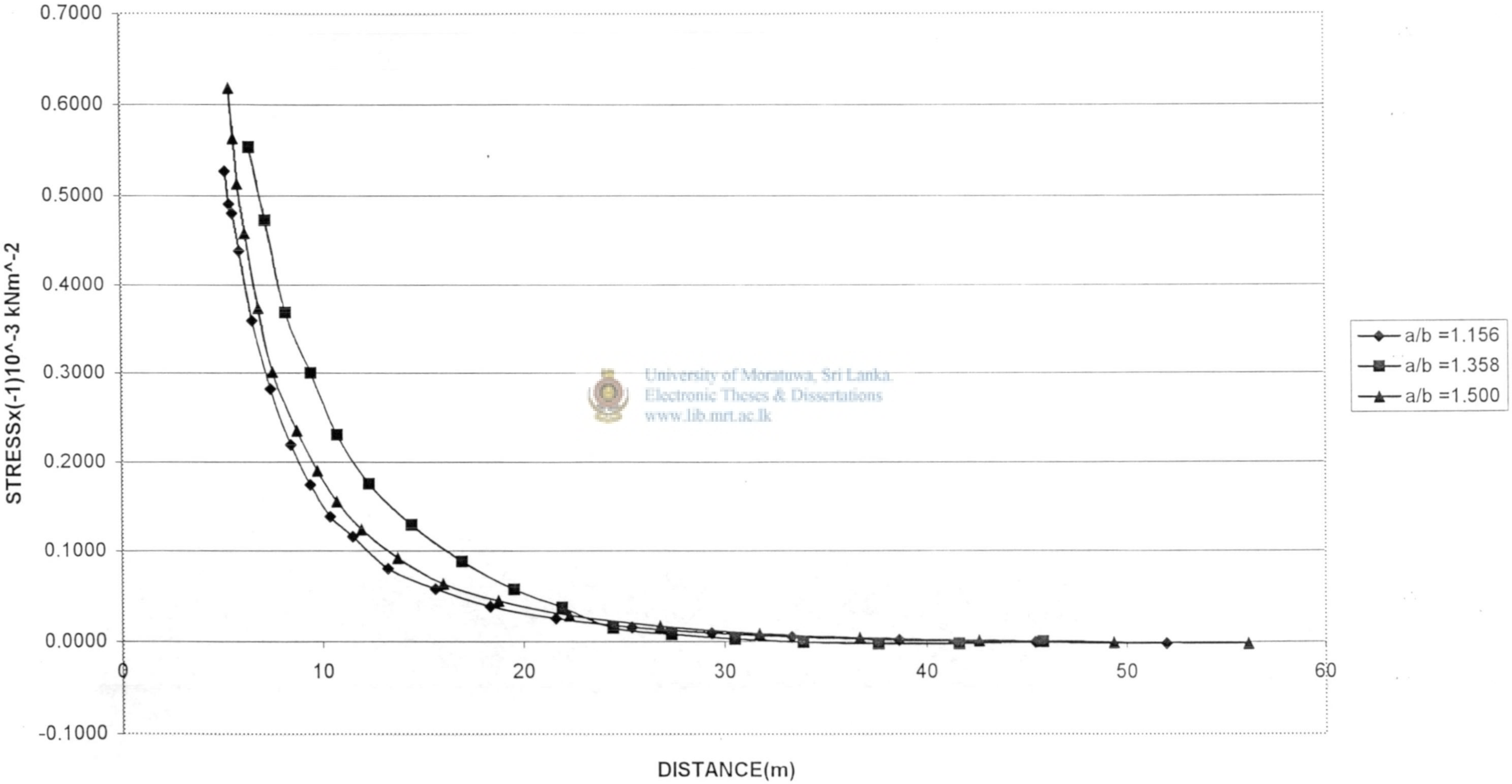

Figure 7.2 Variation of major principal stress along radial line "CD"
(Liner thickness (t) = 0.2m)

VARIATION OF MAJOR PRINCIPAL STRESS ALONG RADIAL LINE "CD"
(FOR LINER THICKNESS t =0.2m)

ELEMENT NUMBER	MAJOR PRINCIPAL STRESSx10^3 (kN/m^2)			
	RATIO OF a/b			
	a/b = 1.156	a/b = 1.358	a/b = 1.500	
6	7.8140	8.2450	9.9410	LINER ELEMENTS
16	0.5621	7.7680	0.7144	
26	0.5275	0.5535	0.6181	
36	0.4909	0.4726	0.5635	
46	0.4805	0.3684	0.5134	
56	0.4385	0.2998	0.4586	
66	0.3593	0.2303	0.3737	
76	0.2818	0.1752	0.3012	
86	0.2191	0.1288	0.2353	
96	0.1740	0.0882	0.1902	
106	0.1381	0.0567	0.1550	
116	0.1158	0.0365	0.1241	
126	0.0802	0.0148	0.0921	
136	0.0570	0.0077	0.0630	
146	0.0377	0.0023	0.0443	
156	0.0246	-0.0007	0.0282	
166	0.0149	-0.0024	0.0161	
176	0.0088	-0.0025	0.0085	
186	0.0048	-0.0004	0.0039	

Table 7.2

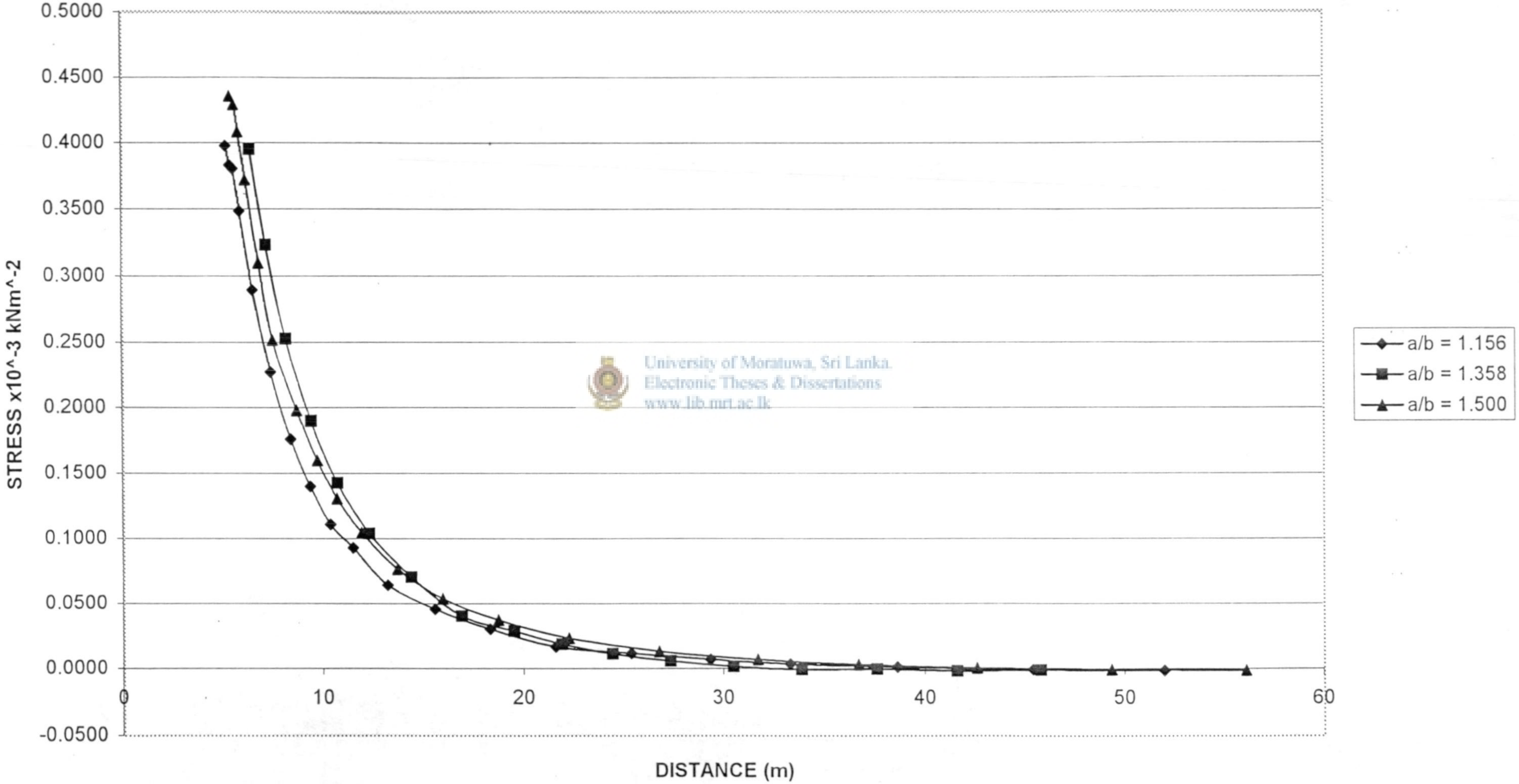

Figure 7.3 Variation of major principal stress along radial line "CD"
(Liner thickness (t) = 0.4m)

VARIATION OF MAJOR PRINCIPAL STRESS ALONG RADIAL LINE "CD"
(FOR LINER THICKNESS t =0.4m)

ELEMENT NUMBER	MAJOR PRINCIPAL STRESSx10^3 (kN/m^2)			
	RATIO OF a/b			
	a/b = 1.156	a/b = 1.358	a/b = 1.500	
6	5.5030	5.3120	6.2190	LINER ELEMENTS
16	5.4820	0.3944	5.8550	
26	0.3975	0.3947	0.4356	
36	0.3830	0.3231	0.4290	
46	0.3802	0.2524	0.4085	
56	0.3485	0.1901	0.3721	
66	0.2893	0.1428	0.3101	
76	0.2273	0.1041	0.2518	
86	0.1767	0.0708	0.1982	
96	0.1401	0.0405	0.1603	
106	0.1110	0.0288	0.1307	
116	0.0931	0.0185	0.1047	
126	0.0644	0.0112	0.0770	
136	0.0457	0.0057	0.0538	
146	0.0302	0.0014	0.0372	
156	0.0169	-0.0007	0.0235	
166	0.0118	-0.0002	0.0133	
176	0.0069	-0.0019	0.0069	
186	0.0037	-0.0011	0.0031	

Table 7.3

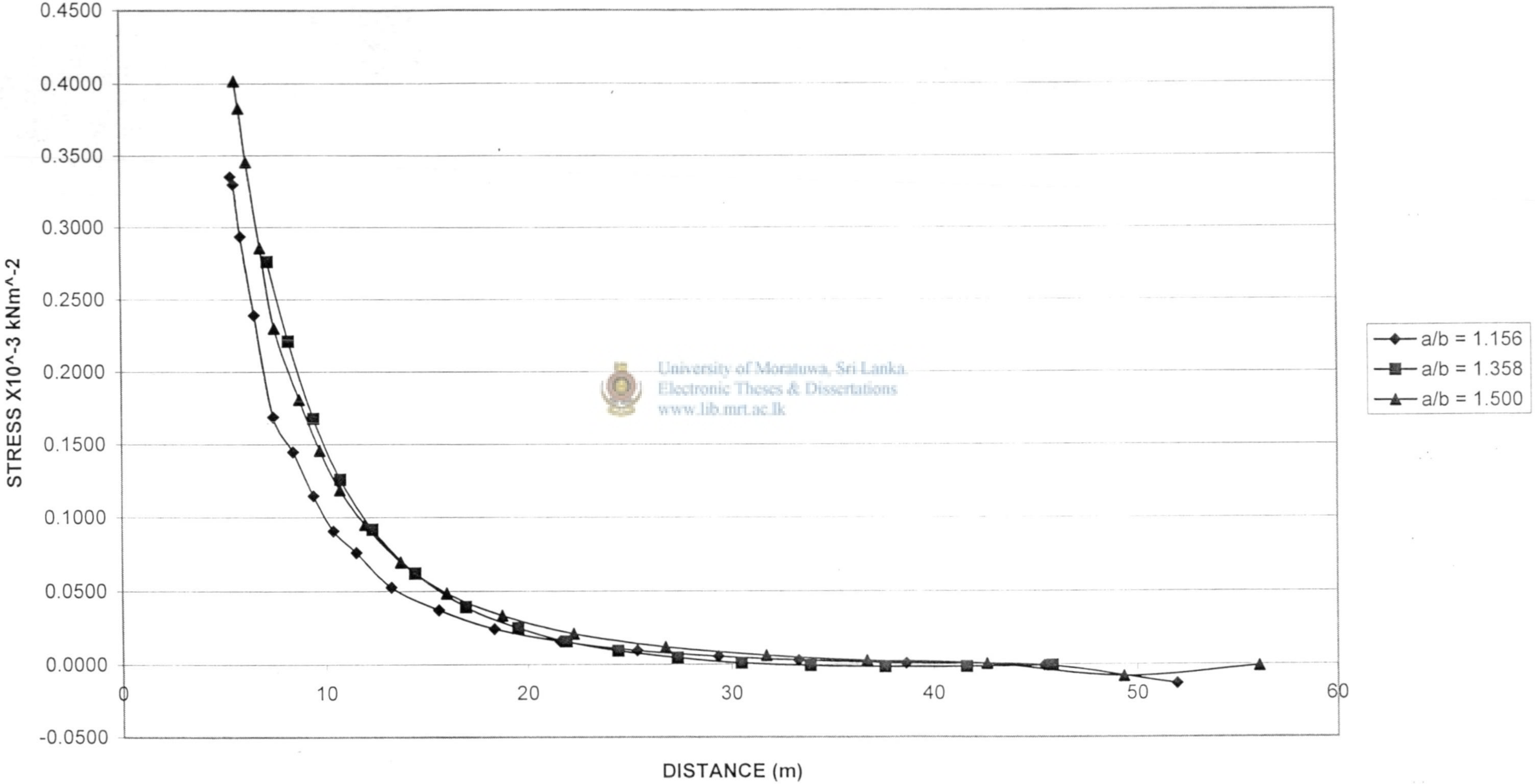

Figure 7.4 Variation of major principal stress along radial line "CD"
(Liner thickness (t) = 0.6m)

VARIATION OF MAJOR PRINCIPAL STRESS ALONG RADIAL LINE "CD"
(FOR LINER THICKNESS t =0.6m)

ELEMENT NUMBER	MAJOR PRINCIPAL STRESSx10^3 (kN/m^2)			
	RATIO OF a/b			
	a/b = 1.156	a/b = 1.358	a/b = 1.500	
6	4.0300	4.4850	5.0880	LINER ELEMENTS
16	4.2230	4.1330	4.8480	
26	4.3780	0.3288	4.7030	
36	0.3350	0.2764	0.4017	
46	0.3296	0.2211	0.3827	
56	0.2936	0.1677	0.3453	
66	0.2390	0.1260	0.2859	
76	0.1687	0.0917	0.2301	
86	0.1447	0.0621	0.1809	
96	0.1146	0.0393	0.1457	
106	0.0906	0.0249	0.1187	
116	0.0760	0.0158	0.0950	
126	0.0527	0.0094	0.0698	
136	0.0372	0.0046	0.0486	
146	0.0245	0.0009	0.0336	
156	0.0159	-0.0008	0.0211	
166	0.0095	-0.0017	0.0119	
176	0.0055	-0.0015	0.0062	
186	0.0029	-0.0007	0.0027	

Table 7.4

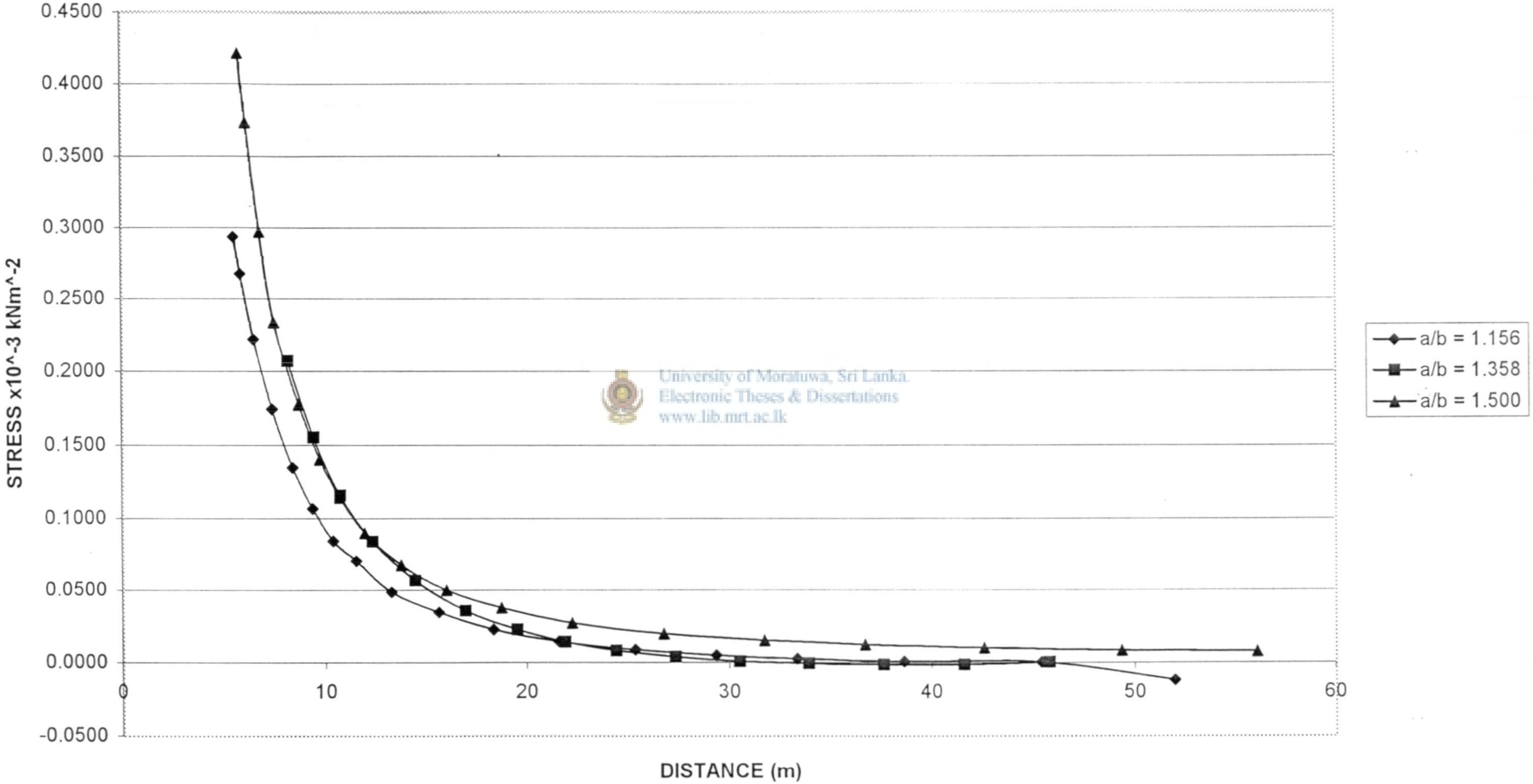

Figure 7.5 Variation of major principal stress along radial line "CD"
(Liner thickness (t) = 0.8m)

VARIATION OF MAJOR PRINCIPAL STRESS ALONG RADIAL LINE "CD"
(FOR LINER THICKNESS t =0.8m)

ELEMENT NUMBER	MAJOR PRINCIPAL STRESSx10^3 (kN/m^2)		
	RATIO OF a/b		
	a/b = 1.156	a/b = 1.358	a/b = 1.500
6	3.6300	3.9790	0.8749
16	3.7690	3.7910	0.8044
26	3.8920	0.3220	0.7079
36	3.9210	0.2650	0.3844
46	0.2938	0.2072	0.4216
56	0.2678	0.1552	0.3732
66	0.2219	0.1159	0.2974
76	0.1741	0.0840	0.2334
86	0.1349	0.0567	0.1775
96	0.1067	0.0356	0.1405
106	0.0843	0.0225	0.1144
116	0.0707	0.1410	0.0900
126	0.0489	0.0083	0.0679
136	0.0345	0.0040	0.0503
146	0.0227	0.0007	0.0377
156	0.0147	-0.0008	0.0273
166	0.0088	-0.0015	0.0198
176	0.0051	-0.0012	0.0152
186	0.0027	0.0005	0.0123

LINER ELEMENTS

Table 7.5

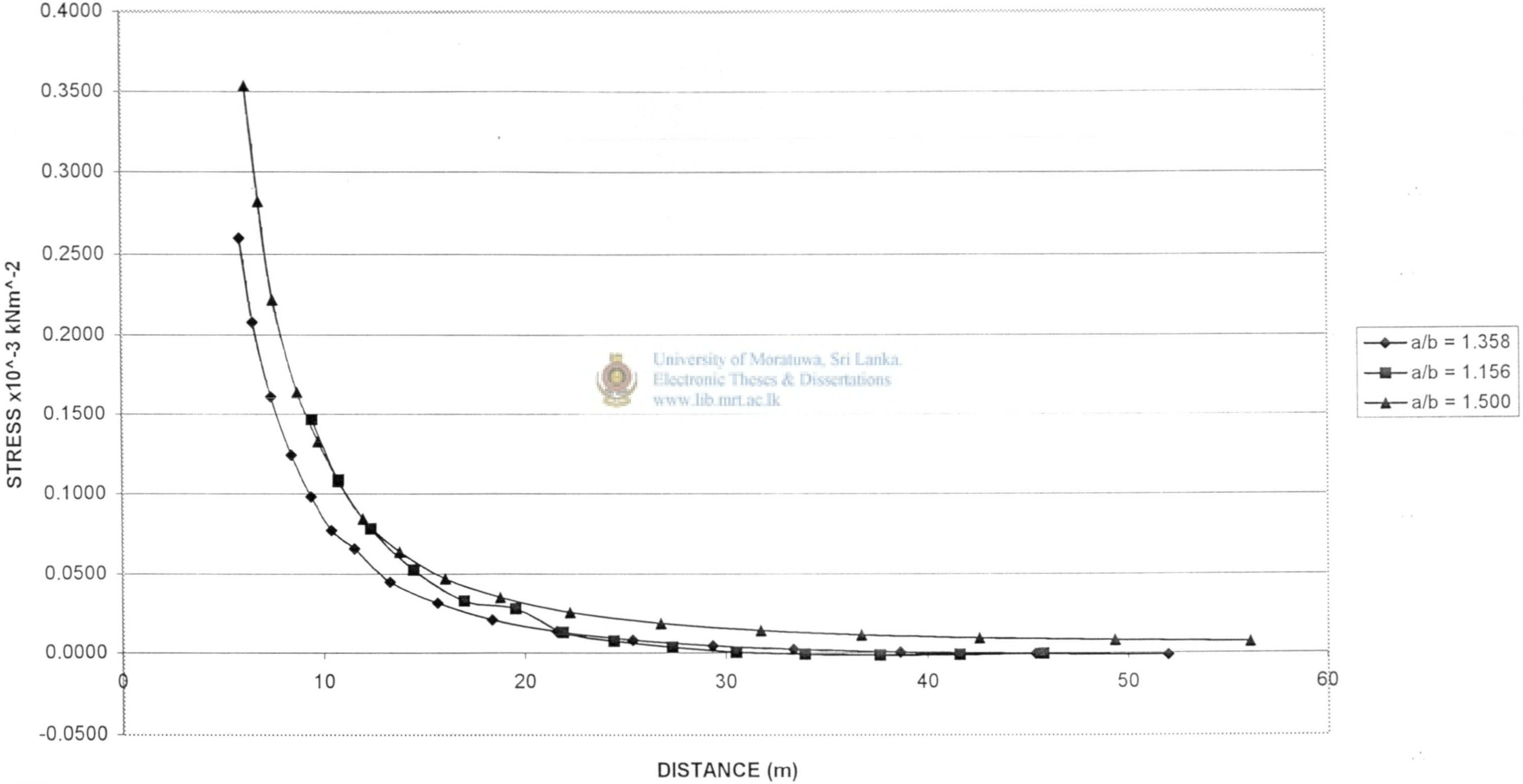

Figure 7.6 Variation of major principal stress along radial line "CD"
(Liner thickness (t) = 1.0m)

VARIATION OF MAJOR PRINCIPAL STRESS ALONG RADIAL LINE "CD"
(FOR LINER THICKNESS t =1.0m)

ELEMENT NUMBER	MAJOR PRINCIPAL STRESSx10^3 (kN/m^2)		
	RATIO OF a/b		
	a/b = 1.156	a/b = 1.358	a/b = 1.500
6	3.1300	3.5370	0.8976
16	3.2830	3.2930	0.8139
26	3.4350	0.2964	0.7237
36	3.5120	0.2560	0.4132
46	3.7070	0.1986	0.3934
56	0.2597	0.1465	0.3538
66	0.2079	0.1086	0.2824
76	0.1610	0.0783	0.2221
86	0.1243	0.0526	0.1638
96	0.0981	0.0329	0.1329
106	0.0773	0.0277	0.1079
116	0.0659	0.0129	0.0847
126	0.0448	0.0075	0.0638
136	0.0316	0.0036	0.0471
146	0.0208	0.0005	0.0352
156	0.0134	-0.0007	0.0255
166	0.0080	-0.0013	0.0184
176	0.0046	-0.0010	0.0140
186	0.0024	-0.0004	0.0114

LINER ELEMENTS

Table 7.6

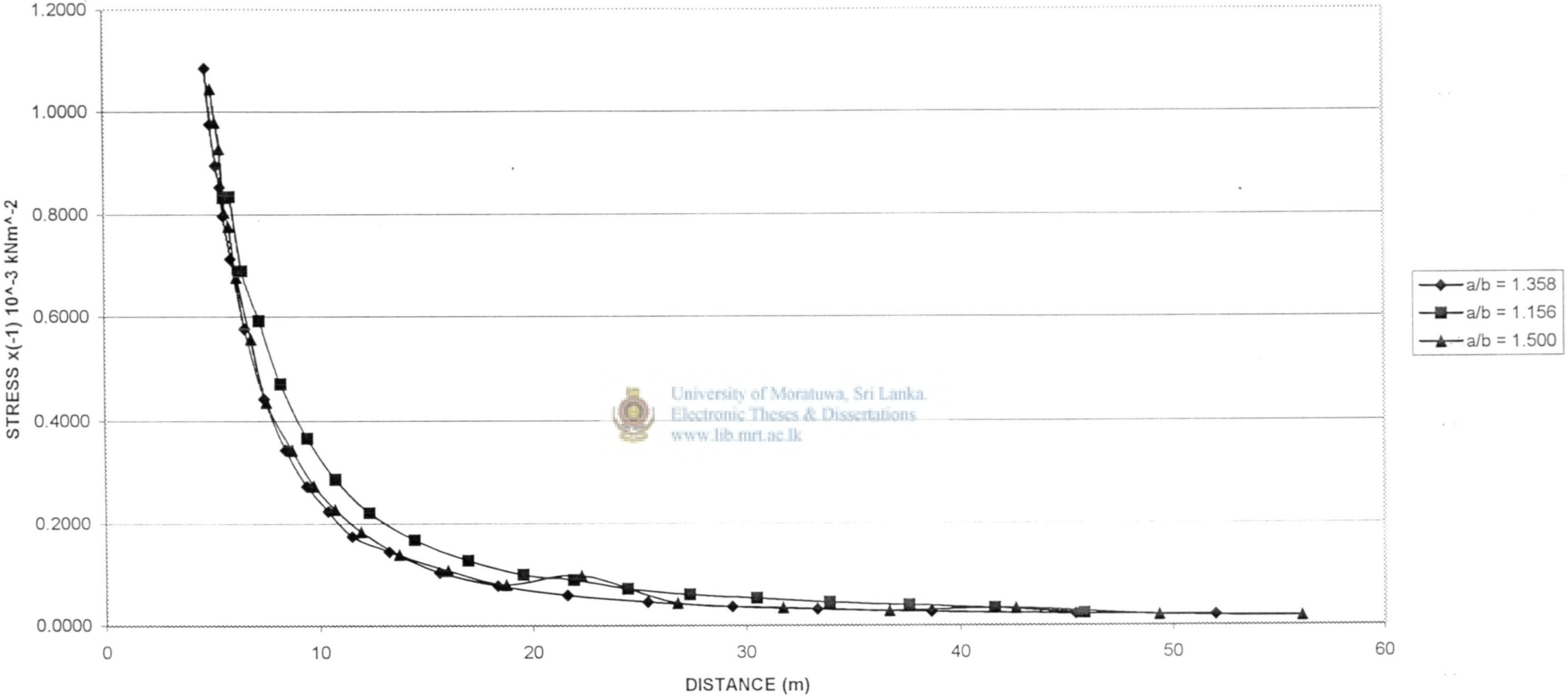

Figure 7.7 Variation of minor principal stress along radial line "CD"
(Without liner)

VARIATION OF MINOR PRINCIPAL STRESS ALONG RADIAL LINE "CD"
(FOR LINER THICKNESS t =0.0m)

ELEMENT NUMBER	MINOR PRINCIPAL STRESSx(-1×10^3) (kN/m^2)		
	RATIO OF a/b		
	a/b = 1.156	a/b = 1.358	a/b = 1.500
6	1.0850	0.8335	1.0450
16	0.9754	0.8354	0.9792
26	0.8958	0.6888	0.9285
36	0.8535	0.5920	0.8046
46	0.7975	0.4716	0.7772
56	0.7122	0.3661	0.6766
66	0.5767	0.2875	0.5571
76	0.4425	0.2218	0.4367
86	0.3437	0.1674	0.3439
96	0.2738	0.1272	0.2752
106	0.2246	0.0987	0.2285
116	0.1746	0.0884	0.1837
126	0.1440	0.0716	0.1390
136	0.1033	0.0607	0.1070
146	0.0780	0.0528	0.0799
156	0.0591	0.0453	0.0970
166	0.0460	0.0396	0.0443
176	0.0372	0.0337	0.0345
186	0.0315	0.0240	0.0285

Table 7.7

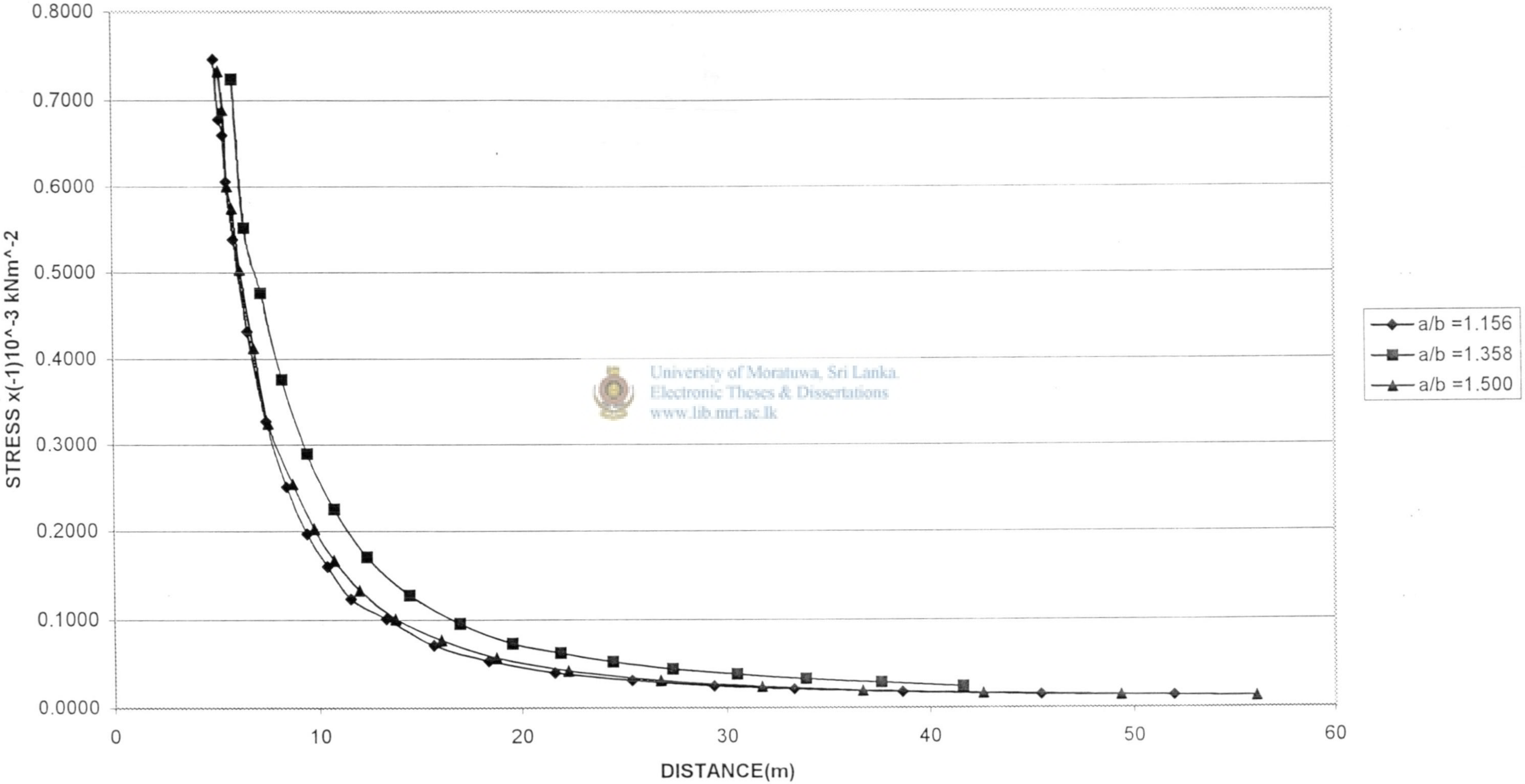

Figure 7.8 Variation of minor principal stress along radial line "CD"
(Liner thickness (t) = 0.2m)

VARIATION OF MINOR PRINCIPAL STRESS ALONG RADIAL LINE "CD"
(FOR LINER THICKNESS t =0.2m)

ELEMENT NUMBER	MINOR PRINCIPAL STRESSx(-1×10^3) (kN/m^2)			
	RATIO OF a/b			
	a/b = 1.156	a/b = 1.358	a/b = 1.500	
6	0.7854	0.4562	0.6004	LINER ELEMENTS
16	0.7463	0.7242	0.7335	
26	0.6783	0.5519	0.6893	
36	0.6600	0.4761	0.6005	
46	0.6058	0.3758	0.5749	
56	0.5381	0.2896	0.5036	
66	0.4319	0.2246	0.4129	
76	0.3268	0.1713	0.3250	
86	0.2506	0.1279	0.2542	
96	0.1973	0.0959	0.2029	
106	0.1604	0.0738	0.1675	
116	0.1234	0.0628	0.1338	
126	0.1013	0.0532	0.1011	
136	0.0719	0.0449	0.0776	
146	0.0540	0.0390	0.0576	
156	0.0407	0.0333	0.0427	
166	0.0316	0.0292	0.0316	
176	0.0255	0.0247	0.0245	
186	0.0215	0.0319	0.0201	

Table 7.8

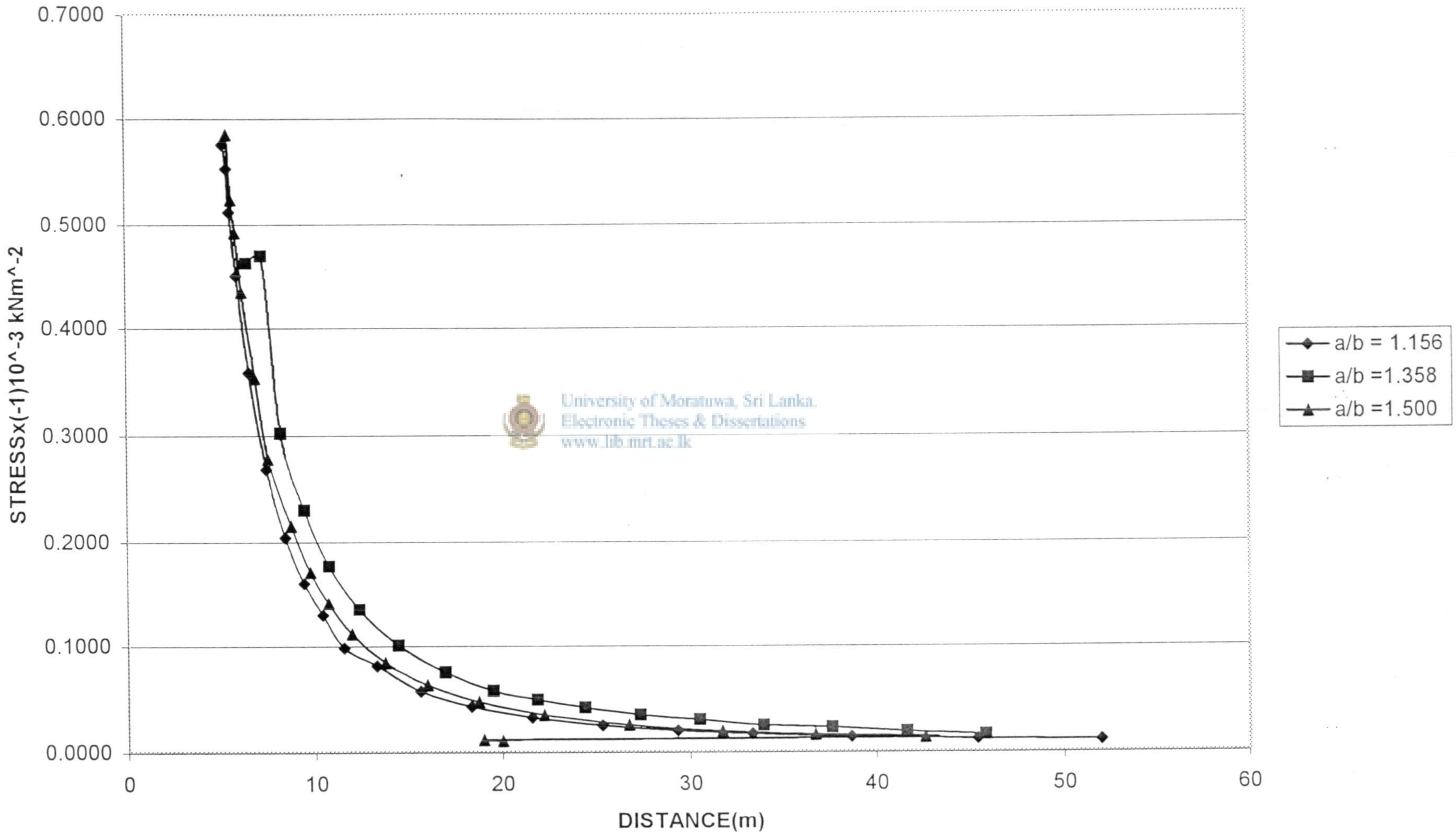

Figure 7.9 Variation of minor principal stress along radial line "CD"
(Liner thickness (t) = 0.4m)

VARIATION OF MINOR PRINCIPAL STRESS ALONG RADIAL LINE "CD"
(FOR LINER THICKNESS t =0.4m)

ELEMENT NUMBER	MINOR PRINCIPAL STRESSx(-1×10^3) (kN/m^2)		
	RATIO OF a/b		
	a/b = 1.156	a/b = 1.358	a/b = 1.500
6	0.8850	0.6347	0.7902
16	0.7886	0.6399	0.7847
26	0.5752	0.4629	0.5849
36	0.5525	0.4696	0.5231
46	0.5114	0.3019	0.4922
56	0.4502	0.2300	0.4345
66	0.3581	0.1768	0.3529
76	0.2683	0.1345	0.2780
86	0.2041	0.1004	0.2150
96	0.1597	0.0749	0.1710
106	0.1292	0.5770	0.1403
116	0.9830	0.0490	0.1113
126	0.0810	0.0415	0.0840
136	0.0571	0.0350	0.0632
146	0.0428	0.0304	0.0473
156	0.0322	0.0250	0.0347
166	0.0249	0.0227	0.0255
176	0.0200	0.0191	0.0196
186	0.0169	0.0161	0.0161

LINER ELEMENTS

Table 7.9

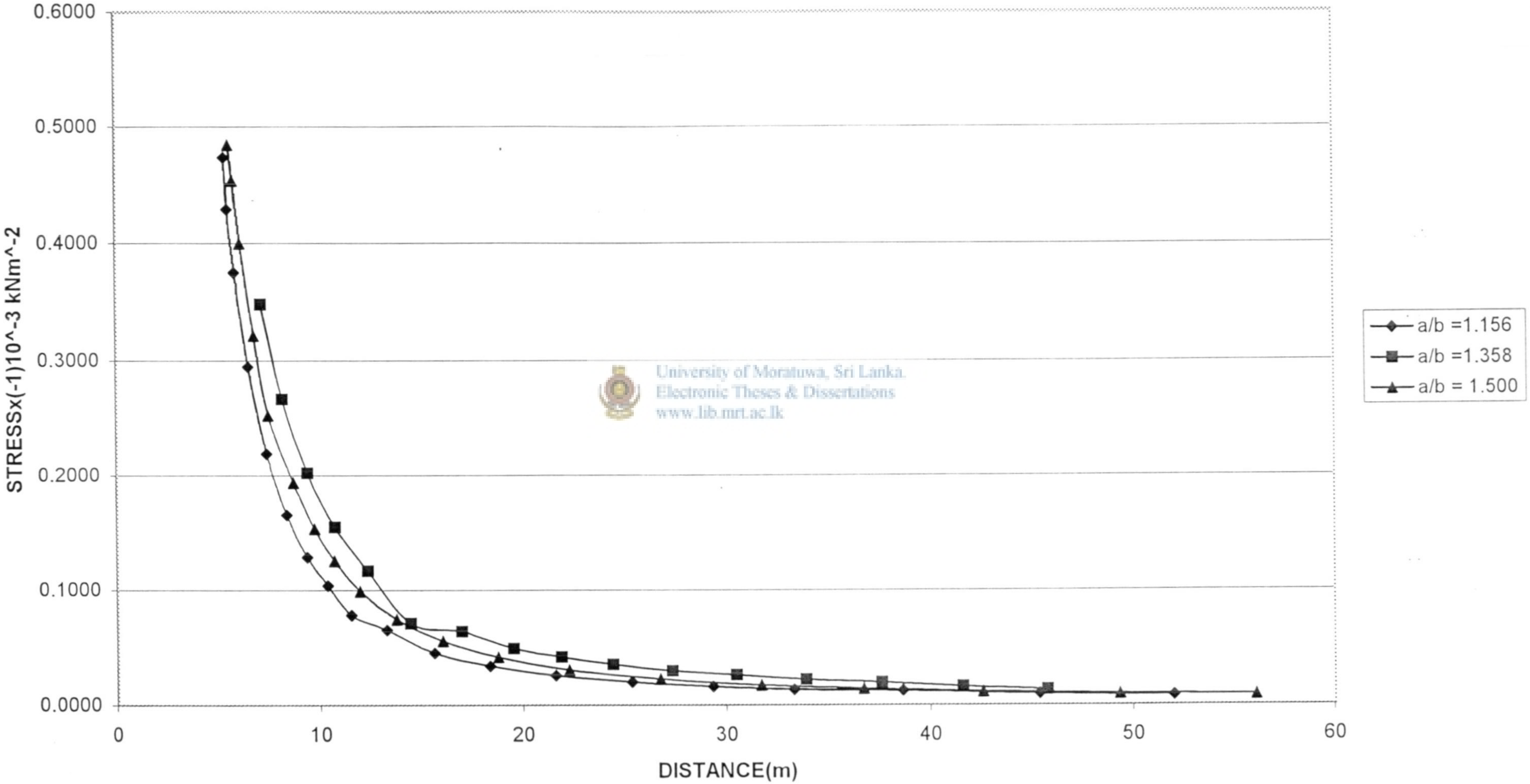

Figure 7.10 Variation of minor principal stress along radial line "CD"
(Liner thickness (t) = 0.6m)

VARIATION OF MINOR PRINCIPAL STRESS ALONG RADIAL LINE "CD"
(FOR LINER THICKNESS t =0.6m)

ELEMENT NUMBER	MINOR PRINCIPAL STRESSx($-1x10^3$) (kN/m^2)		
	RATIO OF a/b		
	a/b = 1.156	a/b = 1.358	a/b = 1.500
6	0.9362	0.6632	0.8159
16	0.8078	0.5000	0.7441
26	0.5255	0.4246	0.6354
36	0.4731	0.3479	0.4845
46	0.4286	0.2667	0.4533
56	0.3748	0.2024	0.4002
66	0.2949	0.1548	0.3217
76	0.2191	0.1172	0.2526
86	0.1657	0.0715	0.1938
96	0.1290	0.0645	0.1538
106	0.1041	0.0495	0.1257
116	0.0784	0.0420	0.0993
126	0.0656	0.0355	0.0749
136	0.0456	0.0298	0.0560
146	0.0341	0.0259	0.0419
156	0.0256	0.0220	0.0306
166	0.0197	0.0193	0.0223
176	0.0158	0.0161	0.0171
186	0.0133	0.0134	0.0140

LINER ELEMENTS

Table 7.10

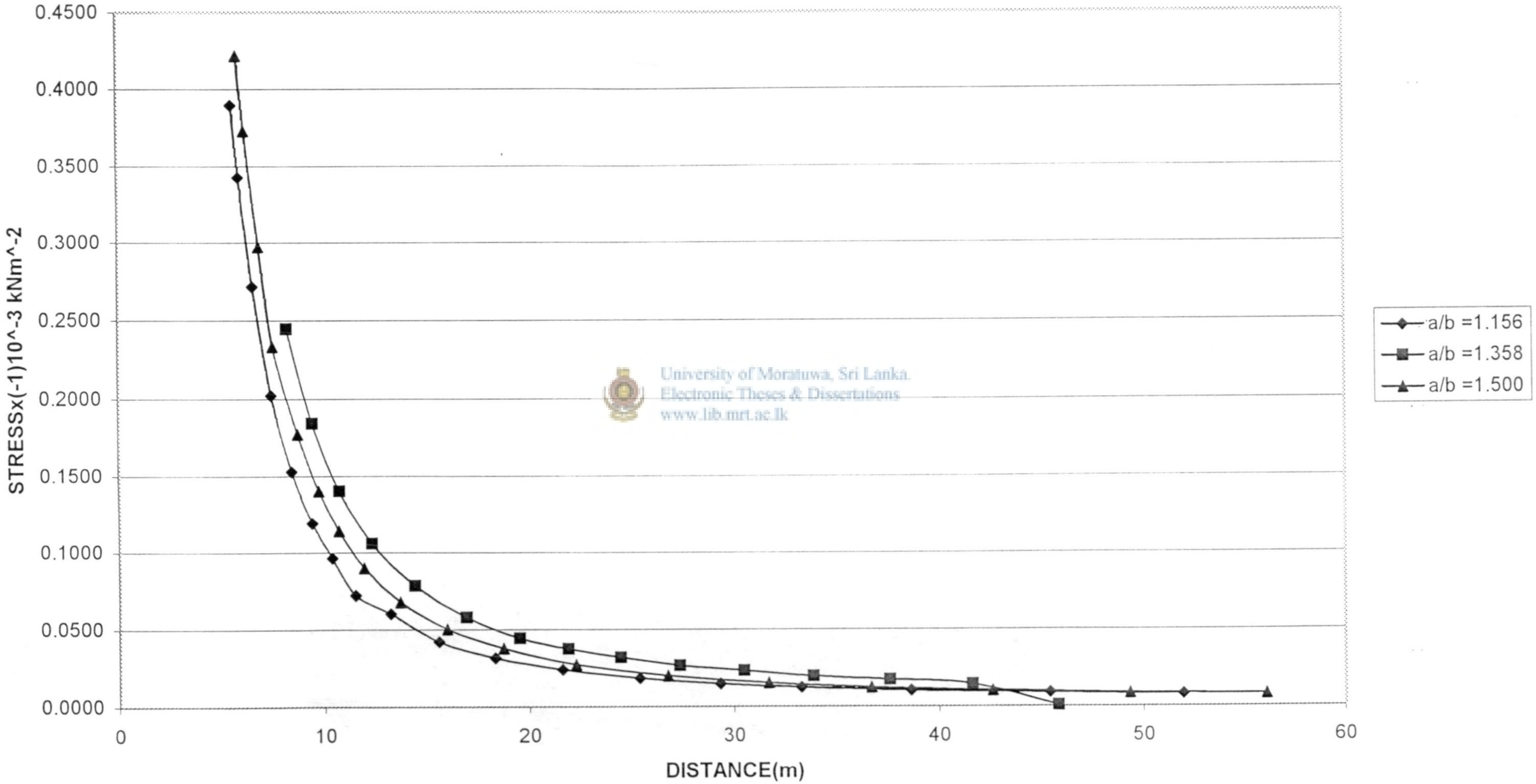

Figure 7.11 Variation of minor principal stress along radial line "CD"
(Liner thickness (t) = 0.8m)

VARIATION OF MINOR PRINCIPAL STRESS ALONG RADIAL LINE "CD"
(FOR LINER THICKNESS t =0.8m)

ELEMENT NUMBER	MINOR PRINCIPAL STRESSx($-1X10^3$) (kN/m^2)		
	RATIO OF a/b		
	a/b = 1.156	a/b = 1.358	a/b = 1.500
6	0.9583	0.6885	0.8749
16	0.8300	0.4903	0.8044
26	0.5930	0.3872	0.7079
36	0.5859	0.3230	0.3844
46	0.3897	0.2448	0.4216
56	0.3426	0.1845	0.3732
66	0.2715	0.1403	0.2974
76	0.2024	0.1059	0.2334
86	0.1531	0.0786	0.1775
96	0.1192	0.0579	0.1405
106	0.0962	0.0443	0.1144
116	0.0723	0.0375	0.0900
126	0.0601	0.0317	0.0679
136	0.0421	0.0265	0.0503
146	0.0316	0.0231	0.0377
156	0.0237	0.0196	0.0273
166	0.0183	0.0172	0.0198
176	0.0146	0.0142	0.0152
186	0.0123	0.0005	0.0123

LINER ELEMENTS

Table 7.11

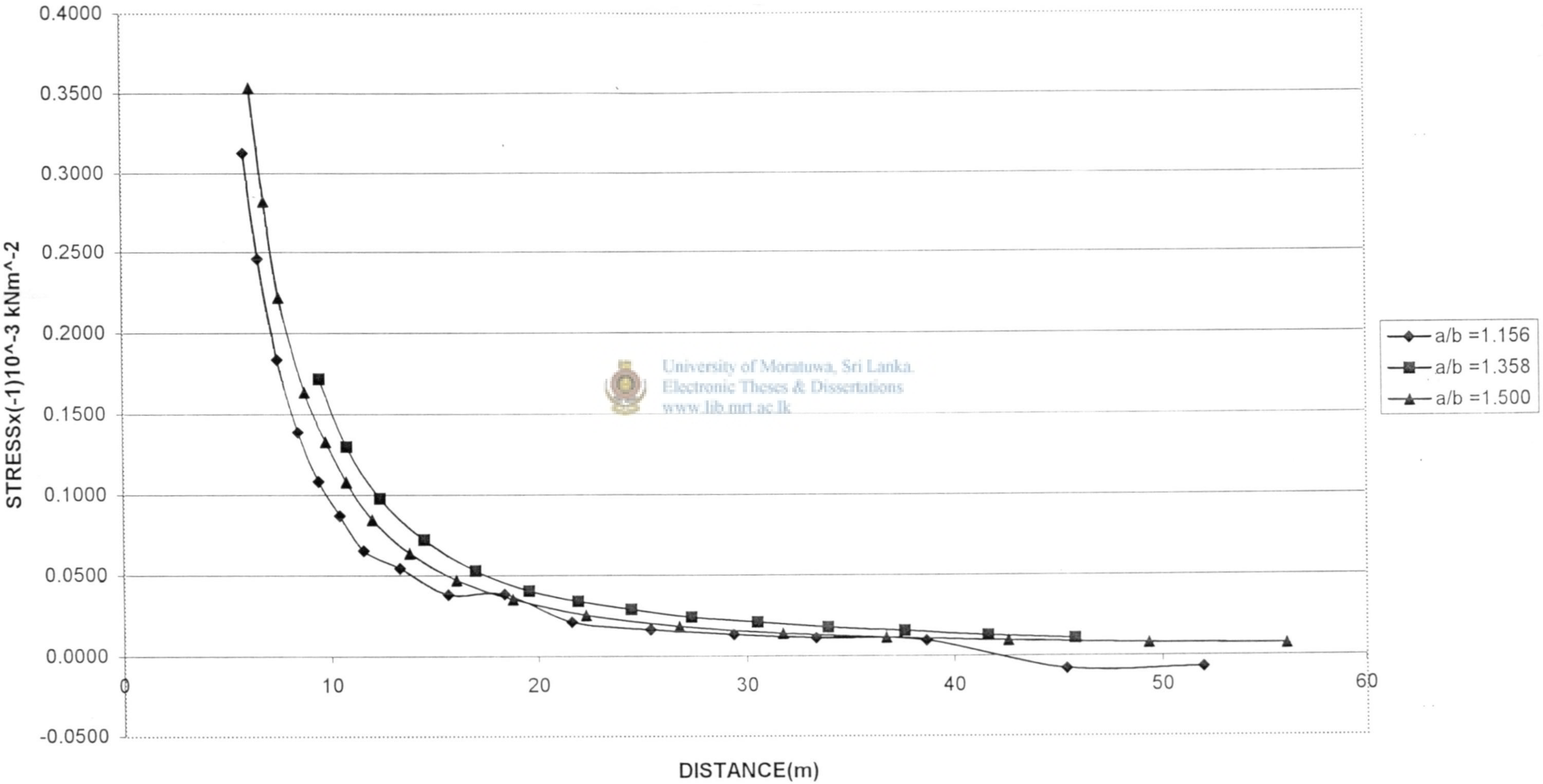

Figure 7.12 Variation of minor principal stress along radial line "CD"
(Liner thickness (t) = 1.0m)

VARIATION OF MINOR PRINCIPAL STRESS ALONG RADIAL LINE "CD"
(FOR LINER THICKNESS t =1.0m)

ELEMENT NUMBER	MINOR PRINCIPAL STRESSx($-1X10^3$) (kN/m^2)			
	RATIO OF a/b			
	a/b = 1.156	a/b = 1.358	a/b = 1.500	
6	0.9813	0.7096	0.8976	LINER ELEMENTS
16	0.8445	0.4717	0.8139	
26	0.6218	0.3651	0.7237	
36	0.5866	0.3107	0.4132	
46	0.3768	0.2308	0.3934	
56	0.3126	0.1719	0.3538	
66	0.2461	0.1297	0.2824	
76	0.1836	0.0975	0.2221	
86	0.1388	0.0721	0.1638	
96	0.1081	0.0529	0.1329	
106	0.0872	0.0404	0.1079	
116	0.0653	0.0341	0.0847	
126	0.0545	0.0288	0.0638	
136	0.0381	0.0241	0.0471	
146	0.0386	0.0209	0.0352	
156	0.0214	0.0177	0.0255	
166	0.0165	0.0156	0.0184	
176	0.0132	0.0128	0.0140	
186	0.0112	0.0106	0.0114	

Table 7.12

CHAPTER 8.0

INFLUENCE OF STIFFNESS OF ROCK ON STRESS AND DEFORMATION IN ROCK SURROUNDING ELLIPTICAL TUNNELS

Figures 8.1 and 8.2 show that stronger rock carries a larger stress than a weaker rock. This implies that for weaker rock, the concrete lining will take most of the imposed load, and will experience higher stress magnitudes than in the case of stronger rock.

Figures 8.5 and 8.6 show that the displacements in rock reduce as the stiffness of rock increases. The numerical results show that this amount of reduction depends on the location of the point, the E_c/E_r ratio, and the tunnel thickness.

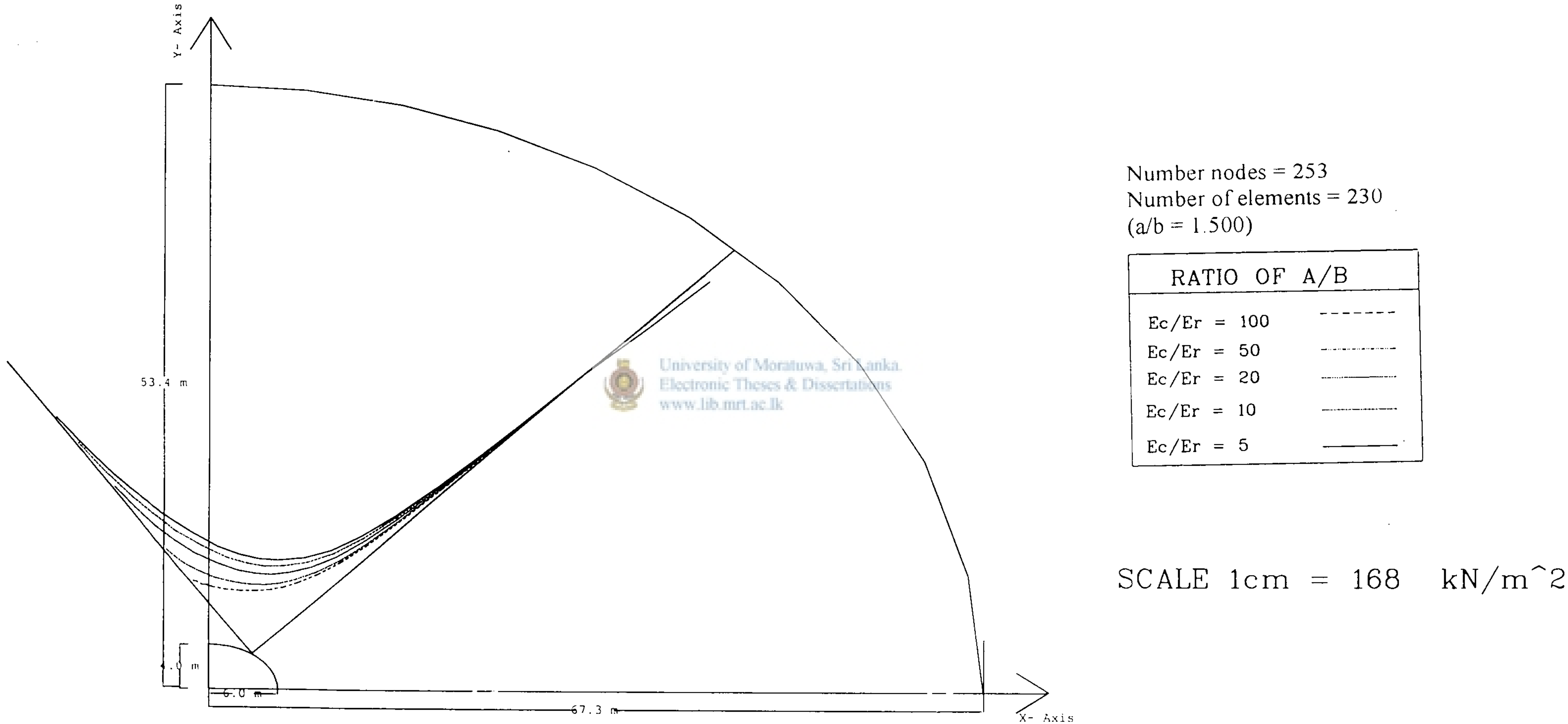

Figure 8.1 Variation of major principal stress along radial line "CD"
(Liner thickness (t) = 0.2m)

VARIATION OF MAJOR PRINCIPAL STRESS ALONG RADIAL LINE "CD"
(FOR FOR ELLIPTICAL TUNNEL - 3, a/b = 1.500)
(LINER THICKNESS = 0.2m)

ELEMENT NUMBER	MAJOR PRINCIPAL STRESS x10^3 kN/m^2					
	RATIO OF E_C/E_R					
	E_C/E_R = 5	E_C/E_R = 10	E_C/E_R = 20	E_C/E_R = 50	E_C/E_R = 100	
6	5.4360	9.9410	15.6800	23.1300	27.2800	LINER ELEMENTS
16	0.8044	0.7144	0.5642	0.3555	0.2473	
26	0.7036	0.6181	0.4916	0.3243	0.2402	
36	0.6491	0.5635	0.4465	0.2971	0.2227	
46	0.5919	0.5134	0.4099	0.2808	0.2180	
56	0.5317	0.4586	0.3664	0.2543	0.2003	
66	0.4335	0.3737	0.3011	0.2159	0.1759	
76	0.3500	0.3012	0.2439	0.1782	0.1476	
86	0.2727	0.2353	0.1920	0.1434	0.1214	
96	0.2207	0.1902	0.1554	0.1168	0.0994	
106	0.1799	0.1550	0.1267	0.0959	0.0824	
116	0.1441	0.1241	0.1015	0.0770	0.0664	
126	0.1059	0.0912	0.0747	0.0570	0.0495	
136	0.0744	0.0640	0.0522	0.0395	0.0343	
146	0.0516	0.0443	0.0361	0.0272	0.0235	
156	0.0329	0.0282	0.0228	0.1710	0.0149	
166	0.0189	0.0162	0.0129	0.0094	0.0082	
176	0.0101	0.0085	0.0067	0.0048	0.0041	
186	0.0047	0.0039	0.0030	0.0021	0.0081	
196	0.0009	0.0008	0.0005	0.0003	0.0004	
206	-0.0132	-0.0001	-0.0009	-0.0004	-0.0001	
216	-0.0227	-0.0018	-0.0013	-0.0005	-0.0008	

Table 8.1

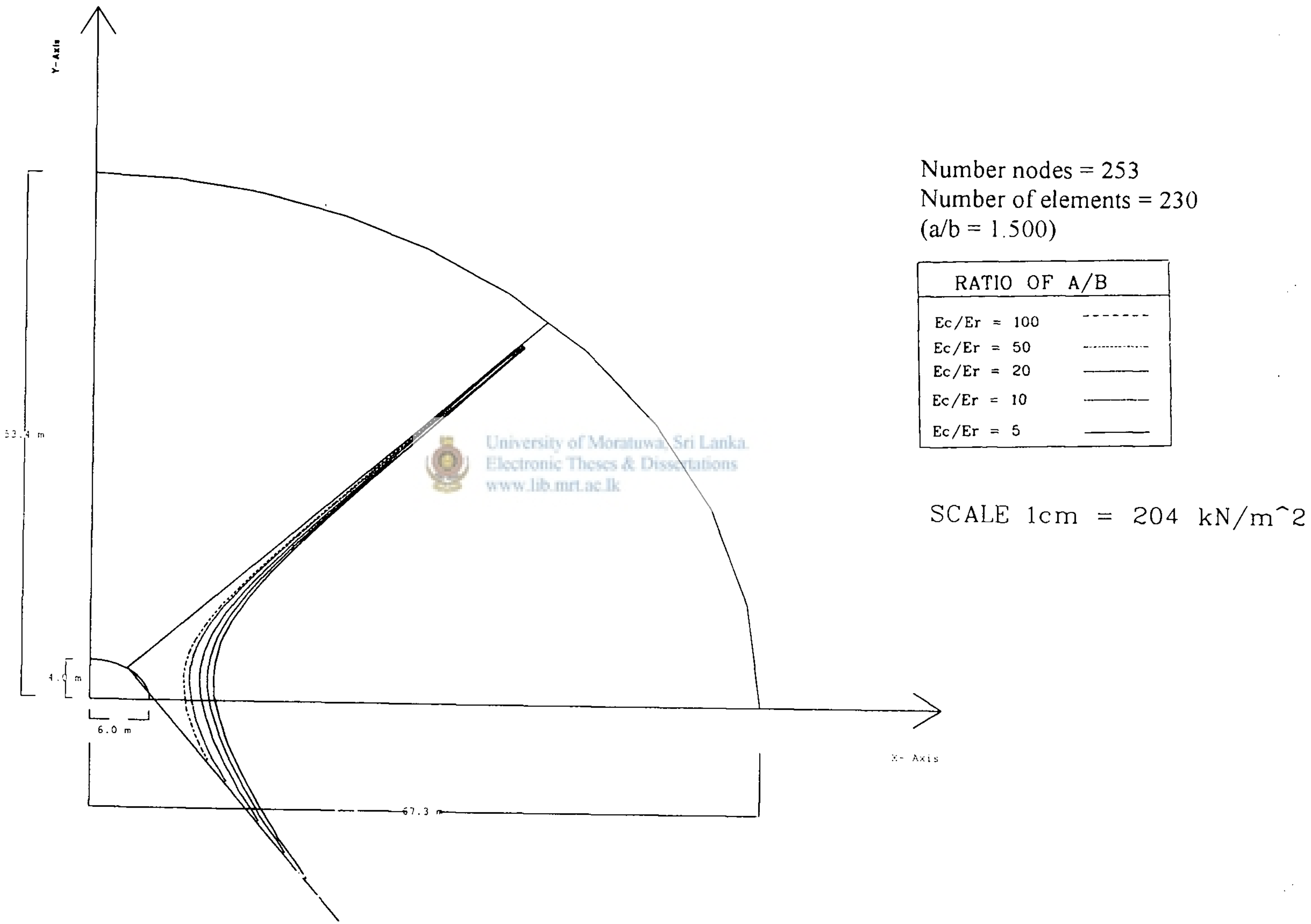

Figure 8.2 Variation of minor principal stress along radial line "CD"
(Liner thickness (t) = 0.2m)

VARIATION OF MINOR PRINCIPAL STRESS ALONG RADIAL LINE "CD"
(FOR FOR ELLIPTICAL TUNNEL - 3, a/b = 1.500)
(LINER THICKNESS = 0.2m)

ELEMENT NUMBER	MINOR PRINCIPAL STRESS $x(-1x10^3)$ kN/m^2					
	RATIO OF E_C/E_R					
	E_C/E_R = 5	E_C/E_R = 10	E_C/E_R = 20	E_C/E_R = 50	E_C/E_R = 100	
6	0.8205	0.6004	0.3280	0.5300	0.3899	LINER ELEMENTS
16	0.8380	0.7335	0.6099	0.4554	0.3698	
26	0.7893	0.6893	0.5705	0.4204	0.3362	
36	0.6869	0.6005	0.4997	0.3767	0.3106	
46	0.6604	0.5749	0.4753	0.3532	0.2872	
56	0.5775	0.5036	0.4176	0.3138	0.2588	
66	0.4757	0.4129	0.3399	0.2528	0.2078	
76	0.3743	0.3250	0.2679	0.0228	0.1668	
86	0.2943	0.2542	0.2075	0.1534	0.1266	
96	0.2354	0.2029	0.1652	0.1218	0.1007	
106	0.1950	0.1675	0.1355	0.0991	0.0817	
116	0.1564	0.1338	0.1075	0.0776	0.0635	
126	0.1183	0.1011	0.0812	0.0585	0.0481	
136	0.0907	0.0770	0.0610	0.0427	0.0342	
146	0.0678	0.0576	0.0457	0.0319	0.0255	
156	0.0505	0.0427	0.0335	0.0228	0.0177	
166	0.0375	0.0316	0.0245	0.0162	0.0122	
176	0.0291	0.0245	0.0189	0.0122	0.0088	
186	0.0240	0.0201	0.0155	0.0097	0.0068	
196	0.0201	0.0107	0.0128	0.0080	0.0054	
206	0.0173	0.0145	0.0110	0.0067	0.0045	
216	0.0154	0.0129	0.0098	0.0060	0.0039	

Table 8.2

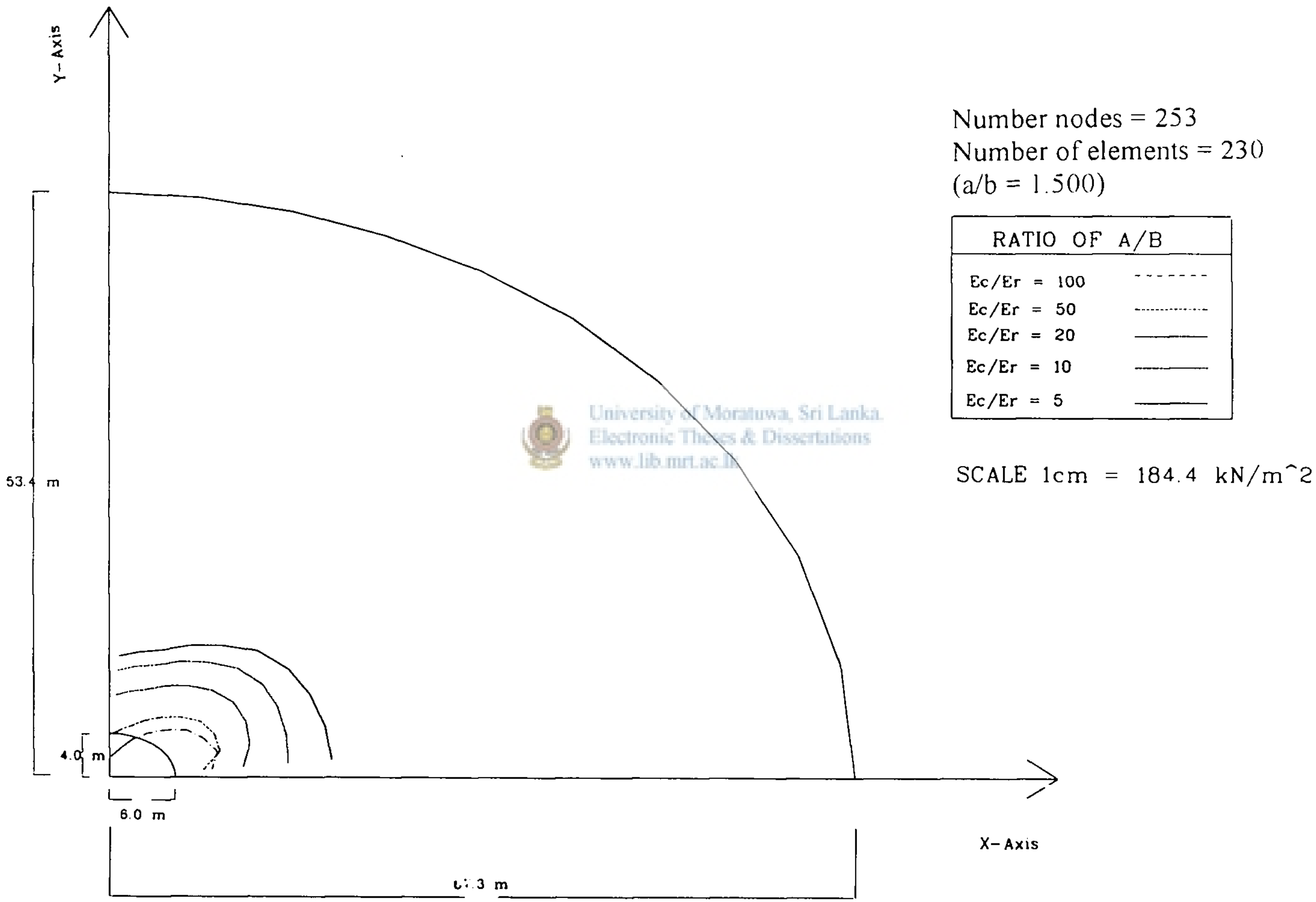

Figure 8.3 Variation of major principal stress along circumferential line "CD"
(Liner thickness (t) = 0.2m)

VARIATION OF MAJOR PRINCIPAL STRESS ALONG CIRCUMFERENTIAL LINE "GH"
(FOR FOR ELLIPTICAL TUNNEL - 3, a/b = 1.500)
(LINER THICKNESS = 0.2m)

NODE NUMBER	MAJOR PRINCIPAL STRESSx10^3 kN/m^2				
	RATIO OF E_C/E_R				
	E_C/E_R = 5	E_C/E_R = 10	E_C/E_R = 20	E_C/E_R = 50	E_C/E_R = 100
51	0.3319	0.2930	0.2253	0.1200	0.0565
52	0.3518	0.3110	0.2414	0.1340	0.0698
53	0.3764	0.3317	0.2594	0.1519	0.0894
54	0.4232	0.3711	0.2930	0.1830	0.1220
55	0.4744	0.4133	0.3285	0.2170	0.1589
56	0.5317	0.4580	0.3664	0.2543	0.2003
57	0.5699	0.4881	0.3952	0.2922	0.2474
58	0.5921	0.4978	0.4021	0.3102	0.2788
59	0.6045	0.4972	0.3933	0.3098	0.3019
60	0.6094	0.4883	0.3660	0.2565	0.2793

Table 8.3

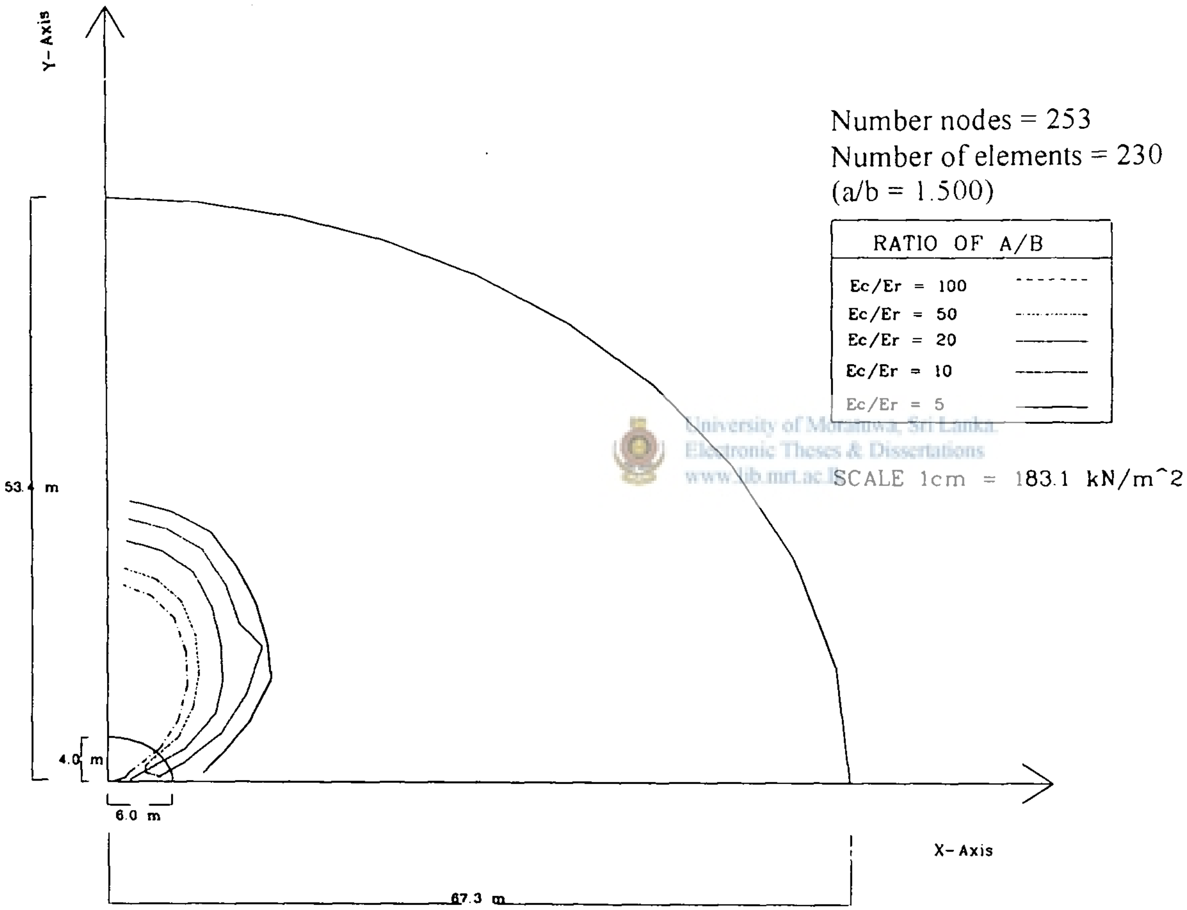

Figure 8.4 Variation of minor principal stress along circumferential line "CD"
(Liner thickness (t) = 0.2m)

VARIATION OF MINOR PRINCIPAL STRESS ALONG CIRCUMFERENTIAL LINE "GH"
(FOR FOR ELLIPTICAL TUNNEL - 3, a/b = 1.500)
(LINER THICKNESS = 0.2m)

NODE NUMBER	MINOR PRINCIPAL STRESSx10^3 kN/m^2				
	RATIO OF E_C/E_R				
	E_C/E_R = 5	E_C/E_R = 10	E_C/E_R = 20	E_C/E_R = 50	E_C/E_R = 100
51	0.7619	0.7187	0.6586	0.5822	0.5356
52	0.7584	0.7080	0.6463	0.5663	0.5176
53	0.7379	0.6844	0.6174	0.5308	0.4794
54	0.6843	0.6247	0.5527	0.4642	0.4143
55	0.6311	0.5611	0.4820	0.3892	0.3390
56	0.5775	0.5036	0.4176	0.3138	0.2588
57	0.5278	0.4492	0.3515	0.2303	0.1689
58	0.4247	0.3395	0.2349	0.1139	0.0636
59	0.3270	0.2184	0.0943	0.1070	0.0512
60	0.2634	0.1374	0.0614	0.1496	0.0136

Table 8.4

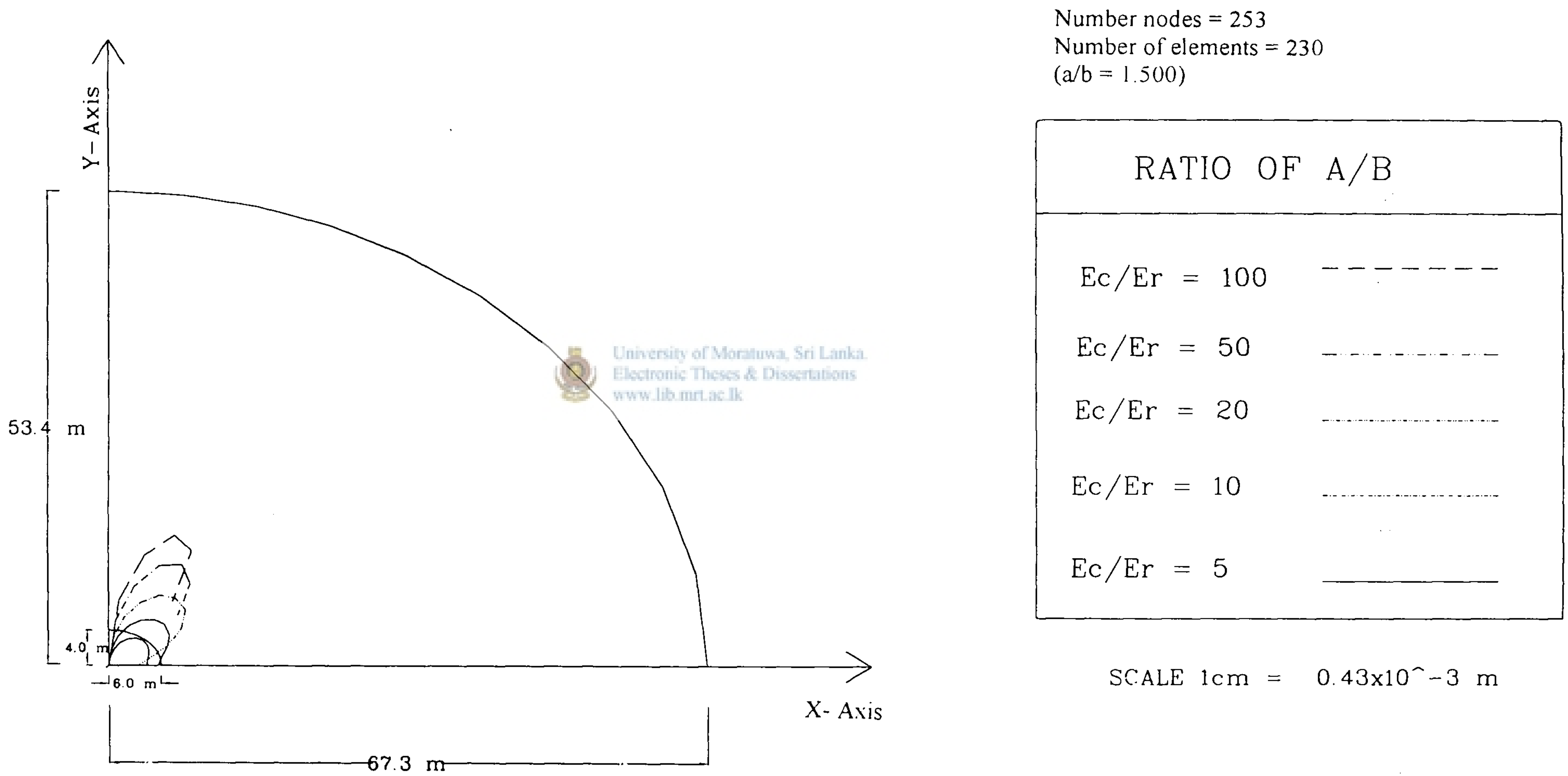

Figure 8.5 Variation of "x" displacement along circumferential line "GH"
(Liner thickness (t) = 0.2m)

VARIATION OF "X" DISPLACEMENTS ALONG CIRCUMFERENTIAL LINE "GH"
(FOR FOR ELLIPTICAL TUNNEL - 3, a/b = 1.500)
(LINER THICKNESS = 0.2m)

NODE NUMBER	"X' DISPLACEMENTS x 10^{-3} (m)				
	RATIO OF E_C/E_R				
	E_C/E_R = 5	E_C/E_R = 10	E_C/E_R = 20	E_C/E_R = 50	E_C/E_R = 100
67	0.0000	0.0000	0.0000	0.0000	0.0000
68	0.1038	0.1862	0.3063	0.5211	0.7491
69	0.1947	0.3476	0.5659	0.9366	1.3010
70	0.2851	0.5027	0.8013	1.2610	1.6430
71	0.3670	0.6352	0.9793	1.4080	1.5980
72	0.4350	0.7326	1.0730	1.3070	1.0200
73	0.4815	0.7872	1.0790	0.9677	-0.0462
74	0.4945	0.7694	0.9298	0.2388	-1.8520
75	0.4799	0.6995	0.6961	-0.6068	-3.7480
76	0.4487	0.6084	0.4561	-1.1337	-5.2640
77	0.4323	0.5635	0.3439	-1.6630	-5.9210

Table 8.5

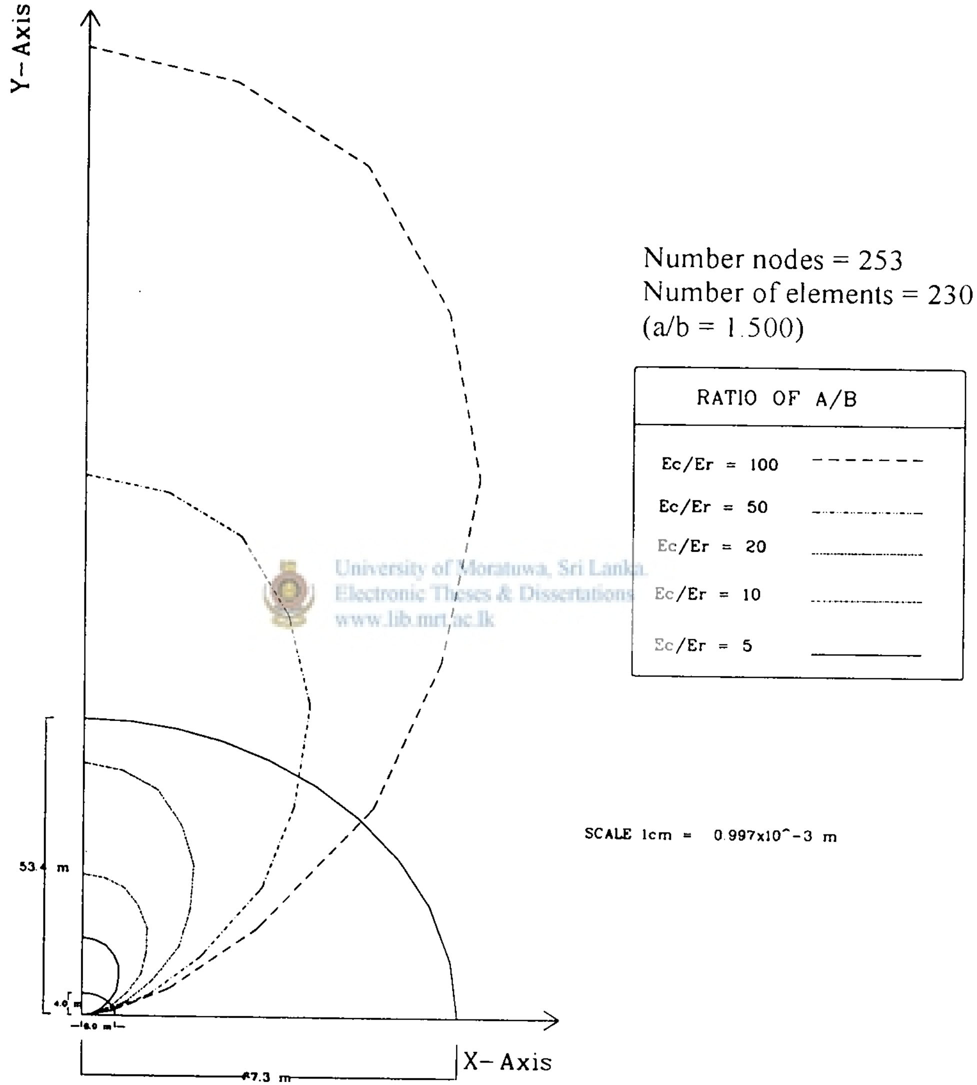

Figure 8.6 Variation of "y" displacement along circumferential line "GH"
(Liner thickness (t) = 0.2m)

VARIATION OF "Y" DISPLACEMENTS ALONG CIRCUMFERENTIAL LINE "GH"
(FOR FOR ELLIPTICAL TUNNEL - 3, a/b = 1.500)
(LINER THICKNESS = 0.2m)

NODE NUMBER	"Y' DISPLACEMENTS x 10^{-3} (m)				
	RATIO OF E_C/E_R				
	E_C/E_R = 5	E_C/E_R = 10	E_C/E_R = 20	E_C/E_R = 50	E_C/E_R = 100
67	1.4140	2.5640	4.5590	9.7440	17.5500
68	1.3950	2.5260	4.4840	9.5510	17.1600
69	1.3530	2.4410	4.3100	9.1020	16.2500
70	1.2460	2.2310	3.9000	8.1120	14.3200
71	1.1180	1.9790	3.4090	6.9300	12.0200
72	0.9353	1.6300	2.7490	5.3810	9.0480
73	0.7676	1.3160	2.1590	4.0130	6.4510
74	0.5409	0.9020	1.4140	2.4000	3.5500
75	0.3506	0.5657	0.8397	1.2670	1.6570
76	0.1709	0.2672	0.3752	0.4925	0.5353
77	0.0000	0.0000	0.0000	0.0000	0.0000

Table 8.6

CHAPTER 9.0

CONCLUSION

The analyses show that introduction of liners contribute in general to reduction of stress levels and deformations in the rock mass surrounding tunnels, and that an optimum liner thickness could be arrived at in practical situations. The reduction in stress magnitudes and displacements at points inside the rock mass depends on the tunnel shape, location of the point, and the stress or displacement quantity being considered.

Stiffer rock experience larger stresses but smaller displacements than weaker rock. Thus for weaker rock, the magnitudes of stress gradients through the concrete liner thickness will be greater (the strains in the concrete liner will be greater than for stronger rock), and points in the rock mass will experience greater deformations. In weaker rock, a thicker concrete liner will be advantageous for stress and deformation reduction in the rock mass.

The effect of elliptical tunnel geometry on stress in the rock mass is not definitive, but there appears to be a certain *a/b* ratio at which the stresses are highest. Results in chapter 7 constitute only a limited parametric analysis, which indicate that the stresses, in general, increase first and then start to decrease after a certain *a/b* value, as the a/b ratio of the ellipse is increased.

This type of finite element analysis offers the tunnel engineers the tools to arrive at an optimum linear thickness and tunnel geometry, by striking a balance between cost and efficiency.

REFERENCES

1. Crouch, S.L. and Starfield, A.M. (1983), Boundary Element Methods in Solid Mechanics, George Allan & Unwin, London, UK.

2. Goodman, R.E. (1976), Methods of Geological Engineering, West Publishing Co., St. Paul, Minnesota, USA.

3. Herget, G. (1988), Stresses in Rock, A.A. Balkema, Rotterdam, The Netherlands.

4. Hocking, G., Brown, E.T., and Waston, J.O. (1976), Three dimensional elastic stress analysis of underground openings by the boundary integral equation method, Proc., 3rd Sympo. Engineering Applications of Solid Mechanics, Toronto, Canada, pp.203-216.

5. Jaeger, C. (1979), Rock Mechanics and Engineering, Second Edition, Cambridge University Press., UK.

6. Obert et al. (1960), Design of underground openings in competent rock, USBM Bull. 587, p.36.

7. Selvedurai, A.P.S. (1979), Elastic Analysis of Soil-Foundation Interaction, Developments in Geotechnical Engineering, Vol. 17, Elservier Scientific Publishing Co., Netherlands.

8. Szechy, Karoly, (1973), The Art of Tunnelling, Second English Edition, Akademiai Kiado, Budapest.

9. Zienkiewicz, O.C. (1977), The finite element method, 3rd Ed, McGraw- Hill Co, London, UK.

10. British Standard, Structural use of concrete, (BS 8110 : Part I : 1985)

APPENDIX A

ANALYSIS OF CIRCULAR TUNNEL, a/b = 1

A circular tunnel geometry was considered to asses the accuracy of numerical results predicted by FEAP, by comparing the numerical results with the analytical solution for a circular lined tunnel given by Jaeger(1979). Material properties, loading and boundary conditions used are identical to those used for elliptical tunnels considered in chapters 4, 5 & 6 for a liner thickness of 0.2m. Finite element mesh used for this analysis is shown in figure A1.

Analytical results and the FEM results were plotted in one graph for comparison purpose (see figures A2 and A3). According to the above results, the deviation of FEM results form analytical results is small. This deviation is close enough for engineer applications. Therefore the results obtained for elliptical tunnels which do not have any analytical solution can be considered as acceptable.

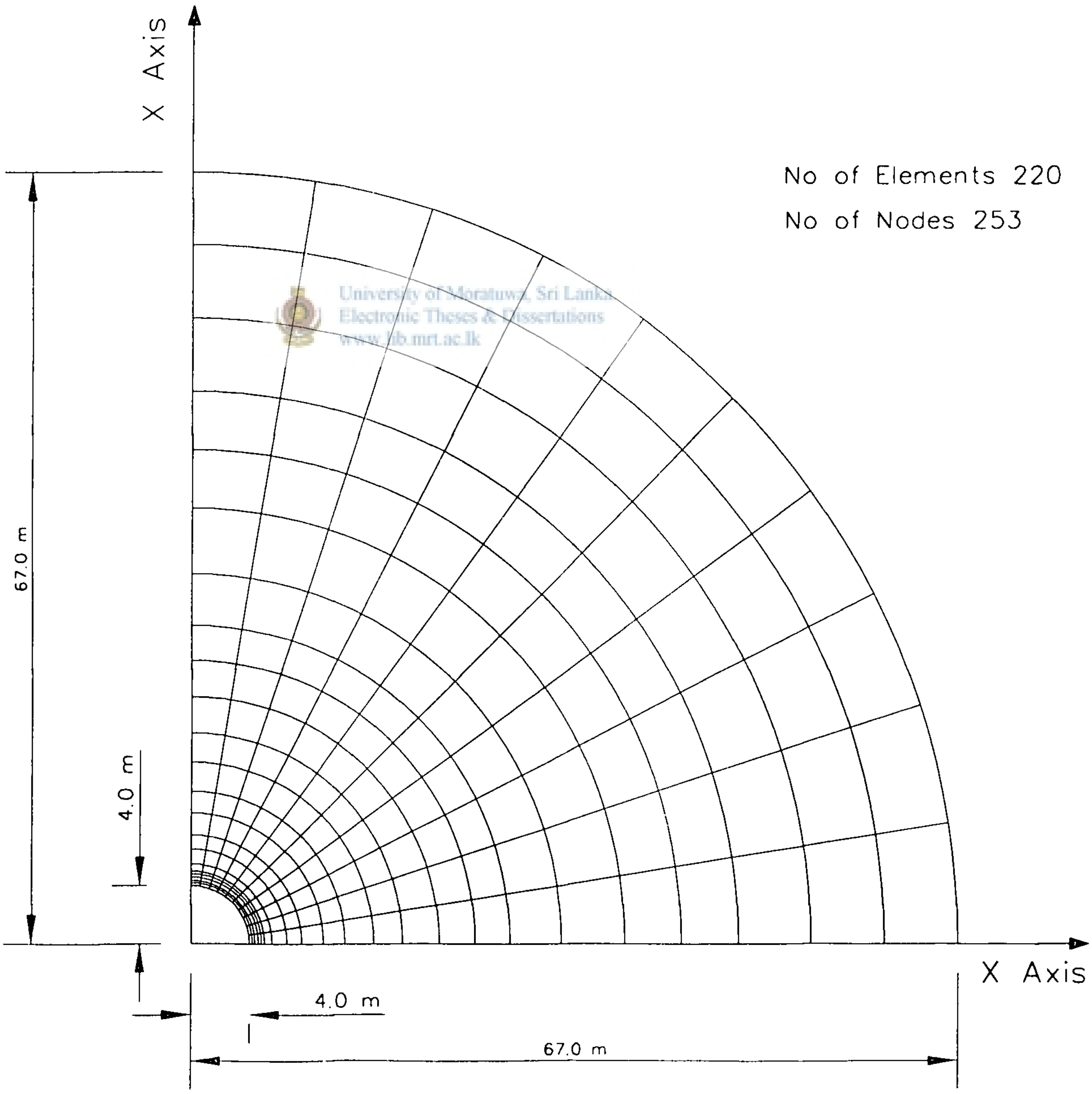

Figure A1 Finite element mesh for circular tunnel with a/b = 1

VARIATION OF MAJOR PRINCIPAL STRESS ALONG RADIAL LINE "CD" FOR CIRCULAR TUNNEL, a/b = 1

ELEMENT NUMBER	MAJOR PRINCIPAL STRESS x 10^3 kNm^{-2}	
	FEAP	ANALITICAL
16	0.5404	0.5622
26	0.4878	0.5134
36	0.4439	0.4707
46	0.4067	0.4330
56	0.3533	0.3772
66	0.2930	0.3144
76	0.2293	0.2461
86	0.1606	0.1731
96	0.1109	0.1215
106	0.0771	0.0859
116	0.0535	0.0615
126	0.0388	0.0462
136	0.0289	0.0360
146	0.0213	0.0281
156	0.0155	0.0220
166	0.0110	0.0173
176	0.0071	0.0133
186	0.0038	0.0098
196	0.0013	0.0072
206	0.0005	0.0054
216	-0.0178	0.0041

Table A1

VARIATION OF MAJOR PRINCIPAL STRESS ALONG RADIAL LINE "CD"
FOR CIRCULAR TUNNEL ,a/b = 1
(LINER THICKNESS t = 0.2m)

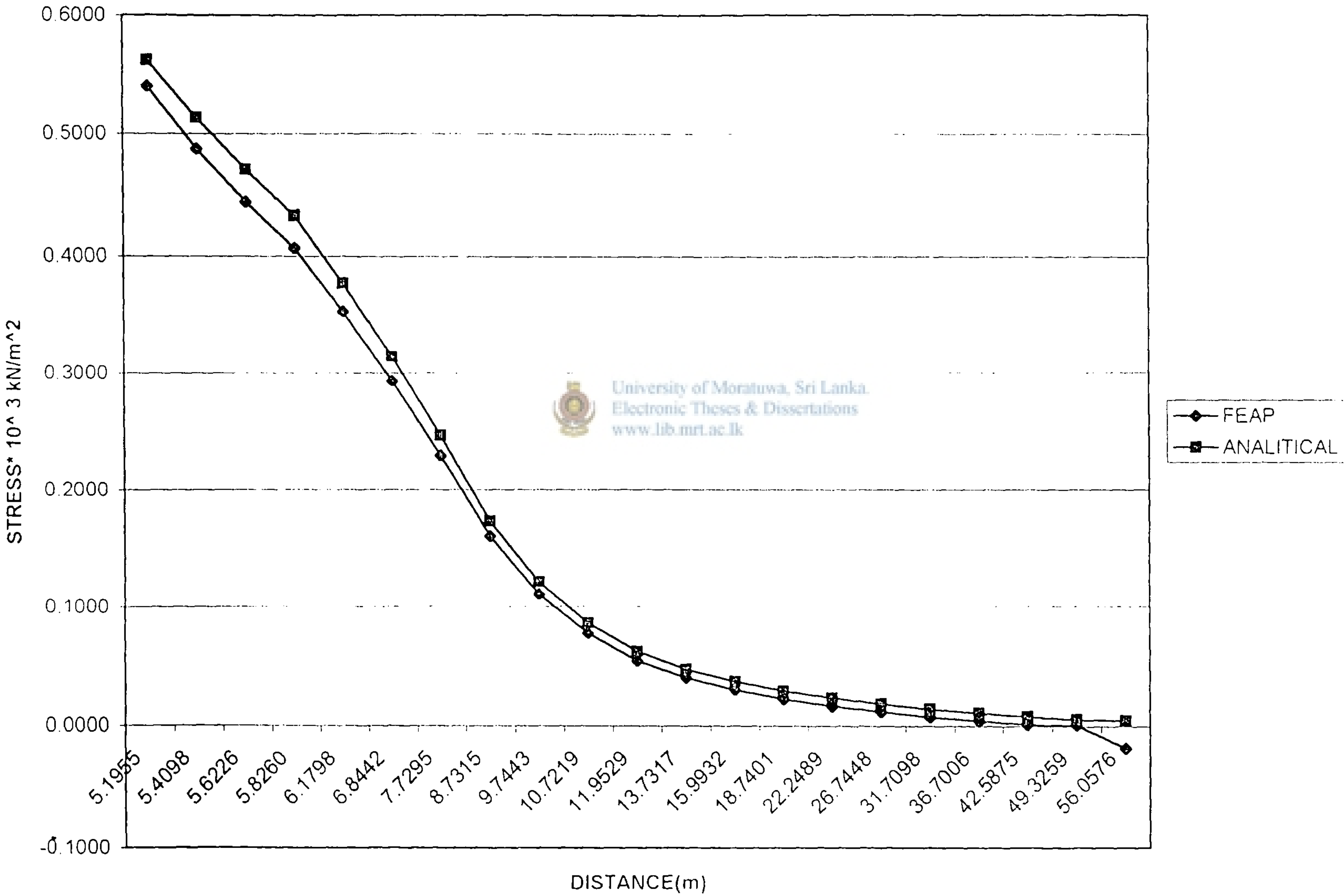

Figure A2 Variation of major principal stress along radial line "CD"
(Liner thickness (t) = 0.2m)

VARIATION OF MINOR PRINCIPAL STRESS ALONG RADIAL LINE "CD" FOR CIRCULAR TUNNEL, a/b = 1

ELEMENT NUMBER	MINOR PRINCIPAL STRESS $x(-1x\ 10^3)\ kNm^{-2}$	
	FEAP	ANALITICAL
16	0.4615	0.5622
26	0.4301	0.5134
36	0.4016	0.4707
46	0.3750	0.4330
56	0.3337	0.3772
66	0.2848	0.3144
76	0.2286	0.2461
86	0.1657	0.1731
96	0.1195	0.1215
106	0.0869	0.0859
116	0.0642	0.0615
126	0.0498	0.0462
136	0.0401	0.0360
146	0.0326	0.0281
156	0.0268	0.0220
166	0.0224	0.0173
176	0.0185	0.0133
186	0.0152	0.0098
196	0.0127	0.0072
206	0.0109	0.0054
216	0.0097	0.0041

Table A2

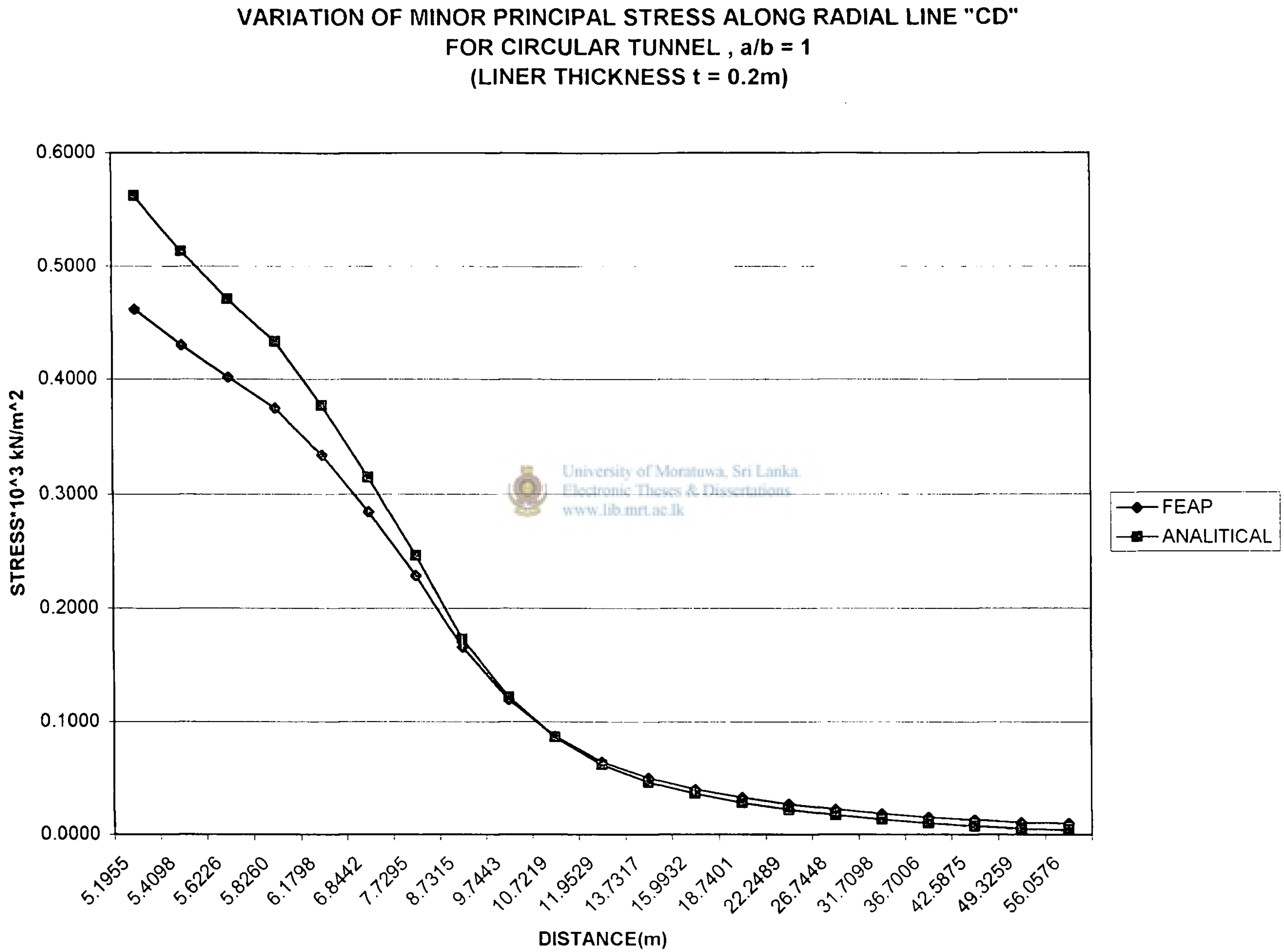

Figure A3 Variation of major principal stress along radial line "CD"
(Liner thickness (t) = 0.2m)

APPENDIX B

CHECK FOR STRAIN IN CONCRETE LINER UNDER INTERNAL FLUID PRESSURE

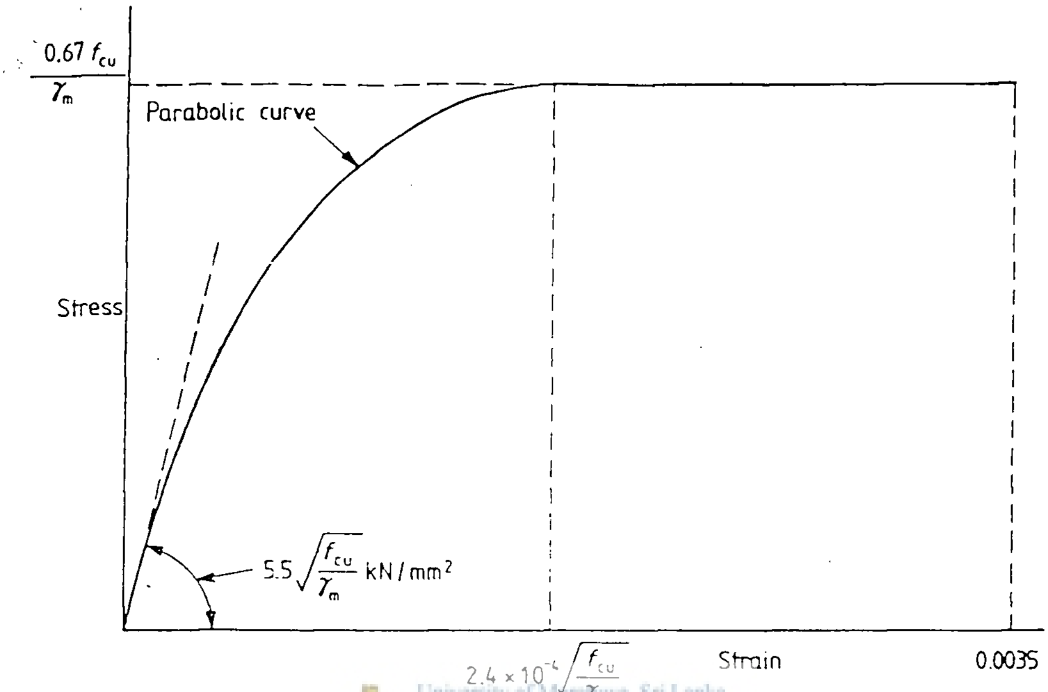

NOTE 1. 0.67 takes account of the relation between the cube strength and the bending strength in a flexural member. It is simply a coefficient and *not* a partial safety factor.

NOTE 2. f_{cu} is in N/mm².

Figure B 1 shows short term design stress-strain curve for normal weight concrete (BS 8110)

$2.4\text{x}10^{-4}(f_{cu}/\gamma_m)^{0.5} = 2.4(25/1.5)^{0.5} = 0.00098$ kN/mm²

$5.5(f_{cu}/\gamma_m)^{0.5} = 5.5(25/1.5)^{0.5} = 22.45$ kN/mm²
= 22450 MPa
= $2.245\text{x}10^7$kPa

$0.67(f_m/\gamma_m) = (0.67\text{x}25)/1.5 = 11.17$N/mm²

$\varepsilon = 1/(2.2485\text{x}10^7/11.1710^3)$
= 0.000497
= 0.0005

From he above calculation it can be seen that the strain in concrete is 0.0005 at failure for grade 25 concrete, if the initial tangent modulus is excepted to prevail.

VARIATION OF MAJOR PRINCIPAL STRAIN
(FOR ELLIPTICAL TUNNEL 3, a/b = 1.500)
(LINER THICKNESS t = 0.2m)

ELEMENT NUMBER	MAJOR PRINCIPAL STRAIN x 10^{-3}				
	E_C/E_R = 5	E_C/E_R 10	E_C/E_R = 20	E_C/E_R = 50	E_C/E_R =100
1	0.1291	0.2369	0.3861	0.5974	0.7325
6	0.2508	0.4419	0.6857	0.1001	0.1175
10	0.2904	0.4435	0.6089	0.7894	0.8674

Table A 3

VARIATION OF MINOR PRINCIPAL STRAIN
(FOR ELLIPTICAL TUNNEL 3, a/b = 1.500)
(LINER THICKNESS t = 0.2m)

ELEMENT NUMBER	MINOR PRINCIPAL STRAIN x (-1)x 10^{-3}				
	E_C/E_R = 5	E_C/E_R 10	E_C/E_R = 20	E_C/E_R = 50	E_C/E_R =100
1	0.9211	0.1401	0.2081	0.3132	0.3967
6	0.1365	0.2106	0.3055	0.4273	0.4897
10	0.1482	0.2056	0.2647	0.3181	0.3228

Table A 4